AD-781 317

STRUCTURAL DYNAMIC PROPERTIES OF TACTICAL MISSILE JOINTS-PHASE 3

George Lasker, et al

General Dynamics

Prepared for:

Naval Air Systems Command

May 1974

DISTRIBUTED BY:

NTIS

National Technical Information Service
U. S. DEPARTMENT OF COMMERCE
5285 Port Royal Road, Springfield Va. 22151

UNCLASSIFIED

Security Classification

AD 781 317

DOCUMENT CONTROL DATA - R & D

ORIGINATING ACTIVITY (Corporate author): Pomona Division of General Dynamics Inc. 1615 W. Mission Boulevard Pomona, California 91766	REPORT SECURITY CLASSIFICATION: UNCLASSIFIED
	GROUP:
REPORT TITLE: STRUCTURAL DYNAMIC PROPERTIES OF TACTICAL MISSILE JOINTS - PHASE 3	
DESCRIPTIVE NOTES (Type of report and inclusive dates): Final (May 1972 thru January 1974)	
AUTHOR(S) (First name, middle initial, last name): George Lasker, John G. Maloney, Michael T. Shelton and David A. Underhill	

REPORT DATE	TOTAL NO. OF PAGES	NO. OF REFS
May 1974	186	7

CONTRACT OR GRANT NO.: N00019-72-C-0507	ORIGINATOR'S REPORT NUMBER(S): CR-6-348-945-003
b. PROJECT NO.	
c.	OTHER REPORT NO(S) (Any other numbers that may be assigned this report)
d.	
DISTRIBUTION STATEMENT: Approved for public release, distribution unlimited.	
SUPPLEMENTARY NOTES	SPONSORING MILITARY ACTIVITY: Naval Air Systems Command Department of the Navy Washington, D.C. 20361

ABSTRACT The results of a third and final phase in a general study of the structural dynamic properties of tactical missile airframe joints are presented. The overall objectives of the study were to provide a better understanding of mechanical joint effects on missile dynamic response and to improve methods for predicting and representing their characteristics in system simulation and response studies.

Finite element structural analysis techniques started in Phase 1 are shown to be capable of providing reliable estimates of joint compliance in complex actual missile structures. A technique for extracting joint compliance values from missile model test data started in Phase 1 is refined to improve convergence and user convenience. A user's manual for the joint compliance extraction digital computer code is included as an appendix to the report. An exploratory study of missile joint self-induced vibration is presented together with an initial evaluation of some promising methods for suppression and control. The report concludes with a proposed rating system for joints intended to integrate the many design considerations such as strength, weight, producibility, and maintainability, in addition to structural dynamic considerations, into overall system requirements.

DD FORM 1 NOV 65 1473 (PAGE 1)

S/N 0101-807-6801

UNCLASSIFIED

Security Classification

UNCLASSIFIED

Security Classification

14 KEY WORDS	LINK A		LINK B		LINK C	
	ROLE	WT	ROLE	WT	ROLE	WT
Tactical Missile Joints						
Dynamics of Joints						
Joint Compliance						
Self Induced Vibration						
Finite Element Applications						
Joint Stiffness						

DD FORM 1 NOV 65 1473 (BACK)

(PAGE 2)

ia

Security Classification

STRUCTURAL DYNAMIC PROPERTIES OF TACTICAL MISSILE JOINTS - PHASE 3

Final Report

(May 1972 to January 1974)

May 1974

CR-6-348-945-003

By

G. Lasker
J. G. Maloney
M. T. Shelton
D. A. Underhill

Prepared Under Contract N00019-72-C-0507

for the

Naval Air Systems Command

by

Pomona Division

General Dynamics, Inc.

1675 W. Mission Blvd.
Pomona, California 91766

Approved for public release; distribution unlimited

ib

FOREWORD

This study has been conducted by the Pomona Division of General Dynamics Corporation for the Naval Air Systems Command under Contract N00019-72-C-0507.

The principal investigator for the study has been Mr. John G. Maloney. Dr. George Lasker has performed the finite element analysis presented in Section 3. The joint compliance extraction technique and computer code work was performed by Mr. M. T. Shelton. The direct technical supervisor has been Mr. David A. Underhill, Structural Dynamics Section Head.

Mr. George P. Maggos has been the Naval Air Systems Command technical monitor.

The authors wish to acknowledge the contributions of Messrs David O. Rife, James B. Samonte and Donald G. VandeGriff for providing assistance in various portions of the study.

TABLE OF CONTENTS

TABLE OF CONTENTS
(Cont'd.)

LIST OF TABLES

LIST OF TABLES
(Cont'd.)

LIST OF FIGURES

LIST OF FIGURES
(Cont'd.)

Section 1.0

SUMMARY

Results of a third and final phase in a general study of the structural dynamic properties of tactical missile joints are presented. This effort, undertaken by the Pomona Division of General Dynamics for the Naval Air Systems Command, has been intended to provide a better understanding of mechanical joint effects on missile dynamic response and improved methods for predicting and representing their characteristics in system simulation and response studies.

Highlights of the results obtained in the first two study phases (References 1 and 2) are reviewed, covering an industry survey, classification scheme, and parametric evaluation of joint compliance effects. Finite element structural analysis techniques started in Phase 1 and completed in this final study phase are shown to be capable of providing reliable estimates of joint compliance in complex actual missile structures.

Experimental methods are reviewed and a joint compliance extraction code designed to solve for joint properties from modal test data is described in some detail. This method, also started in the Phase 1 study, has been refined during the present phase to improve convergence and user convenience. A user's manual for this code is included as an Appendix.

An exploratory study of missile joint self-induced vibration is presented together with an initial evaluation of some promising methods for suppression and control. The report concludes with a discussion of a proposed rating system for tactical missile joints with the objective of offering the designer some perspective on integrating the many considerations such as strength, producibility, and maintainability, in addition to compliance, into overall system requirements.

Section 2.0

INTRODUCTION

The structural dynamic properties of tactical missile joints can play an extraordinarily important role in weapon system structural response characteristics. This report deals with the third and final phase of an exploratory study of the primary structural dynamic characteristics of missile mechanical joints and the analytical and experimental tools identified and developed for predicting their behavior.

The most conspicuous attribute of the average tactical missile joint is flexural compliance under applied bending moment. The first phase study was largely devoted to an examination of this characteristic starting with a literature search and an industry survey to sample others' experience followed by a parametric study of joint compliance effects, elastic coupling, the significance of stiffness discontinuities and the importance of considering actual load paths through joint elements. Based on the industry survey, it was concluded that investigators generally represent missile joints in analytical modeling by flexural springs selected by trial and error to match measured response characteristics. Joint compliance effects were typically found to account for more than 30 percent of the total elastic deformation of a missile in its primary bending modes.

A joint classification scheme proposed in a NASA study reported in Reference 3 suggested factors of ten increase in compliance progressing from each level - Excellent, Good, Moderate, and Loose. Thus, a "Moderate" joint would be 10 times as compliant as a "Good" joint and 100 times as compliant as an "Excellent" joint. Viewed in terms of stiffness loss in a typical missile airframe, a "Good" joint represents a local reduction in section properties of approximately 60 percent over a span of one half body diameter. A "Moderate" joint would correspondingly reduce local section properties 95 percent. Such gross structural inefficiencies are attributed to poor distribution of load paths through joint interfaces. Figure 2-1 shows the powerful influence of joint compliance on the first mode frequency of a missile idealized as a uniform beam.

From the standpoint of the structural dynamic analyst charged with the responsibility for developing adequate math models in developmental studies, methods for accurately estimating joint compliance are of paramount importance. The advent of finite element structural analysis techniques has offered some very promising tools for realistically representing detailed elastic behavior with joint elements. Finite element modeling of idealized joints was started in an exploratory effort during Phase 1 and - based on encouraging results - considerably expanded during Phase 2 to encompass an actual missile joint design for which accurate compliance test data were available for correlation purposes. This effort has been continued during the present and final study phase with emphasis on computational economy and is presented in Section 3.0.

Experimental methods when test hardware is available offer another important approach to the determination of missile joint structural dynamic properties. An ideal test configuration for evaluating joint properties is considered to be a simple uniform structure on a free-free suspension to avoid external constraints and with the subject joint located at mid-span. The joint bending compliance then has a dominant effect on odd numbered modes (1, 3, . . .) and the joint shear compliance is exposed by even numbered modes (2, 4, . . .). Simple tests were performed during Phase 1 on tubular models to illustrate the basic test approach and to explore the effects of load path discontinuities. Actual missile joint hardware was employed in a series of four similar tests during the Phase 2 study, with data on two joint configurations being provided in a colloborative effort by Naval Weapon Center, China Lake personnel. One joint test of particular interest involved a shear joint with 18 radial screws. Joint compliance was evaluated parametrically as a function of number of fasteners, producing the surprisingly consistent and well ordered results shown in Figure 2-2. An exploratory generalization of this shear joint behavior is shown in Figure 2-3 with the cautionary comment that the derived compliance expression must be viewed with some skepticism since it considers only joint diameter and number of fasteners. Test data for two unrelated specimens are compared with the empirical compliance expression in the figure, however, and show better agreement than might be expected. The 8 fastener data point is taken from the 8-inch diameter shear joint tested at the Naval Weapons Center, China Lake and reported in the Phase 2 study. The 3 and 6 fastener data points are taken from the segmented tube test data in Phase 1 extrapolated to a "fastener" arc length of 2 degrees in order to correspond to the 1/4 inch bolts used with the 13.5 inch diameter data source.

The opportunity to test single joints in the "ideal" configuration is the exception rather than the rule, however, and more generally dynamic testing is performed on total airframes with many joints. The traditional approach consists of hand tuning compliance values to produce matching results between the mathematical model and measured mode shapes and frequencies. Since this is a laborious, time consuming, and often frustrating task, an automated and systematic approach is desirable. To these ends, an exploratory effort based on the optimization method of steepest descent was developed in Phase 1 of the study. This method of extracting joint compliance values from a set of measured missile elastic mode frequencies and shapes was shown to be feasible. However, various limitations in the implemented method precluded full development. A more general approach developed by Hall, Calkin and Sholar, Reference 4, appeared in the literature and in Phase 2 their method was applied to the problem of extracting joint compliances. The result is a digital computer code. In Phase 3 refinements were added to the joint compliance extraction technique code to increase its utility and a user's manual was prepared for the code. Section 4 and the Appendix of the present report present the Phase 3 efforts on the joint compliance extraction technique.

Another important characteristic of missile airframe joints is that of self-induced vibration. This behavior is most usually associated with joint designs having inherently low interface preloads, and its presence can create unnecessarily severe environments in laboratory testing as well as in both captive and free-flight. Section 5 of this report describes an investigation of this phenomena covering both full scale and model exploratory testing.

The final section of this report, Section 6, illustrates a method of integrating the structural dynamic properties of joints with other important mechanical attributes that airframe joints must possess to meet overall system requirements.

FIGURE 2-1

FREQUENCY RATIO VS. JOINT STIFFNESS RATIO
UNIFORM BEAM - MIDSPAN JOINT

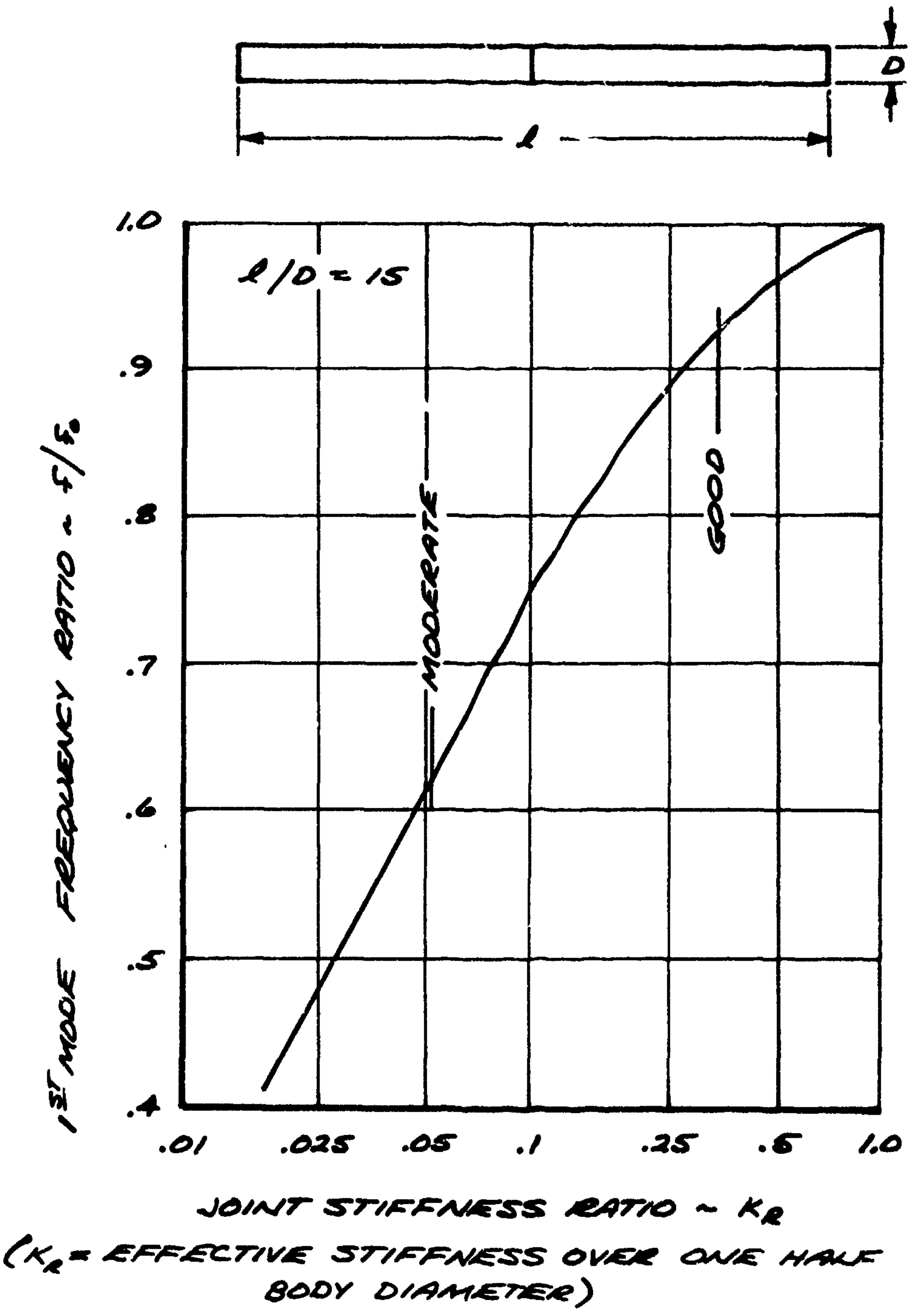

FIGURE 2-2

13.5 INCH DIAMETER SHEAR BOLT JOINT
FLEXURAL COMPLIANCE VS. NUMBER OF FASTENERS

$C_\theta = 12.71(10)^{-8}/n^{1.404}$ RAD./IN-LB.

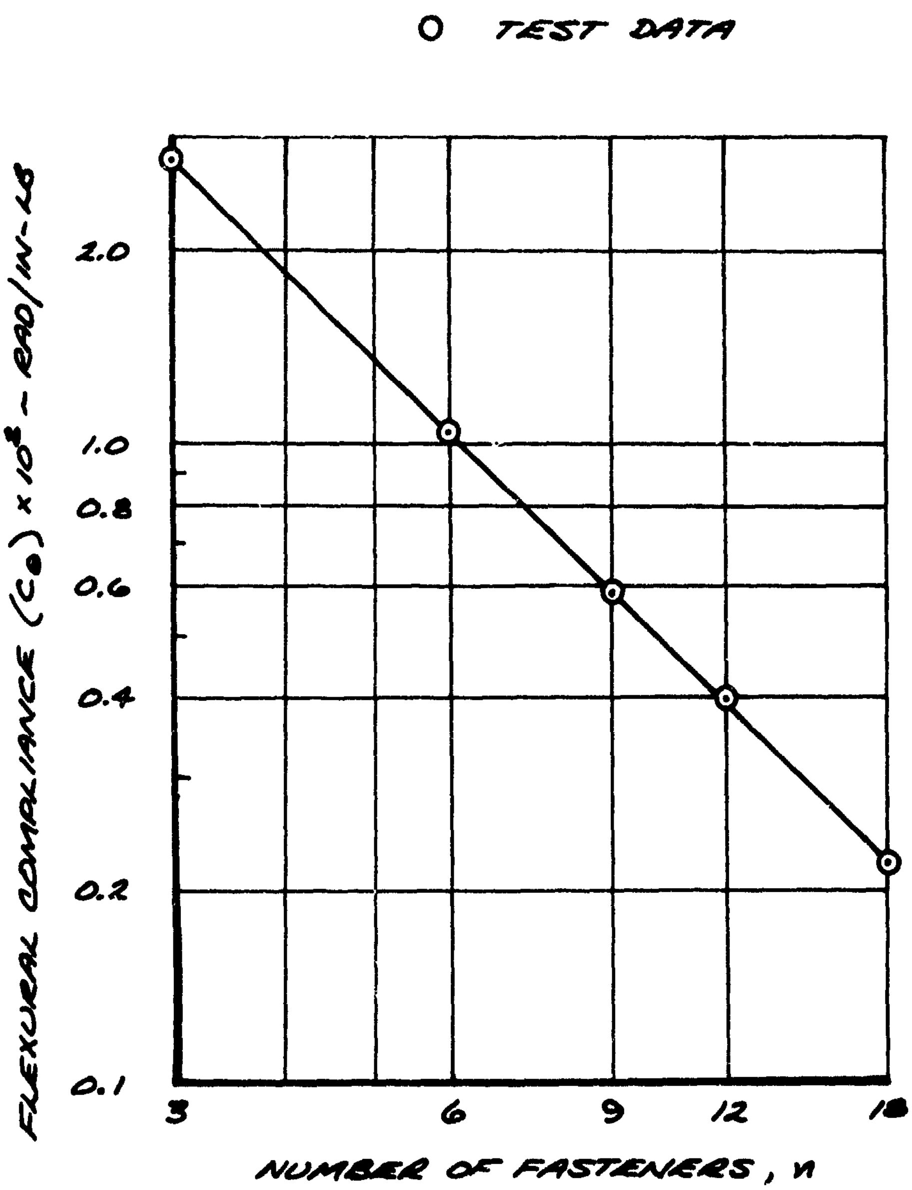

FIGURE 2-3

GENERALIZED SHEAR JOINT COMPLIANCE VERSUS NUMBER OF FASTENERS

$$D^3 C_\theta = 31.3\,(10)^{-5} / n^{1.404}$$

WHERE D = JOINT DIA. IN INCHES

C_θ = COMPLIANCE, RAD./IN-LB.

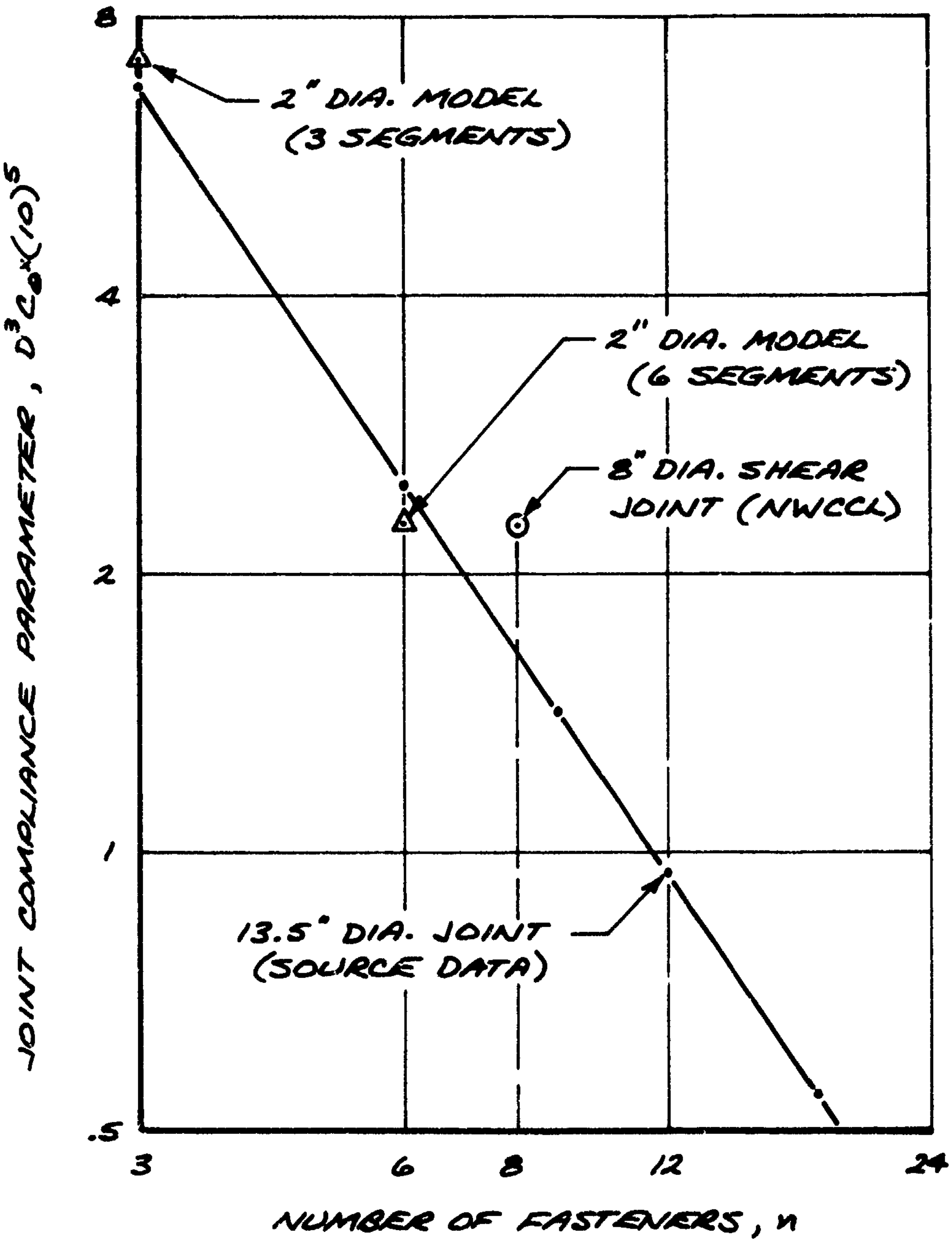

Section 3.0

JOINT COMPLIANCE ANALYSIS

Finite element structural analysis methods have been shown in earlier study phases to offer considerable promise as means of predicting tactical missile mechanical joint properties. In the Phase 2 portion of the investigation a finite element type of analysis was performed on an eighteen fastener shear joint. The analysis made use of the NASTRAN computer program. The math model used described the structure on each side of the joint by means of a set of conical shell elements. Bolts were then described by discrete springs. Each spring constrains two corresponding points on each side of the joint. The solution process is based on a Fourier series expansion about the circumference. Thus forces and displacements are determined by summing a set of harmonic components. The compliance associated with various harmonics can be zero. The zero compliance harmonics are well defined for uniform bolt patterns. Thus for a joint with n bolts, the compliance associated with all harmonics are zero except for harmonics 0, 1, n-1, n + 1, 2 n-1, 2 n + 1, ...

In Phase 2 the problem was formulated and computations were performed entirely on NASTRAN. The cost per computer run was quite high even though only twelve harmonics were used. Two effects played a role in the high cost. If the structure was geometrically axisymmetric the stiffness matrix for each harmonic would be uncoupled from all others, however, due to the bolts the structure is asymmetric. Thus a coupling between harmonics results with a corresponding high computer solution time. The problem is aggravated to a considerable degree by the fact that the zero harmonics cannot be excluded from the solution process. Thus to solve this problem using say 50 harmonics is almost prohibitive.

On examining this problem it became apparent that it was not inherently expensive but rather due to limitations within the NASTRAN program. It also became apparent that a small efficient computer program could be written which used certain NASTRAN outputs. This was done as part of the Phase 3 finite element analysis effort.

The new computer program uses NASTRAN generated stiffness coefficients associated with each harmonic and the structure on each side of the joint.

3.1 PROBLEM FORMULATION

Consider two axisymmetric shells with a common axis of symmetry which are attached together with respect to a discrete set of points around the circumference as shown in Figure 3-1.

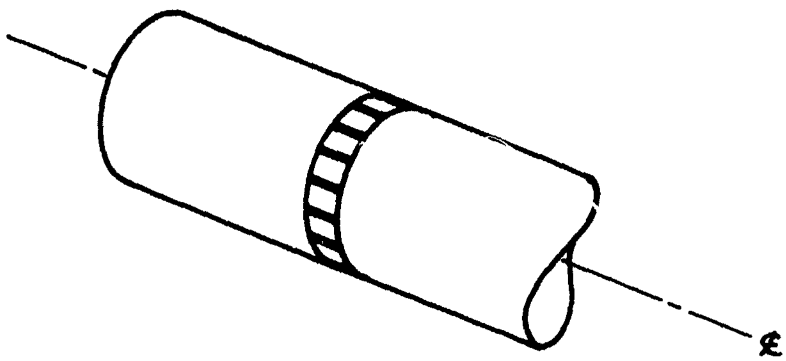

Figure 3-1. Sketch Showing Two Axisymmetric Shells Attached at a Discrete Set of Points

We require the attachments to be positioned so that they are symmetric with respect to a plane of symmetry which includes the missile longitudinal axis. The attachment forces do not act at points but rather over a small area defined by the thickness of the shell and an arc length defined by the enclosed angle ϵ as shown in Figure 3-2.

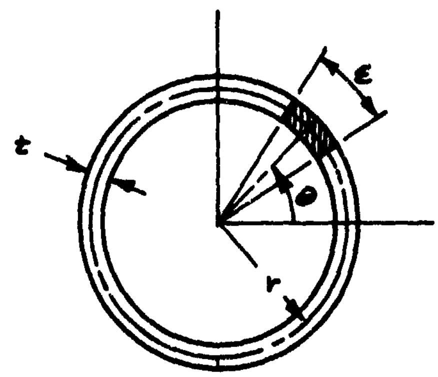

Figure 3-2. Area Over Which Bolt Acts as Defined in Math Model

Also the distribution of the load over the area is taken as uniform. Let ρ be the resultant bolt force acting on the area. The stress $\sigma(\theta)$ can then be expanded into a cosine series in the form

$$\sigma(\theta) = \frac{1}{t} \sum a_n \cos n\theta \tag{3.1}$$

On doing so we obtain

$$\sigma(\theta) = \frac{2p}{t\epsilon} \sum_{n=1}^{\infty} \frac{\sin(n\epsilon/2)}{n} \cos(n\theta) \tag{3.2}$$

or

$$a_n = \frac{2p}{n\epsilon} \sin(n\epsilon/2) \tag{3.3}$$

The use of the cosine series imposes the requirement that the horizontal plane be a plane of symmetry The quantity $t\sigma(\theta)$ has units of load per unit arc length. The quantity $f(\theta) = t\sigma(\theta)$ can be expressed in the form

$$f(\theta) = f_1 \cos(\theta) + f_2 \cos(2\theta) + f_3 \cos(3\theta) + \cdots \tag{3.4}$$

where

$$f_n = \frac{2p}{n\epsilon} \sin(n\epsilon/2) \tag{3.5}$$

It can be interpreted as a generalized force associated with the n th harmonic. Let f_{ni} be the generalized force associated with the n th harmonic and the i th bolt. Let the joint have b bolts and let p_i be the force resultant for the i th bolt acting at θ_i. Then the harmonic generalized forces f_n associated with the set of bolts used on the joint are

$$f_n = \sum_{i=1}^{b} f_{ni} = \sum_{i=1}^{b} \frac{2p_i}{n\epsilon} \sin(n\epsilon/2) \cos(n\theta_i) \tag{3.6}$$

Let us define a matrix with elements a_{ij}

$$a_{ij} = \frac{2}{i\epsilon} \sin(i\epsilon/2) \cos(n\theta_j) \tag{3.7}$$

Let f_i and p_j respectively be elements of column vectors $\{f_i\}$ and $\{p_j\}$. Then from (3.6) and (3.7) one can see that the following relationship holds

$$\{f_i\} = [a_{ij}]\{p_j\} \tag{3.8}$$

Let $[s_{ij}]$ be a diagonal matrix where element s_{ij} is a spring stiffness constant associated with the i th bolt and let $\{v_j\}$ be a column matrix associated with bolt elongations. Then the following relationship holds.

$$\{p_j\} = [s_{jk}]\{v_k\} \tag{3.9}$$

If we could assign a point on the circumference to each bolt then bolt elongation could be expressed by a set of generalized displacements u_n as follows:

$$v_i = \sum_{n=1}^{\infty} u_n \cos(n\theta_i) \tag{3.10}$$

Since the bolt load is associated with an area as shown in Figure 3-2 we cannot associate the bolt displacement with only one point. We will give an indirect definition which will implicitly contain an averaging over this area. Let the problem be limited to m harmonics and let $[c_{ij}]$ be an m by b matrix which relates bolt elongations $\{v_i\}$ to generalized harmonic displacements $\{u_j\}$ as follows

$$\{v_i\} = [c_{ij}]\{u_j\} \tag{3.11}$$

Then virtual bolt elongations $\{\delta v_i\}$ and virtual generalized displacements $\{\delta u_j\}$ are related by

$$\{\delta v_i\} = [c_{ij}]\{\delta u_j\} \tag{3.12}$$

We require the following to hold

$$\{p_i\}^T\{\delta v_i\} = \{f_j\}^T\{\delta u_j\} \tag{3.13}$$

That is, we require the virtual work associated with virtual elongation $\{\delta v_i\}$ to be equal to the virtual work associated with the corresponding generalized variables. On substituting from (3.8) and (3.12) into (3.13) we obtain

$$\{p_i\}^T [c_{ij}] \{\delta u_j\} = \{p_i\}^T [a_{ij}]^T \{\delta u_j\} \tag{3.14}$$

Equation (3.14) can hold for all virtual displacements $\{\delta u_j\}$ and all loads $\{p_i\}$ if and only if

$$[c_{ij}] = [a_{ij}]^T \tag{3.15}$$

Therefore from (3.7) and (3.15) it follows that

$$c_{ij} = \frac{2}{j\epsilon} \sin\left(\frac{j\epsilon}{2}\right) \cos(n\theta_i) \tag{3.16}$$

From (3.8), (3.9), (3.11), and (3.15) it follows that

$$\begin{aligned} \{f_i\} &= [a_{ij}] \{p_j\} \\ &= [a_{ij}] [s_{jk}] \{v_k\} \\ &= [a_{ij}] [s_{jk}] [a_{k\ell}]^T \{u_\ell\} \end{aligned} \tag{3.17}$$

Let

$$[\bar{s}_{i\ell}] = [a_{ij}] [s_{jk}] [a_{k\ell}]^T \tag{3.18}$$

Thus $[\bar{s}_{i\ell}]$ is a stiffness matrix which describes the stiffness of the set of joint bolts with respect to the generalized (harmonic) variables $\{f_i\}$ and $\{u_\ell\}$. Then (3.17) has the form

$$\{f_i\} = [\bar{s}_{ij}] \{u_j\} \tag{3.19}$$

We will now define the variables associated with the axisymmetric structures on each side of the joint. These structures will be interpreted as two free structures whose relative displacements are constrained by the bolt attachments. We will assume that there is no relative radial or circumferential motion across the joint. Since the two structures are unconstrained except by the joint it follows that the zero and first harmonics of longitudinal relative displacements are respectively associated with relative longitudinal translation and pitch rigid body motions. The higher harmonics on the other hand are associated with shell deformation.

Using NASTRAN we can compute the displacement u_n associated with each higher harmonic load f_n acting on the joint. We can then compute two sets of stiffness coeffi-ients associated with each of the structures as follows:

$$K_{ii}' = \frac{f_i'}{u_i'}$$
$$K_{ii}'' = \frac{f_i''}{u_i''} \tag{3.20}$$

where the single and double primes are used to distinguish the two structures. From the above discussion it follows that

$$K_{11}' = K_{11}'' = 0 \tag{3.21}$$

The joint displacements can be described by relative generalized (harmonic) displacement parameters $\{u_i\}$ described earlier. They are related to the harmonic displacement parameters for the two structures as follows:

$$u_i = u_i' - u_i'' \tag{3.22}$$

Then from (3.17) and (3.19) it follows that

$$u_i = \frac{f_i'}{K_{ii}'} - \frac{f_i''}{K_{ii}''} \tag{3.23}$$

This is a consequence of the orthogonality of the set of cosine functions. Similarly joint equilibrium and harmonic function orthogonality requires

$$f_i' = - f_i'' = f_i \tag{3.24}$$

where f_i indicates that the prime will not be required below. Substituting (3.24) into (3.23) and simplifying we obtain

$$u_i = \left(\frac{K_{ii}' + K_{ii}''}{K_{ii}' K_{ii}''} \right) f_i \tag{3.25}$$

or

$$f_i = K_{ii} u_i \tag{3.26}$$

where

$$K_{ii} = \frac{K_{ii}' K_{ii}''}{K_{ii}' + K_{ii}''} \tag{3.27}$$

The parameters K_{ii} describe the effective stiffness associated with the set of harmonics for the axisymmetric structure on both sides of the joint. Let $[K_{ij}]$ be a diagonal matrix with diagonal elements K_{ii}. Then (3.26) can be expressed in the following matrix form

$$\{f_i\} = [K_{ij}] \{u_j\} \tag{3.28}$$

Note that

$$K_{11} = 0 \tag{3.29}$$

Partition equation (3.19) and (3.28) as follows

$$\begin{Bmatrix} f_1 \\ \{f_i\}_2 \end{Bmatrix} = \begin{bmatrix} \bar{S}_{11} & [\bar{S}_{ij}]_{12} \\ [\bar{S}_{ij}]_{21} & [\bar{S}_{ij}]_{22} \end{bmatrix} \begin{Bmatrix} u_1 \\ \{u_j\}_2 \end{Bmatrix} \tag{3.30}$$

$$\begin{Bmatrix} f_1 \\ \{f_i\}_2 \end{Bmatrix} = \begin{bmatrix} 0 & 0 \\ 0 & [K_{ij}]_{22} \end{bmatrix} \begin{Bmatrix} u_1 \\ \{u_j\}_2 \end{Bmatrix} \tag{3.31}$$

From (3.30) and (3.31) we obtain

$$f_1 = \bar{S}_{11} u_1 + [\bar{S}_{ij}]_{12} \{u_j\}_2 \tag{3.32}$$

$$\{f_i\}_2 = [\bar{S}_{ij}]_{21} u_1 + [\bar{S}_{ij}]_{22} \{u_j\}_2 \qquad (3.33)$$

$$\{f_i\}_2 = [K_{ij}]_{22} \{u_j\}_2 \qquad (3.34)$$

From (3.33) and (3.34) we obtain

$$\{u_j\}_2 = \left[[K_{ij}]_{22} - [\bar{S}_{ij}]_{22} \right]^{-1} [\bar{S}_{jk}]_{21} \, u_1 \qquad (3.35)$$

On substituting (3.35) into (3.32) we obtain

$$f_1 = \left(\bar{S}_{11} + [\bar{S}_{ij}]_{12} \left[[K_{jk}]_{22} - [\bar{S}_{jk}]_{22} \right]^{-1} [\bar{S}_{kl}]_{21} \right) u_1 \qquad (3.36)$$

Let A_{11} equal the quantity in brackets. Then (3.36) has the form

$$f_1 = A_{11} \, u_1 \qquad (3.37)$$

The parameter u_1 is a measure of the maximum relative displacement around the circumference. We wish to relate the joint stiffness to more common parameters M and ϕ which correspond to joint bending moment and joint relative rotation. Now u_1 and ϕ are related by

$$u_1 = r\phi \qquad (3.38)$$

where r is defined in Figure 3-2. We will define the relationship between M and f_1 by requiring that the following hold for all virtual displacements δu_1 and $\delta\phi$.

$$M\delta\phi = f_1 \delta u_1 \qquad (3.39)$$

On substituting (3.38) into (3.39) we obtain

$$M\delta\phi = f r \delta\phi \qquad (3.40)$$

For the above to hold for all virtual changes it follows that

$$M = rf \qquad (3.41)$$

On substituting (3.38) into (3.37) and the resultant into (3.41) we obtain

$$M = r^2 A_{11} \phi \tag{3.42}$$

The equivalent joint stiffness designated by H is related by

$$H = r^2 \left(\bar{S}_{11} + [\bar{S}_{ij}]_{12} \left[[K_{jk}]_{22} - [\bar{S}_{jk}]_{22} \right]^{-1} [\bar{S}_{kl}]_{21} \right) \tag{3.43}$$

3.2 TEST CASE AND RESULTS

A computer program which can compute the effective joint stiffness as described above was written. The structural configuration used in the Phase 2 study was used in this study since comparative test data were available. Figure 3-3 describes the joint and Figure 3-4 describes the finite element model of shell elements used in all the NASTRAN analyses.

The NASTRAN computer program was used to compute the longitudinal harmonic stiffness coefficient designated by K'_{ii} and K''_{ii} for the first 108 harmonics. These stiffness coefficients are given in Table 3-1 and a log-log plot of the stiffness coefficient versus harmonic number is given in Figure 3-5.

As can be seen from Figure 3-5 the value of stiffness appears to approach a straight line for higher values of harmonic number. A straight line on a log-log plot implies the following continuous function relationship

$$\frac{K}{K_1} = \left(\frac{n}{n_1}\right)^{\alpha} \tag{3.44}$$

where K is the dependent stiffness variable, n is the independent harmonic number variable, (K_1, n_1) is a point on the line and α is a coefficient related by

$$\alpha = \frac{\mathrm{LOG}\left(\frac{K_2}{K_1}\right)}{\mathrm{LOG}\left(\frac{n_2}{n_1}\right)} \tag{3.45}$$

where (K_2, n_2) is a point on the line. For the two lines in Figure 3-5 associated with the two structures connected by the joint, the data used to compute higher harmonic stiffness coefficients are given in Table 3-2.

Table 3-2

Data Used in Equation (3.44) to Compute Stiffness Coefficients for Harmonics Greater than 108

	Structure 1	Structure 2
K_1	1.57×10^7	4.35×10^7
K_2	3.32×10^8	9.90×10^8
n_1	10	10
n_2	100	100

As pointed out earlier many harmonics do not influence the computation. Table 3-3 shows the harmonics which influence the computations as a function of number of fasteners.

Each bolt has an effective arc length over which it acts. As noted earlier this arc length is defined by the enclosed angle ϵ. Let us define the quantity R as the ratio of ϵ over the angle subtended by the bolt. The R can be interpreted as the effective number of bolt diameters over which the bolt load distributes at the joint.

The larger the value of R the higher the joint stiffness will be. To establish correct values of R computed values of stiffness were compared to measured results obtained in the Phase 2 study. Table 3-4 summarizes the Phase 2 measured values of stiffness.

Table 3-4

Phase 2 Measured Values of Stiffness for Various Numbers of Fasteners ($\times 10^8$ Inch Pounds per Radian)

Number of Fasteners	Stiffness
3	0.358
6	0.971
9	1.680
12	2.573 (interpolated)
18	4.440

Table 3-5 gives computed values of joint stiffness for the three fastener joint, for various values of R and for different values of the highest harmonic used in the calculations. The value of R equal to 6.24 gives results which are almost equal to the measured values. Table 3-6 shows results for 3, 6, 9 and 18 fastener cases using R equal to 6.24. Although the results match the experimental values for the three fastener case, they are quite in error for the 18 fastener case. The compliances of the 18 fastener case for various values of R are given in Table 3-7. As can be seen a value of R close to 1.5 is required if the 18 fastener case is to match measured results. Using a linear interpolation between the compliance values for R equal to 1.5 and 2.0 we conclude that a value of R equal to 1.544 will give a value very close to the measured compliance. Table 3-8 gives results for R equal to 1.544. Since R equal to 6.24 gives correct values for the 3 fastener case and R equal to 1.544 gives correct values for the 18 fastener case, we used a linear interpolation to establish values of R for the 6, 9 and 12 fastener case. Computed joint stiffness for these cases are given in Table 3-9. Figure 3-6 gives curves of stiffness versus number of fasteners of the measured results and of the computed results for R equal to 1.544 and 6.24.

As can be seen from the results described above there does not appear to be a simple way of describing bolt shell interaction. For the joint in question one shell surface overlaps the other and the bolt load acts on the two contacting surfaces. The above results imply that the fewer the bolts the more compliant the joint but the larger the effective contact area between the shells becomes. The results suggest that a more detailed analytical description of the bolt area is required.

Figure 3-7 shows the curve of joint stiffness versus R for the three fastener case. A dashed straight line referred to as the "reference line" is also shown in this figure. Before continuing our discussion of this curve note Figure 3-8 which shows curves of stiffness versus highest harmonic used in the computation for various values of R. In essence these curves show the way in which the cosine series converges. Note that the cosine series converges slower for smaller values of R and that all curves are monotonically decreasing. Now re-examine Figure 3-7. The separation of the curve for low values of R can partly be explained by the slow convergence, i.e., the values shown for the lower values of R are somewhat separated from the values at the point of convergence. The separation from the reference line associated with higher values of R can be explained in a different way. The assumption was made in the derivation that the load distribution along the arc length associated with the bolt load is uniform. This does not introduce very much error for small R however for large R the error is significant.

3.3 CONCLUSIONS

The analysis described here was motivated by the fact that comparable analyses performed using the NASTRAN computer program would have been prohibitive. A joint stiffness analysis performed entirely on NASTRAN during the Phase 2 study cost approximately $300.00 per run for a case which used 12 harmonics. In the present analysis the determination of K' and K" were made once for 109 harmonics using NASTRAN at a cost of $2000.00 and all subsequent runs cost from $0.10 to $0.30. The relatively high cost in generating the K's motivated use of formulas (3.44) for generating higher K values.

One of the problems with using NASTRAN to solve the complete problem is that one would have to use all the harmonics up to the highest one used. One could not exclude harmonics. Thus a run using the present method which used up to harmonic number 400 and costing $0.30 would have cost in excess of $5000.00 if done directly on NASTRAN. In the present study over 100 runs were made at a modest cost.

An unexpected problem was the one associated with selecting an appropriate bolt load distribution parameter (R). The effective load path area for each fastener in the shear bolt joint analyzed appears to decrease as the number of fasteners increases. It should be noted, however, that joint compliance estimates within 10 to 20 percent will in most cases be more than adequate for missile modal analysis purposes. Accuracy in compliance estimates is more important for compliant joints which have a greater influence on airframe modal characteristics than for stiff joints which have little effect on airframe response characteristics.

A useful effort which was not attempted in this study would be to develop a simple expression for estimating K_1, n_1, and α used in equation (3.44). Such an expression would allow the determination of joint compliance for shells of revolution.

TABLE 3-1 NASTRAN Computed Stiffness Coefficients for the Structure on Each Side of the Joint for 108 Harmonics (amts x 10^8 pounds per inch)

	Structure 1	Structure 2		Structure 1	Structure 2		Structure 1	Structure 2
1	0.04291	0.06535	37	0.95935	2.66935	73	2.12083	6.30799
2	0.04239	0.08109	38	0.98724	2.75904	74	2.15987	6.42760
3	0.04219	0.11913	39	1.01313	2.84877	75	2.19932	6.54837
4	0.04415	0.06769	40	1.04307	2.93862	76	2.23918	6.67031
5	0.05090	0.21266	41	1.07109	3.02867	77	2.27945	6.79342
6	0.06247	0.24588	42	1.09974	3.11901	78	2.32014	6.91770
7	0.07684	0.48946	43	1.12753	3.20969	79	2.36125	7.04316
8	0.08313	0.30330	44	1.15600	3.30079	80	2.40277	7.16979
9	0.11140	0.33731	45	1.18467	3.39238	81	2.44471	7.29760
10	0.13189	0.37756	46	1.21356	3.48451	82	2.48706	7.42659
11	0.15477	0.42459	47	1.24271	3.57724	83	2.52984	7.55677
12	0.18000	0.47815	48	1.27211	3.67062	84	2.57303	7.68813
13	0.20748	0.53858	49	1.30180	3.76470	85	2.61664	7.82067
14	0.23698	0.60538	50	1.33178	3.85953	86	2.66068	7.95439
15	0.26821	0.67771	51	1.36207	3.95515	87	2.70513	8.08928
16	0.33244	0.75520	52	1.39268	4.05158	88	2.75000	8.22535
17	0.33442	0.83705	53	1.42362	4.14888	89	2.79530	8.36258
18	0.36869	0.92249	54	1.45490	4.24706	90	2.84102	8.50097
19	0.40330	1.01082	55	1.48653	4.34616	91	2.88716	8.64049
20	0.43800	1.10136	56	1.51851	4.44621	92	2.93373	8.78115
21	0.47251	1.19358	57	1.55085	4.54722	93	2.98072	8.92287
22	0.50669	1.28663	58	1.58356	4.64922	94	3.02810	9.06563
23	0.54040	1.38028	59	1.61664	4.75223	95	3.07597	9.20931
24	0.57356	1.47360	60	1.65010	4.85627	96	3.12423	9.35370
25	0.60612	1.37804	61	1.68394	4.96135	97	3.17292	9.49853
26	0.63806	1.66562	62	1.71816	5.06749	98	3.22203	9.64273
27	0.66940	1.75835	63	1.75278	5.17471	99	3.27157	9.78316
28	0.70015	1.85126	64	1.78778	5.04321	100	3.32153	9.89900
29	0.73036	1.94382	65	1.82318	5.39240	101	3.37193	10.26364
30	0.76009	2.03090	66	1.85898	5.50289	102	3.42274	10.29839
31	0.78938	2.12750	67	1.89517	5.61450	103	3.47399	10.43826
32	0.81829	2.21863	68	1.93102	5.72724	104	3.52566	10.58834
33	0.84690	2.30934	69	1.96877	5.84112	105	3.57776	10.74234
34	0.70160	2.39970	70	2.00617	5.95611	106	3.63029	10.89874
35	0.90340	2.48976	71	2.04398	6.07225	107	3.68329	11.05698
36	0.93142	2.57962	72	2.08220	6.18955	108	3.73663	11.21680

TABLE 3-3 Harmonics Having Non Zero Stiffness Coefficients for the Varicus Fastener Arrangements

Number Of Fasteners									
3		6		9		12		18	
2	40	5	79	8	118	11	157	17	235
4	41	7	83	10	125	13	167	19	251
5	43	11	85	17	127	23	169	35	253
7	44	13	89	19	134	25	179	37	269
8	46	17	91	26	136	35	181	53	271
10	47	19	95	28	143	37	191	55	287
11	49	23	97	35	145	47	193	71	289
13	50	25	101	37	152	49	203	73	305
14	52	29	103	44	154	59	205	89	307
16	53	31	107	46	161	61	215	91	323
17	55	35	109	53	163	71	217	107	325
19	56	37	113	55	170	73	227	109	341
20	58	41	115	62	172	83	229	125	343
22	59	43	119	64	179	85	239	127	359
23	61	47	121	71	181	95	241	143	361
25	62	49	125	73	188	97	251	145	377
26	64	53	127	80	190	107	253	161	379
28	65	55	131	82	197	109	263	163	395
29	67	59	133	89	199	119	265	179	397
31	68	61	137	91	206	121	275	181	413
32	70	65	139	98	208	131	277	197	415
34	71	67	143	100	215	133	287	199	431
35	73	71	145	107	217	143	289	215	433
37	74	73	149	109	224	145	299	217	449
38	76	77	151	116	226	155	301	233	451

TABLE 3-5 Computed Joint Stiffness for Three Fasteners and Various Values of the Ratio of ϵ over the Bolt Diameter Enclosed Angle ($x10^7$ inch pound per radian)

Highest Harmonic	R(Values of ϵ Over Bolt Diameter Enclosed Angle)							
	½	1	3	5	6	6.2	6.24	10
1	10388.0	10387.0	10378.0	10359.0	10345.0	10342.7	10342.2	10270.0
3	12.6700	12.6730	12.7050	12.7760	12.8372	12.8372	12.8851	13.1129
6	5.1253	5.1308	5.1905	5.3076	5.3955	5.4142	5.4183	5.9090
9	3.8632	3.8708	3.9532	4.1160	4.2386	4.2347	4.2703	4.9572
12	3.3277	3.3374	3.4449	3.6567	3.8157	3.8496	3.8567	4.7262
15	3.0494	3.0618	3.1941	3.4531	3.6449	3.6855	3.6941	4.6893
18	2.8862	2.9009	3.0572	3.3584	3.5769	3.6225	3.6321	4.6884
36	2.4698	2.5013	2.8092	3.2721	3.5359	3.5865	3.5971	4.6569
64	2.2466	2.3132	2.7897	3.2592	3.5231	3.5741	3.5848	4.6497

Table 3-6

Computed Equivalent Joint Stiffness (x 10^8 inch pound per radian) for 3, 6, 9, 18 Fasteners. All Computations Use 6.24 for the Value of ϵ Over the Bolt Diameter Enclosed Angle

Highest Harmonic	3	6	9	18
1	1034.22	2068.40	3102.62	6205.2
3	1.28851	- -	- -	- -
6	.54183	2.0828	- -	- -
9	.42703	- -	4.3292	- -
12	.38567	1.1690	- -	- -
15	.36941	- -	- -	- -
18	.36321	1.0632	2.5469	48.734
36	.35971	1.0470	2.4721	31.067
54	- -	- -	2.4547	29.7569
64	.35848	- -	- -	- -
72	- -	1.0412	2.4509	29.589
109	- -	1.0406	2.4486	29.356

Table 3-7

Computed Joint Stiffness for Eighteen Fasteners and Various Values of the Ratio of ϵ over the Bolt Diameter Enclosed Angle (x 10^8 inch pounds per radian)

Highest Harmonic	Values of ϵ Over Bolt Diameter Enclosed Angle			
	0.5	1.0	1.5	2.0
1	6232.9	6232.0	6230.2	6230.2
17	10.9580	11.2330	-	-
35	5.0374	5.2411	-	-
53	4.0392	4.3071	-	-
71	3.5954	3.9403	-	-
109	3.1513	3.6822	-	-
181	2.9575	-	4.4163	5.2684
253	2.9178	-	4.4128	5.2620
325	2.9140	-	4.4092	5.2597

Table 3-8

Computed and Measured Equivalent Joint Stiffness ($\times 10^8$ Inch Pounds per Radian) for 3, 6, 9, 12, and 18 Fasteners. All computations use 1.544 for the value of R.

Number of Fasteners	Highest Harmonic Number	Computed Joint Stiffness	Measured Joint Stiffness
3	55	.2445	.358
6	109	.6089	.971
9	163	1.163	1.680
12	217	1.962	2.573*
18	325	4.480	4.440

*Interpolated

Table 3-9

Computed Equivalent Joint Stiffness
($\times 10^8$ Inch Pounds per Radian)

Number of Fasteners	Highest Harmonic Number	R	Computed Stiffness	Test Data
3	55	6.240	0.3585	0.358
6	109	5.301	0.9430	0.971
9	163	4.361	1.8306	1.680
12	217	3.422	2.9524	2.573*
18	325	1.544	4.4798	4.440

*Interpolated

FIGURE 3-3

SHEAR BOLT JOINT

TEST SPECIMEN AND SECTION MODELED USING FINITE ELEMENTS

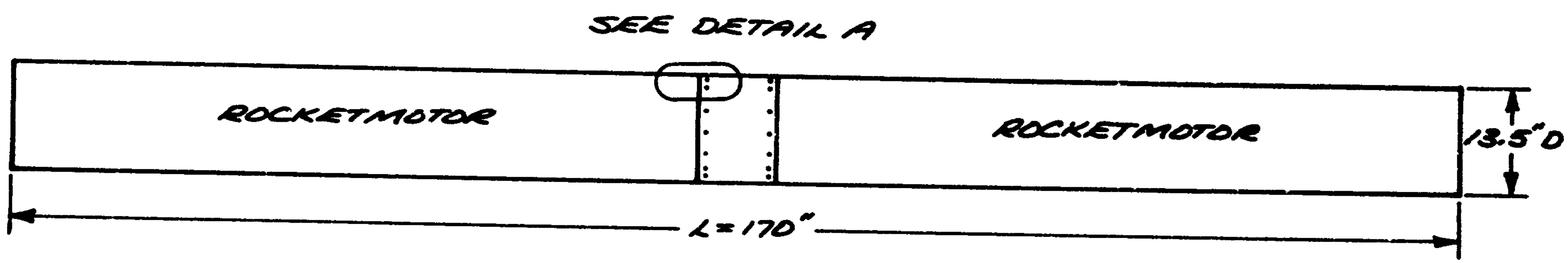

TEST SPECIMEN

DETAIL A

SECTION MODELED WITH FINITE ELEMENTS

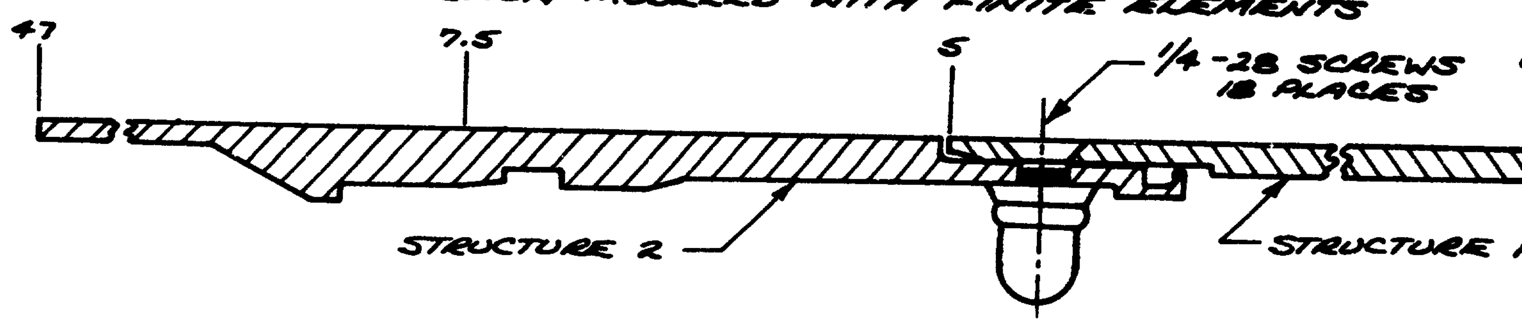

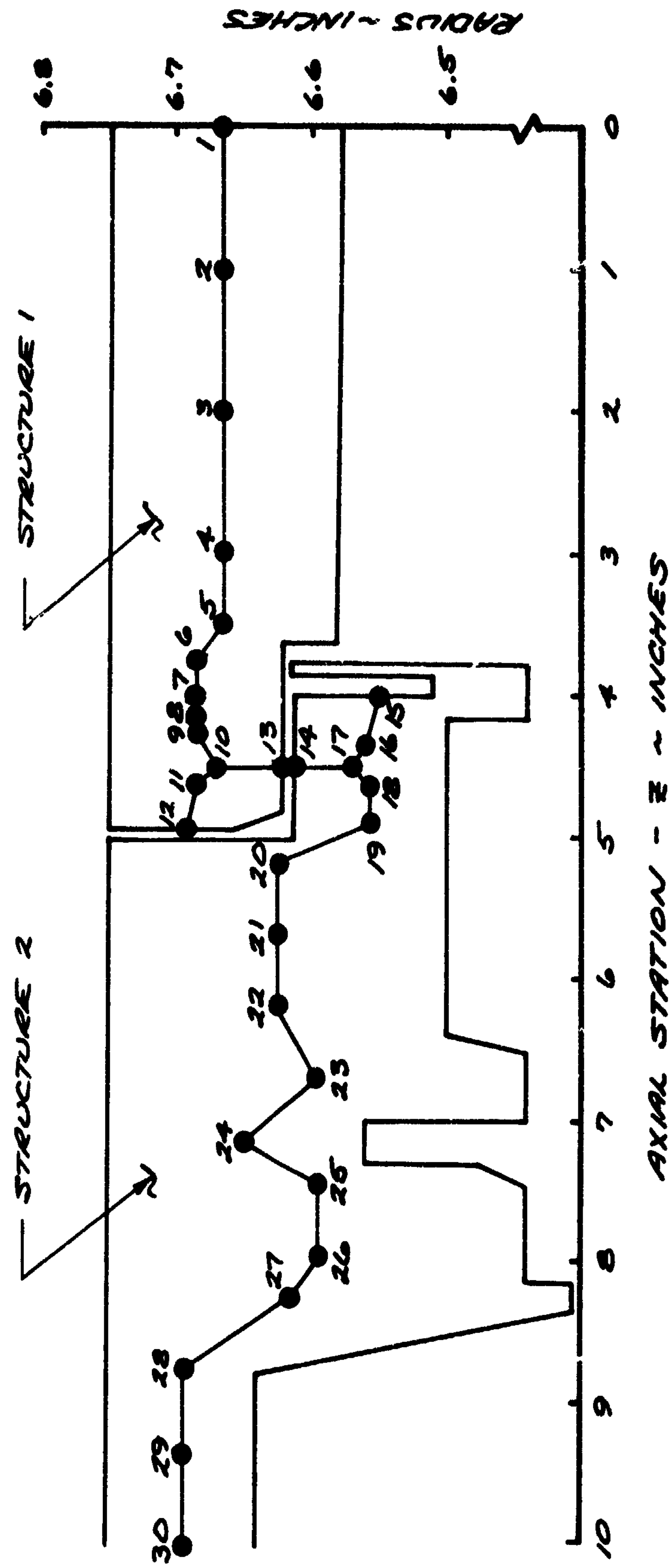

FIGURE 3-4

SHELL ELEMENT MODEL IN THE REGION OF THE SHEAR BOLT JOINT

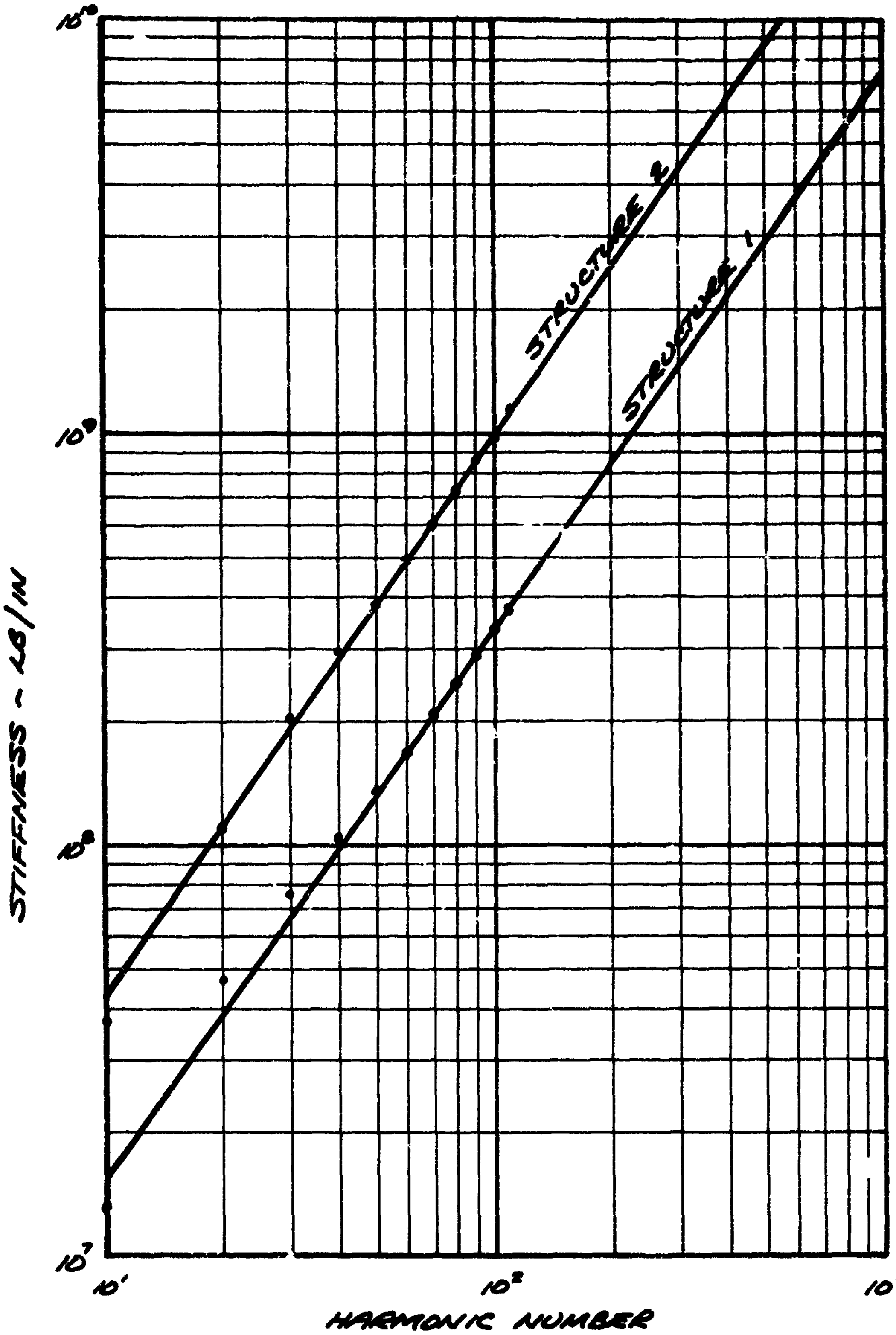

FIGURE 3-5 LOG-LOG PLOTS OF NASTRAN COMPUTED STIFFNESS COEFFICIENTS VERSUS HARMONIC NUMBER FOR THE TWO STRUCTURES

FIGURE 3-6

CURVE OF STIFFNESS VERSUS NUMBER OF FASTENERS FOR R = 1.544, R = 6.24 AND MEASURED RESULTS

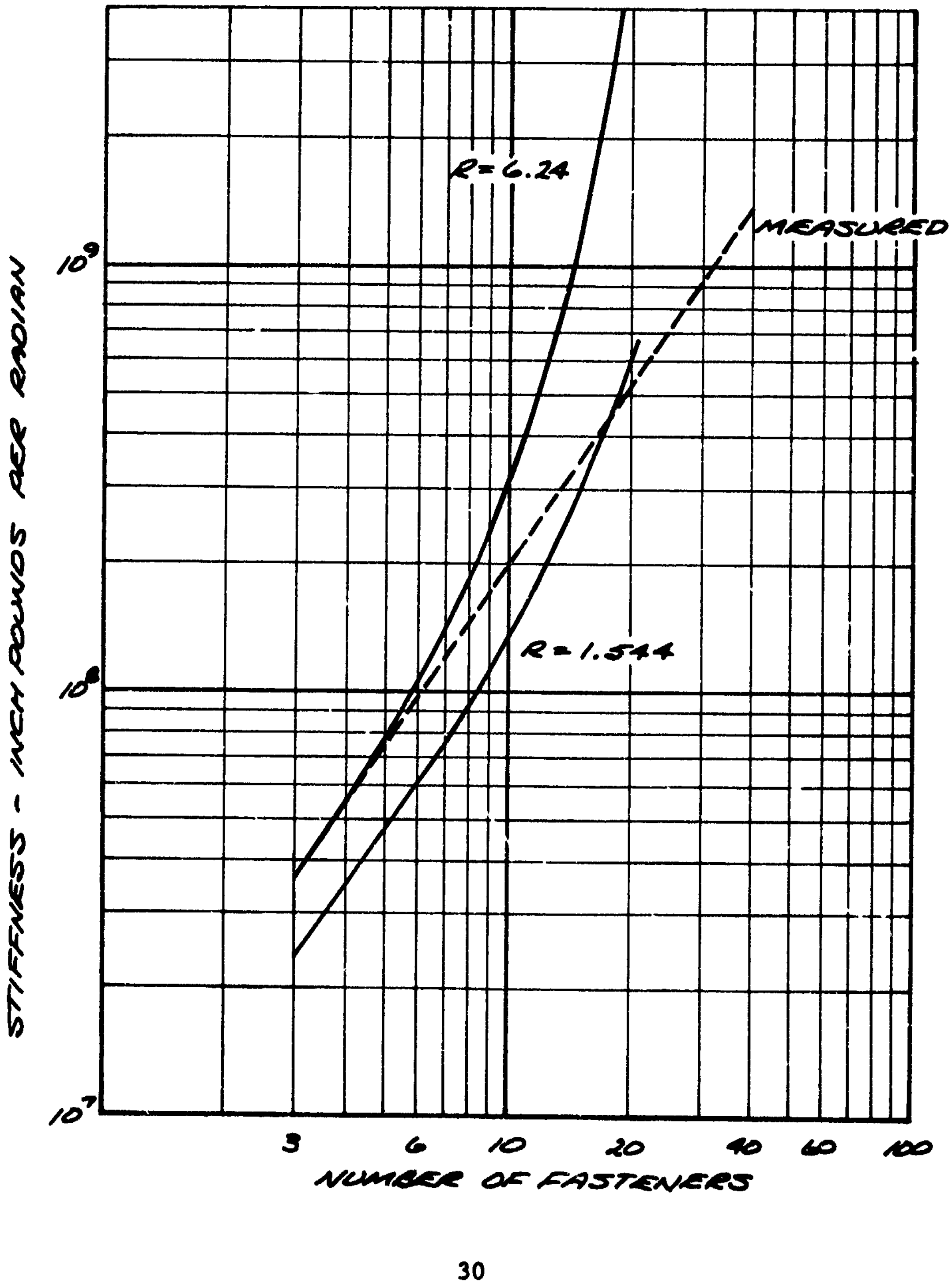

FIGURE 3-7

CURVE OF JOINT STIFFNESS VERSUS R (RATIO OF ε OVER THE BOLT DIAMETER ENCLOSED ANGLE) FOR THE THREE FASTENER CASE.

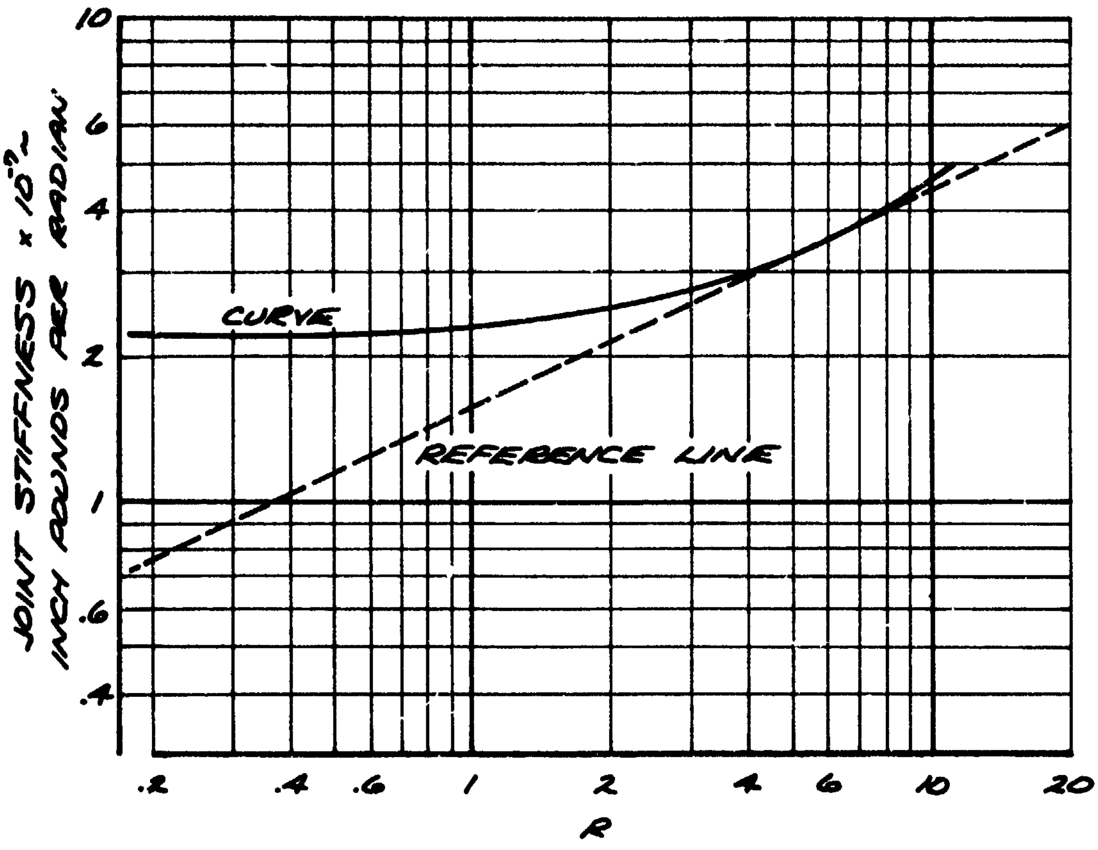

FIGURE 3-8

CURVES OF COMPUTED JOINT STIFFNESS VERSUS HIGHEST HARMONIC FOR THREE FASTENER JOINT AND VARIOUS VALUES OF R (RATIO OF E OVER BOLT DIAMETER ENCLOSED ANGLE.)

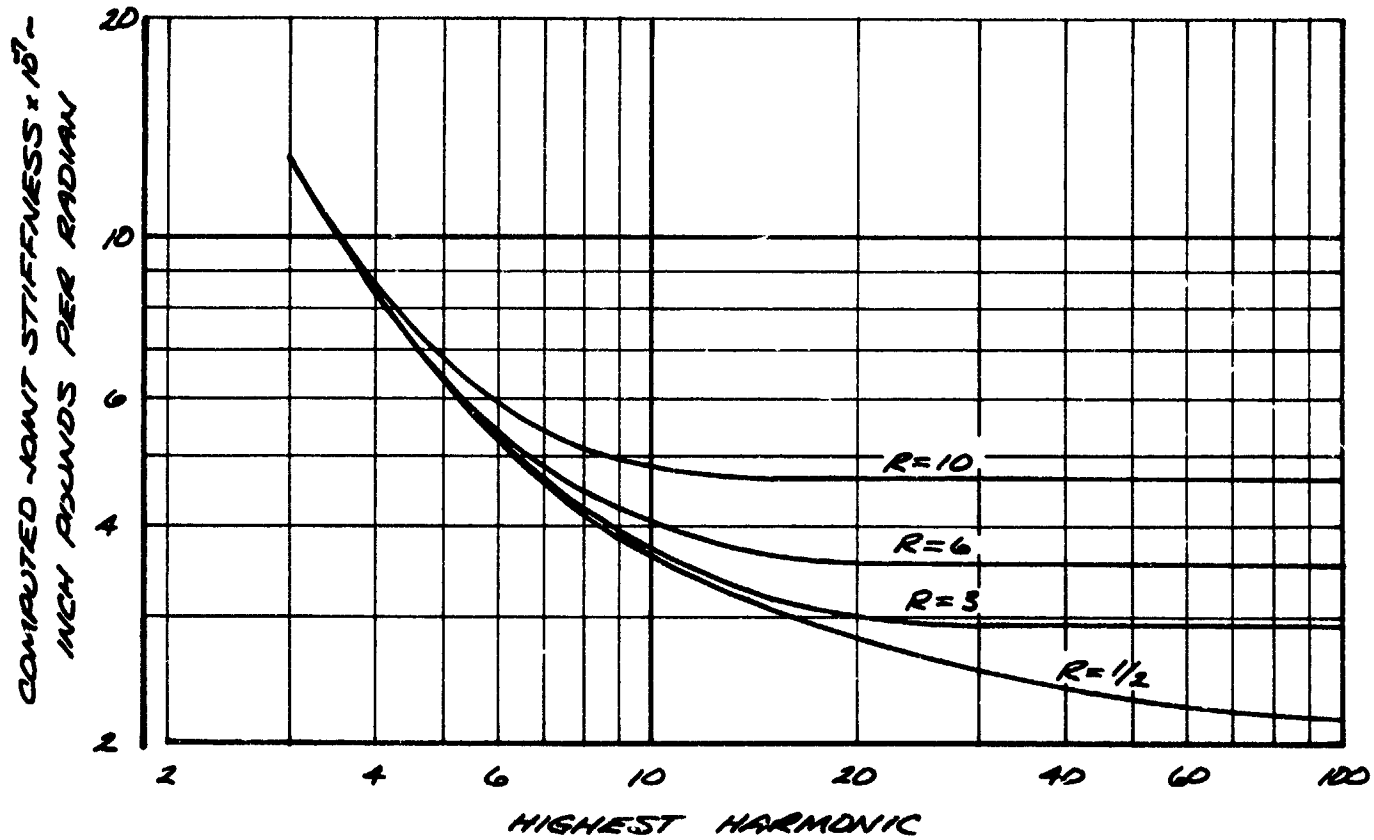

Section 4.0

JOINT COMPLIANCE EXTRACTION TECHNIQUE DEVELOPMENT

Tactical missile joint compliances often represent one of the major uncertainties in developing an acceptable analytical model for dynamic response studies. This uncertainty tends to be reinforced if large differences are discovered between theoretical and experimental mode shapes and frequencies. If one assumes that errors in assumed joint compliances are totally responsible for the theory/test mismatch, then a method of solution for effective joint compliances is suggested through an iterative "best fit" between modal analysis and modal test data. Since distributed mass and missile airframe stiffness parameters are generally well defined, the assumption that all errors lie in the effective joint compliances is not usually unreasonable. For many years at the Pomona Division of General Dynamics a somewhat arbitrary trial and error "hand tuning" procedure was employed to arrive at a set of joint compliances which would yield an acceptable fit between analysis and test data. This procedure can become quite time consuming and cumbersome, however, when more than two or three unknown joint compliances are involved.

A joint compliance extraction technique was developed during Phase 1 of the study of structural dynamic properties of tactical missile joints (Reference 1). It utilized a steepest-descent method to solve for variable unknown spring rates based upon a weighted best fit match between experimental and theoretical mode shapes and natural frequencies. The method was tailored specifically to beam representations of missile structures. Unfortunately, the method as implemented had several limitations. One of the restrictions was that the number of modes used had to equal or exceed the number of unknown joints to obtain meaningful results. Also, only bending cases with free-free boundary conditions could be run, and no method of handling appendages had been devised.

Late in the Phase 1 study, a general method for estimating structural parameters from dynamic test data appeared in Reference 4 which looked promising for use in the extraction of missile airframe joint compliances. Subsequently this method was applied in Phase 2 to simple test cases with encouraging results. As confidence was gained in the optimization method, the method was programmed for use with a Control Data Corporation 6400 computer. Originally only first order gradient terms were used. The first order gradient method worked well with a small (two degree of freedom) system, but was inadequate for larger systems. Next a second order gradient method in which the second order terms were approximated by differences was tried and techniques developed to improve convergence of the method. The resulting computer program is called program JOINTS.

During the present and final phase of this study (Phase 3) a number of program refinements and improvements have been introduced and evaluated. These program additions include the following:

1. A time saving option is provided for generation of "Standard" weighting factors which weights all test mode shapes and frequencies equally. Provision still exists, of course, for input of alternate weighting factors if preferred.

2. Program logic has been added to preclude missing or skipping over needed theoretical modes by assuring theoretical/test mode correspondence both in number of nodes and polarity. This prevents sizable errors which can result from mode mismatching and avoids numerous program restarts, thus saving turn around time between computer runs.

3. An option is offered to use a greater number of theoretical modes than experimental modes in the calculation of the gradients of the cost function. This feature aids solution convergence when only a few experimental modes are available.

4. An interpolation/extrapolation program called FILLIN has been added which takes experimental modal data at any arbitrary set of test missile stations and generates modal displacement and slope data at missile stations consistent with the lumped parameter modal analysis model. This operation offers a substantial labor savings in the preparation of input data for the joint compliance extraction program.

Section 4.1 presents the theory that program JOINTS is based upon. Rationale in selecting iteration bite size and the considerations involved in choosing experimental mode shape and frequency weighting factors are discussed in Section 4.2 together with a review of some of the results obtained with a hypothetical test case during the Phase 2 study. Section 4.3 presents a discussion and summary of the new program features added during the present phase and Section 4.4 offers a program application test case based on a set of actual tactical missile modal test data. The joint compliance extraction technique user's manual, including a listing of the programs, and appropriate test cases are presented in the Appendix.

4.1 METHOD OF ANALYSIS

The joint compliance extraction technique is designed to determine mechanical joint compliances of an elastic missile structure by generating the "best" least square fit between a linear lumped parameter mathematical model and a given set of experimental modal data. A major assumption in the method is that the joint compliances constitute the principal unknowns in the lumped parameter system, with both distributed mass and stiffness being precisely defined. Weighting factors which involve mode number, shape, and frequency acknowledge the existence of accuracy limitations in the test data. The joint compliances yielding a best fit are found by minimizing a quadratic function of the differences between corresponding theoretical and experimental eigenvalues and eigenvectors. This function, referred to as the cost function, is expressed as follows:

$$F = \frac{1}{2} \sum_{i=1}^{N_1} \left\{ W_{if} \left(\omega_{ie}^2 - \omega_{it}^2 \right)^2 + \left(\underline{X}_{ie} - \underline{X}_{it} \right)^T W_{ix} \left(\underline{X}_{ie} - \underline{X}_{it} \right) \right\} \quad (4.1)$$

The frequencies and mode shapes are denoted by ω and $\underline{X}$, respectively. The weighting factor matrix is W and the index i is the mode number. If the mode shape slopes are used, they are treated as additional components of the $\underline{X}$'s. The subscripts e and t denote experimental and theoretical values, respectively. The minimization of the cost function constitutes a nonlinear programming problem which is the subject of this section. Optimization problems not amenable to standard methods are more the rule than the exception. In this case the optimization is accomplished by a steepest descent method especially developed for this study. The basic concept originally appeared in Reference 4. Before proceeding with a detailed discussion of the method, the structural mathematical model utilized will be described.

4.1.1 System Model. The fundamental structural dynamic considerations of a tactical missile are often handled with a linear lumped parameter mathematical model. The one used in this study is typical. More expressly, the mathematical model simulates a beam-like body with a series of lumped masses connected by weightless beams. Discrete shear, compressive; torsional, and flexural springs may be included at any point in the model. The model can be used to analyze bending, torsion, and longitudinal motion. The model contains provisions for including appendages attached to the main body at arbitrary angles with arbitrary attachment springs. The appendages are modeled similarly to the main body. The boundary value problem that results from this representation can be expressed as an eigenvalue problem:

$$\left[K - \omega_{it}^2 M \right] X_{it} = 0 \qquad i = 1, 2, \cdots N \quad (4.2)$$

where M and K are mass and stiffness matrices, respectively. The subroutine within the computer program which solves the eigenvalue problem uses the Holzer-Myklestad method. This numerical method utilizes transfer matrices from point to point on the model and finds the eigenvalues by satisfying the boundary conditions using an iterative procedure. A complete description of the method is found in Reference 5. Limitations of the method and economy preclude extraction of all N modes where N is typically 50 to 200. It will be seen later that the lack of a complete set of modes introduces approximations into the optimization method and necessitates modifications.

4.1.2 Solution Method. The "best fit" values of the joint compliances, defined in a least square error sense, are determined by minimizing the cost function which is accomplished with a modified steepest descent method. Steepest descent or gradient methods as they are also known, iteratively converge on the location of the minimum, since an analytical solution of the condition for an extremum, $\nabla F = 0$, is not possible. The successive estimates of the minimizing values of the independent variables, in this case a vector the components of which are the unknown spring rates of the structural joints $\underline{k}$, are

$$\underline{K}^{(n+1)} = \underline{K}^{(n)} - \theta \nabla F \Big|_{\underline{K}^{(n)}} \quad (4.3)$$

The superscript indicates the number of the estimate. If the quantity θ is a constant, the algorithm is a first order method commonly referred to as the steepest descent method. It is based on the intuitive notion that if one proceeds in the direction of the steepest descent, which Equation 4.3 does, in small steps one must arrive at a local minimum. It can also be proven rigorously (Reference 6). A very efficient second order method may be derived by applying the Newton-Raphson algorithm to the gradient of the cost function which yields the successive approximation,

$$\underline{K}^{(n+1)} = \underline{K}^{(n)} - S \left[\frac{\partial^2 F}{\partial K_i \, \partial K_j} \right] \nabla F \Big|_{\underline{K}^{(n)}} \quad (4.4)$$

The matrix of second partial derivatives must be non-singular. Theoretically, the step size, S, is a scalar. However, in this study, it was necessary to generalize its definition. Equation 4.4 serves as the basis for the algorithm developed. The reasons for the modifications that were necessary will be explained as they are encountered.

The j^{th} component of the gradient of the cost function is

$$\frac{\partial F}{\partial K_j} = \sum_{i=1}^{N_1} \left\{ W_{if} \left(\omega_{it}^2 - \omega_{ie}^2 \right) \frac{\partial \omega_{it}^2}{\partial K_j} + \left(\underline{X}_{it} - \underline{X}_{ie} \right)^T W_{ix} \frac{\partial \underline{X}_{it}}{\partial K_j} \right\} \quad (4.5)$$

where k_j is the jth unknown spring rate. In order to calculate the partial derivatives of the eigenvalues and eigenvectors with respect to the k_j's, a departure was made from Reference 4. Here the modes were normalized to unity with respect to the generalized mass M,

$$\underline{X}_{it}^{T} M \underline{X}_{jt} = \delta_{ij} \tag{4.6}$$

Also a joint compliance positioning matrix, K^j, is introduced which locates the unknown spring rates within the full spring matrix -

$$K = \bar{K} + \sum_{j=1}^{N_J} K^{j} k_j \tag{4.7}$$

$\bar{K}$ is the matrix of known spring elements. Because of the peculiarities of the method used to solve the eigenvalue problem, the spring matrix, K, is not directly available and so neither are the variable spring positioning matrices, the K^j's. However, they can be derived by considering the strain energy stored in the jth spring. For simplicity, assume that a separate spring rate is assigned to each joint. Then the strain energy associated with the jth spring is:

$$U_j = \frac{1}{2} k_j \left('x_j - x_j' \right)^2 \tag{4.8}$$

where $'x_j$ and x_j' are the slopes to the left and to the right of the joint for the case of a rotational spring. The strain energy is also $U_j = 1/2 k_j \underline{x}'^T K^j \underline{x}'$. Equating the two expressions and then the coefficients of like terms, it can be deduced that the matrix, Kj, must be the null matrix except for a submatrix,

$$\begin{pmatrix} 1 & -1 \\ -1 & 1 \end{pmatrix} \tag{4.9}$$

corresponding to the coordinates on either side of the joint. Then according to Reference 7 the partial derivatives are

$$\frac{\partial \omega_{it}^2}{\partial k_j} = \underline{X}_{it}^{T} K^{j} \underline{X}_{it} \tag{4.10a}$$

$$\frac{\partial \underline{X}_{it}}{\partial k_j} = \sum_{\ell \neq i}^{N} \frac{\underline{X}_{\ell t}^{T} K^{j} \underline{X}_{it}}{\omega_{it}^2 - \omega_{\ell t}^2} \underline{X}_{\ell t} \tag{4.10b}$$

Equations (4.10a) and (4.10b) can be expanded in terms of components of the normal coordinates by utilizing the strain energy relationship for each joint.

$$\frac{\partial \omega_{it}^2}{\partial K_j} = x_{it,mj}\left(x_{it,mj} - x_{it,mj+1}\right) + x_{it,mj+1}\left(-x_{it,mj} + x_{it,mj+1}\right)$$

$$= \left(x_{it,mj} - x_{it,mj+1}\right)^2 \qquad (4.11a)$$

$$\frac{\partial \underline{X}_{it}}{\partial K_j} = \sum_{\ell \neq i}^{N} \left(\omega_{it}^2 - \omega_{\ell t}^2\right)^{-1} \left\{ x_{\ell t,mj}\left(x_{it,mj} - x_{it,mj+1}\right)\right.$$

$$\left. + x_{\ell t,mj+1}\left(-x_{it,mj} + x_{it,mj+1}\right)\right\} \underline{X}_{\ell t} \qquad (4.11b)$$

where the indices mj and $mj+1$ refer to the components of the normal coordinates to the left and right of the jth joint respectively. The partial derivatives of the mode shapes were derived using the second formulation of Reference 7 which requires a complete set of theoretical modes. As pointed out previously the sum has to be truncated for reasons of accuracy and economy. This is usually the case in dynamic problems. Here the justification is a posteriori. The number of therotical modes used in the computation of their derivatives is an option to be selected by the user.

$$\frac{\partial \underline{X}_{it}}{\partial K_j} \cong \sum_{\ell \neq i}^{N_1} \frac{\underline{X}_{\ell t}^T K^j \underline{X}_{it}}{\omega_{it}^2 - \omega_{\ell t}^2} \underline{X}_{\ell t} \qquad (4.12)$$

The second partial derivative of the cost function with respect to the unknown spring rates, k_q and k_j, is

$$\frac{\partial^2 F}{\partial K_q \partial K_j} = \sum_{i=1}^{N_1} \left\{ W_{if}\left[\frac{\partial \omega_{it}^2}{\partial K_q}\frac{\partial \omega_{it}^2}{\partial K_j} + \left(\omega_{it}^2 - \omega_{ie}^2\right)\frac{\partial^2 \omega_{it}^2}{\partial K_q \partial K_j}\right]\right.$$

$$\left. + \frac{\partial \underline{X}_{it}^T}{\partial K_q} W_{ix} \frac{\partial \underline{X}_{it}}{\partial K_j} + \left(\underline{X}_{it} - \underline{X}_{ie}\right)^T W_{ix} \frac{\partial^2 \underline{X}_{it}}{\partial K_q \partial K_j}\right\} \qquad (4.13)$$

The second partials of the eigenvalues and mode shapes are

$$\frac{\partial^2 \omega_{it}^2}{\partial K_q \partial K_j} = \frac{\partial X_{it}^T}{\partial K_q} K^j X_{it} + X_{it}^T K^j \frac{\partial X_{it}}{\partial K_q} \tag{4.14a}$$

$$\frac{\partial^2 X_{it}}{\partial K_q \partial K_j} \cong \sum_{\ell \neq i}^{N_i} (\omega_{it}^2 - \omega_{\ell t}^2)^{-1} \Bigg\{ \Bigg[-(\omega_{it}^2 - \omega_{\ell t}^2)^{-1} \left(\frac{\partial \omega_{it}^2}{\partial K_q} - \frac{\partial \omega_{\ell t}^2}{\partial K_q} \right) X_{\ell t}^T K^j X_{it}$$

$$+ \frac{\partial X_{\ell t}^T}{\partial K_q} K^j X_{it} + X_{\ell t}^T K^j \frac{\partial X_{it}}{\partial K_q} \Bigg] X_{\ell t}$$

$$+ X_{\ell t}^T K^j X_{it} \frac{\partial X_{\ell t}}{\partial K_q} \Bigg\} \tag{4.14b}$$

During Phase 2 it was felt that direct calculation of the second partial derivatives of the eigenvalues and eigenvectors using the above equations were prohibitive because of computer memory size limits. It was subsequently realized that direct calculation of the second partial derivatives is very likely economically feasible since many of the terms are zero. However, since only a small number of unknown missile joints are assumed, the method employed in program JOINTS approximates the second partials by taking differences of the first partials. Such a numerical process tends to be accuracy sensitive and demands careful monitoring. Without resorting to double precision arithmetic, the step size must be large enough to yield a sufficient number of significant figures . On the other hand, too large a step size may enclose a region too large for the cost function to be represented by a quadratic. The procedure settled upon was the following. Using the current estimate $\underline{k}^{(n)}$, the gradient of the cost function is computed with Equations (4.5), (4.11a) and (4.12). The current estimates of the unknown springs are successively incremented one at a time in the direction dictated by the corresponding component of the gradient:

$$K_j'^{(n)} = K_j^{(n)} \left[1 - r \cdot SGN \left(\frac{\partial F}{\partial K_j} \bigg|_{K^{(n)}} \right) \right] \tag{4.15}$$

The relative increment, r, is the same for all the unknown spring rates and fixed for a particular problem. The gradient is calculated at $\underline{k}'^{(n)}$ and the ratios of the differences of the respective components and the spring rate increments are computed. In order to improve the estimates of the second partial derivatives, corresponding off-diagonal estimates which theoretically should be equal are averaged as indicated below.

$$\frac{\partial^2 F^{(n)}}{\partial K_i \partial K_j} = \frac{\partial^2 F^{(n)}}{\partial K_j \partial K_i} \approx \frac{1}{2} \left\{ \left(K_i'^{(n)} - K_i^{(n)}\right)^{-1} \left[\frac{\partial F^{(n)}}{\partial K_j}\right]_{K_i}^{K_i'} \right. \tag{4.16}$$

$$\left. + \left(K_j'^{(n)} - K_j^{(n)}\right)^{-1} \left[\frac{\partial F^{(n)}}{\partial K_i}\right]_{K_j}^{K_j'} \right\}$$

The Hessian, the matrix of second partial derivatives, is then inverted. The correction terms in Equation (4.4) are computed using a value of 1.0 for S. The sign and magnitude of each correction component are compared to those of the increment used to estimate the second partials. If the signs agree or if the magnitude is less than 2-1/2% of the current spring rate, the second order correction is utilized. If not, equation (4.15) is used. If the new spring rates, $\underline{k}^{(n+1)}$, result in an increase in the cost function, the correction terms to $\underline{k}^{(n)}$ are halved repeatedly until a decrease in the cost function is obtained. In any case, each variable spring rate is kept within prespecified limits. These procedures which taken together may be considered a complicated method of selecting a varying step size, S, evolved heuristicly. Modifications which can be made to improve them and put them on a more rigorous basis are possible.

4.2 SPECIAL PARAMETERS

This section discusses two of the parameters important to the proper functioning of the method of solution. Both of these parameters are input quantities in the present version of Program JOINTS. These parameters are the set of weighting factors and the step size - r.

4.2.1 Weighting Factors. Ideally the weighting in the cost function should reflect both the relative accuracy of the experimental data and the relative importance of the information to be obtained from applications of the mathematical model. Often for missiles constructed with thin cylindrical shells, the experimental data will diverge from beam behavior in progressively higher modes. For many dynamic analyses (such as dynamic loads analyses and autopilot elastic mode coupling analyses), the contribution of the higher modes is less significant than the lower modes. If the above conditions hold for any given problem, then the weighting factors should decrease in some way with increasing mode number.

A derivation of the weighting factors is now developed. The cost function (Equation 4.1) may be broken down into two terms (mode shape and frequency) for each mode

$$F_i = F_{if} + F_{ix} \tag{4.17}$$

where

$$F_{if} = \frac{1}{2} W_{if} \left(\omega_{ie}^2 - \omega_{it}^2 \right)^2 \tag{4.18}$$

$$F_{ix} = \frac{1}{2} \left(\underline{X}_{ie} - \underline{X}_{it} \right)^T W_{ix} \left(\underline{X}_{ie} - \underline{X}_{it} \right) \tag{4.19}$$

Rewriting F_{ix} as a summation yields

$$F_{ix} = \frac{1}{2} W_{ix} \sum_{k} \left(\underline{X}_{ie_k} - \underline{X}_{it_k} \right)^2 \tag{4.19a}$$

To see the size of terms produced in the cost function by an error in the eigenvalue or eigenvector, a relative error of size ϵ is assumed in each of the measured quantities. Then the cost function terms will be equated by proper selection of weighting factors. That is, an error of ϵ will be assumed in both ω^2 and X, and weighting factors will then be found which give equal size terms in the cost function. If the theoretical eigenvalues and eigenvectors are assumed correct, then an error of ϵ in the eigenvalue can be written as

$$\omega_{it}^2 = (1+\epsilon)\, \omega_{ie}^2 \tag{4.20}$$

The frequency terms in the cost function become

$$F_{if} = \frac{1}{2} W_{if} \left[\omega_{ie}^2 - (1+\epsilon)\, \omega_{ie}^2 \right]^2$$

$$F_{if} = \frac{1}{2} W_{if} \left[-\epsilon\, \omega_{ie}^2 \right]^2$$

$$F_{if} = \frac{1}{2} W_{if}\, \epsilon^2 \omega_{ie}^4 . \tag{4.21}$$

This means that an error of ϵ in the eigenvalue will produce a residual term in the cost function proportional to the product of the fourth power of the frequency and the square of the error. Considering the same error applied to the mode shape contribution to the cost function yields

$$F_{ix} = \frac{1}{2} W_{ix} \sum_{\ell} \left[X_{ie_\ell} - (1+\epsilon) X_{ie_\ell} \right]^2$$

$$F_{ix} = \frac{1}{2} W_{ix} \sum_{\ell} \epsilon^2 X_{ie_\ell}^2 \tag{4.22}$$

The above equation shows that an error of ϵ in the eigenvector will produce a residual term in the cost function proportional to the product of the square of the eigenvector and the square of the error. Since the mode shapes are normalized to a unity generalized mass, then

$$1 = \sum_{\ell} m_\ell X_{ie_\ell}^2 \tag{4.23}$$

If assumptions are made that the test specimen is a slender beam with uniform mass and station distributions, then the above equation may be rewritten as

$$1 = \bar{m} \sum_{\ell} X_{ie_\ell}^2$$

$$\sum_{\ell} X_{ie_\ell}^2 = 1/\bar{m} \tag{4.23a}$$

and the mode shape portion of the cost function becomes inversely proportional to the mass

$$F_{ix} = \frac{1}{2} W_{ix} \epsilon^2 \frac{1}{\bar{m}} \tag{4.24}$$

where $\bar{m} = \frac{\text{mass of beam}}{\text{Number of stations}}$

F_{ix} is independent of frequency, and is dependent upon the mass, number of beam stations, and the square of the error.

To equate the size of the frequency terms in the cost function with each other, the following weighting factors were selected

$$W_{if} = \frac{\omega_{N/e}^4}{\omega_{ie}^4} \tag{4.25}$$

where

$\omega_{N/e}$ = highest experimental mode frequency

Equating the mode shape and frequency terms of the cost function yields

$$W_{ix} \frac{1}{\bar{m}} = \frac{\omega_{N_{1e}}^4}{\omega_{ie}^4} \omega_{ie}^4 = \omega_{N_{1e}}^4$$

$$W_{ix} = \omega_{N_{1e}}^4 \bar{m}$$

$$W_{ix} = \frac{\omega_{N_{1e}}^4 m}{N} \qquad (4.26)$$

where m = mass of the missile (Lb-Sec^2/In)

N = number of internal stations

The above weighting factors then approximately weight the mode shape and frequency errors equally. These factors have been built into Program JOINTS along with a set of adjustable weighting factor coefficients. If unequal weights are desired, weighting factor coefficients are input to the program and these coefficients are multiplied by the above factors to obtain the new weighting factors used by the program. That is

$$W_{if} = WFC_{if} \left(\frac{\omega_{N_{1e}}^4}{\omega_{ie}^4} \right) \qquad (4.27)$$

$$W_{ix} = WFC_{ix} \left(\frac{\omega_{N_{1e}}^4}{N} m \right) \qquad (4.28)$$

where WFC_{if} and WFC_{ix} are input separately for each mode.

Some consideration was given to including provisions for weighting some mode components more than others, but this was concluded to be an impractical and unwarranted complexity in the operation of the program.

4.2.2 "Bite" Size Selection. The bite size being discussed in this section is r in equation (4.15), the increment each spring is altered during the intermediate calculation in the computation of the second order partials. The choice of the spring increment size, r, can cause a problem unless care is taken in its selection. The step size must be large enough to prevent incurring numerical accuracy problems, yet small enough to give an adequate estimate of the second order gradients of the cost function.

The present tolerance ratio on the frequency solution in the modal analysis routine in Program JOINTS is 1 x 10^{-5}. That is, the theoretical frequency solutions will be no worse than .001 percent. In selecting a value of r to be used in Program JOINTS, a change in each individual spring equal to r times the spring rate should produce frequency changes greater than .01 percent in the theoretical modes. This change in frequency is dependent upon the joint locations and magnitude of compliances. Reference 1 (Phase 1 Report) provides an extensive discussion of these parameters. Another constraint on the step size to be considered is that if the originally assumed joint compliances are 'far from convergence' a first order gradient method is used rather than the second order gradient method. If the first order method is used, r is the amount the compliance is altered each iteration. If r is small, the solution time may be very large. The phrase 'far from convergence' is defined as a region which is determined by the directions indicated for changes in individual spring rates from the first order and the second order gradient methods. If the two methods indicate opposite directions should be taken for the change in spring rate, the first order method is used. As the cost function minimum is approached, the first and second order terms agree in sign for the change in spring rate so the magnitude determined from the second order method is used. This choice of either the first or second order method is made independently for each spring.

To illustrate the effect of the step size r, consider the non-uniform bending beam model shown in Figure 4-1. It consists of five beam sections connected by four flexural joints, each of "moderate" to "good" stiffness for the assumed test airframe. The Holzer Myklestad method (identical to what is used in Program JOINTS) was used to generate the required modal data for this test case. Since the modal data are "exact" for the lumped parameter model, a precise means for judging the accuracy of the JOINTS program solution is provided. Selected flexural joints were then assumed to be unknown, and arbitrary (incorrect) initial values selected.

Figure 4-2 shows the results obtained with Program JOINTS by using two modes to solve for three joint compliances. For this case, the compliance of the first of the four joints was assumed to be known correctly and the compliance of the last three were assumed high by a factor of two. The value of the intermediate step size, r, used in this case was 25%. Figure 4-2 shows the result of eighteen iterations. The convergence is seen to be quite slow. Other values of r have been considered with interesting results. Figure 4-3 shows the same example as Figure 4-2, except the value of r was changed from 25% to 1%. Here convergence to the three correct joint flexural compliances is achieved in four iteration cycles or about four times as fast. This points out the importance of the intermediate step size, r, used in approximating the second partial derivatives. In both of these examples, three unknown spring rates were solved using only two modes.

Figure 4-4 illustrates further the importance of the intermediate step size, r, in the convergence of the method. Values of r considered in Figure 4-4 range from 25% to 1%. Very little difference is seen between 1% and 5%, suggesting that both approximate the second order gradients well. For this case, it can be seen that 25%, 20%, and 15% were all too large a value for r. All three values of r will produce the correct joint compliances but the run time is much longer for the larger values of r. The value of r for best convergence will not be the same for all cases. In fact, for some problems it might be more efficient to make two computer runs using two different values of r. In the beginning, use of a larger value of r may be required if the program employs the first order gradient method. However, the solution may be speeded up by using a smaller value of r as the cost function minimum is approached and the program uses the second order gradient method.

4.3 PROGRAM FEATURES ADDED

This section discusses some of the techniques developed during the Phase 3 study to increase the efficiency of Program JOINTS and to decrease the work required by the user. Covered in this discussion are the program generation of weighting factors, logic in JOINTS to correct for modes being missed by the eigenvalue extraction subroutine, and the benefits of using the input parameter 'CLOSE'. In addition, this section introduces the computer program (Program FILLIN) written as an aid for the user of Program JOINTS. Program FILLIN accepts measured modal data in a general format and interpolates between those data points to obtain a new set of data in the format appropriate for use in Program JOINTS. The changes to the input data are necessitated because Program JOINTS compares the experimental and theoretical modal data at identical missile stations.

4.3.1 Weighting Factor Generation. In the original program format, the weighting factors required to use Program JOINTS had to be calculated by the user. As an added convenience, it was decided to accomplish the major portion of the weighting factor computation within the program. Equations 4.25 and 4.26 of section 4.2.1 present the equations of the weighting factors now used in the program. The option is retained to input weighting factor coefficients desired by the user, but these weighting factor coefficients (WFC_{if} and WFC_{ix} in equations 4.27 and 4.28) modify the factors computed by the program and do not replace them. If no values are input for WFC_{if} and WFC_{ix} , these coefficients are each assumed equal to 1.0. If the user, for example, wishes to weight the first mode shape and frequency a factor of two more than the other modes, he simply inputs the value 2.0 for WFC_{1f} and WFC_{1x} and 1.0 for all other modes.

4.3.2 'Missing' Mode Logic. Another option built into Program JOINTS during Phase 3 is a check to guard against missing modes in the eigenvalue extraction routine. This is accomplished by checking the computed modes against the experimental modes. For bending cases, the number of slope sign changes in each theoretical mode shape is compared with each measured mode. Like modes are matched and if any modes are missing the program will go back and compute the missing modes. Because of the way the Myklestad subroutine treates redundant appendages, this check should not be used with a model that has redundant appendages.

4.3.3 Number of Theoretical Modes. Another improvement introduced to Program JOINTS is to allow the calculation and inclusion of more theoretical modes than experimental modes in the partial derivatives of the mode shape given in equation (4.11b) The partial derivative of the eigenvector for the i^{th} mode is expressed as the sum of contributions from all modes except the i^{th} mode. This sum is truncated at however many modes are available for the calculation. If only one mode is available, then the partial is approximated by zero. If two modes are available, then the partial is approximated by contributions from one mode. For a distributed system, the partial derivative would be computed from an infinite sum. The larger the number of modes, the closer the sum should approximate the partial derivatives. Using more modes in approximating the partial derivatives can be expected to produce more accurate values, aid in the problem solution, and accelerate the rate of convergence. The amount of computer time used per iteration cycle, however. is directly proportional to the number of theoretical modes used in the solution. Because of this cost consideration, the user would be advised to use an equal number of theoretical modes in the solution when three or more measured modes are available.

4.3.4 Input Parameter 'CLOSE'. The input parameter 'CLOSE', Table A-3,used in Program JOINTS is another parameter designed to save computer time. If a value is not input for 'CLOSE' into Program JOINTS, a continuous search is made for the required number of modes between specified frequency limits. Computer time may be saved by eliminating as much of the searching as possible. A way of eliminating the unnecessary searching is to start below but very near the answer. The reason for starting just below the answer is that the frequency search is done in an increasing order. For a model which matches the experimental data fairly closely, the search starting frequency for each mode may be selected close to the experimental frequencies. If a value of 'CLOSE' is input, the search for the i^{th} mode starts at the frequency equal to 'CLOSE' times the experimental frequency for the i^{th} mode.

Starting the search for the modes near the required solution has saved considerable computer time in several of the test cases. Using the tactical missile application of Section 4.4 as an example, a value of 'CLOSE' equal to 0.9 cost approximately 30% less than an identical run where a continuous search was used. However, care must be taken that 'CLOSE' times the experimental frequency for the i^{th} mode will not be less than the theoretical frequency for the $(i-1)^{th}$ mode, in which case the $(i-1)^{th}$ mode will be repeated for the i^{th} mode.

4.3.5 Test Data Preparation. One of the goals of the Phase 3 study was to simplify the tasks of the person using Program JOINTS. During the Pnase 2 study, it became obvious that for Program JOINTS to be easily useable, a scheme was needed to reduce the amount of work required to get the experimental data in the format necessary for the program. As the cost function is formulated, the mode shape deflection and slope at every internal station are compared with a measured mode shape deflection and slope at that station. However, seldom are the measurements made at the station locations required by the mathematical model. In addition, the quantities most usually measured during test are the modal deflections and not the slopes. One way of handling this problem is to plot the measured deflection data. From these plots, a new set of modal deflections and slopes are read at the desired stations and key punched on cards. As an example of the size of this problem, the tactical missile test case discussed in Section 4.4 has a total of 78 stations. The number of data points read per mode is 156, and three modes were used for that case. It was for this reason that Program FILLIN was written.

Program FILLIN accepts modal data measured at a set of missile stations and the mathematical model data to be used in Program JOINTS. The program then interpolates using several simple curve fitting techniques. The program is primarily designed for bending mode cases. The method of interpolation to be used at a particular station is determined by the station type and the relative locations of stations at which experimental values are available The types of stations considered include those not at a joint, those immediately to the right or left of joints, and those at the ends of the main beam or an appendage. The first class of stations includes the majority of stations. For these stations interpolation was accomplished with a sliding parabolic least square curve fit to four experimental values. That is the two nearest experimental values on either side of the station are used for the least square fit. If two experimental values are not available on both sides of the station, linear interpolation or if necessary extrapolation is resorted to. This also applies to stations at ends of appendages and to modal slopes at stations immediately to the right or left of rotational spring joints and to modal displacements at stations immediately to the right or left of shear spring joints. Modal slopes at a shear joint are the average of the two straight line slopes on each side of the joint.

One of the limitations of Program FILLIN is that appendages with 180° attachment angles will have slope values with the sign opposite to the Myklestad subroutine. This occurs because the Myklestad routine uses a different coordinate systems on appendages than it does on the main beam while FILLIN uses only one coordinate system. Another limitation of

FILLIN is that inaccuracies can occur at stations near joints and in slopes at roots of appendages. However, one of the advantages of the least square curve fit is that the method will smooth the experimental data.

4.4 TACTICAL MISSILE TEST CASE

To show the utility of Programs FILLIN and JOINTS, a set of measured bending modal data for an actual tactical missile were selected as a test case. The set of modal data had previously been matched with a mathematical modal by a trial and error method. This method took approximately sixty computer runs. Previous test cases based on hypothetical models had shown that the method arrives at the correct joint compliances rapidly when an exact math model is used with no errors in the input data. The results obtained with this test case illustrate how well the program works when matching a lumped parameter model to actual measured data with its inherent experimental errors.

Figures 4-5, 4-6, and 4-7 present the three experimental modes and the curve fit values obtained from Program FILLIN for the tactical missile. There are slight discrepancies between the measured data points and the curve fit values, especially near the front end of the missile where few data points exist. The forward end of the missile is a radome shell and quite stiff for the weight it supports. It therefore bends very little in the lower bending modes. When the program fits the data points with a quadratic equation, the match is not perfect. Nevertheless the interpolated modal displacements and slopes are believed to be reasonable representations of the measured modes. Since the method tends to smooth the data, a test case with larger experimental errors in the measured modes would look more impressive.

The output displacements and slopes from Program FILLIN are punched on cards in the format for Program JOINTS. However, the punched output must be checked and corrected as 180 degree appendages will have the sign of the slopes out of phase with the Myklestad program. This is due to a different sign convention in the Myklestad subroutine for 180 degree appendages.

The data output from Program FILLIN was then used as the input modal data for Program JOINTS. The set of weighting factors selected for this application were chosen to equate all three modes (both frequencies and mode shapes) equally. The first three joint compliances (which represented airframe joints) were started approximately 300% higher than the hand tuned values. The fourth joint compliance represented the attachment compliance for an internal appendage. The originally assumed value of the fourth compliance was started high by 30% over the hand tuned value.

Figure 4-8 shows the rate of convergence obtained by Program JOINTS for the tactical missile application. The program was run for a total of eight iteration cycles. However, the cost function did not improve significantly after the third cycle. The final (iteration cycle eight) joint compliances obtained agree quite well with the hand tuned values. Figures 4-9, 4-10, and 4-11 present a comparison of the experimental and theoretical modes. It is apparent from the figures that a good match has been obtained between the two sets of data.

Next, a new set of weighting factors was chosen to see what effect different weighting factors had on the solution. It should also be noted that the test data was represented well by the beam model in the above solution. The set of frequency weighting factor coefficients selected were 100, 10, and 1 for the first, second, and third modes respectively. The corresponding mode shape weighting factor coefficients were 1, 0.1, and 0.01. Figure 4-12 shows the solution (No. 2) obtained for this condition. Comparison of Figures 4-8 and 4-12 shows that both sets of compliances obtained are close to the hand tuned values. The following is a comparison of the experimental frequencies and the frequencies obtained for the two sets of weighting factors.

Mode No.	Experimental Frequency (Hz)	Theoretical Frequency (Hz)	
		Solution No. 1	Solution No. 2
1	59.3	59.5	59.3
2	116.	114.4	116.0
3	153.	154.2	153.6

As shown above, the case where the frequencies are weighted more heavily than the mode shapes (solution number 2) does in fact exhibit a better match between the experimental and theoretical frequencies.

4.5 STATUS OF THE EXTRACTION TECHNIQUE

The joint compliance extraction technique in its present format is believed to offer a useful, convenient, and reliable method for estimating effective compliances of missile joints from modal test data. The method presumes that the missile airframe distributed stiffness and mass properties are known, the modal characteristics can be adequately modeled as a lumped parameter beam, and that all discrepancies between modal analysis and modal test data can be attributed to uncertainties in the joint compliance values. As in any analytical method, additional refinements and areas for improvement will become evident as applications are further explored with actual test data.

LIST OF SYMBOLS FOR SECTION 4.0

F = Cost Function of Error Terms

N_1 = Number of Experimental Modes

$\sum_i$ = Summation on Index i

ω = Mode Frequency

X = Mode Shape

W = Weighting Factor

$(\ )^T$ = Transpose of $(\ )$

K = Stiffness Matrix

M = Mass Matrix

N = Number of Internal Stations in Model

k = Unknown Spring Components

n = Iteration Number

θ = Step Size

∇F = $\frac{\partial F}{\partial K}$ = Gradient of F

S = Step Size

$[\ ]^{-1}$ = Inverse of $[\ ]$

δ_{ij} = Kronecker Delta $\begin{cases} = 1 & i = j \\ = 0 & i \neq j \end{cases}$

$\bar{K}$ = Matrix of Known Spring Elements

N_J = Number of Joints

U = Strain Energy

${}'X_j, X_j'$ = Slope to the Left and Right of Joint j

k' = Intermediate Spring Rate Used in Computing the Second Order Derivatives of F

LIST OF SYMBOLS FOR SECTION 4.0 (Cont'd.)

r = Intermediate Step Size Used to Obtain K'

$SGN(\ )$ = The Sign of ( )

ϵ = Relative Error Size

λ = ω^2 = Eigenvalue

m = Mass of Missile

WFC = Weighting Factor Coefficients

SUBSCRIPTS

e = Experimental

t = Theoretical

x = Mode Shape

f = Frequency

i, j, ℓ, m, q = Indices or Counters

FIGURE 4-1

NON-UNIFORM BENDING BEAM PROPERTIES

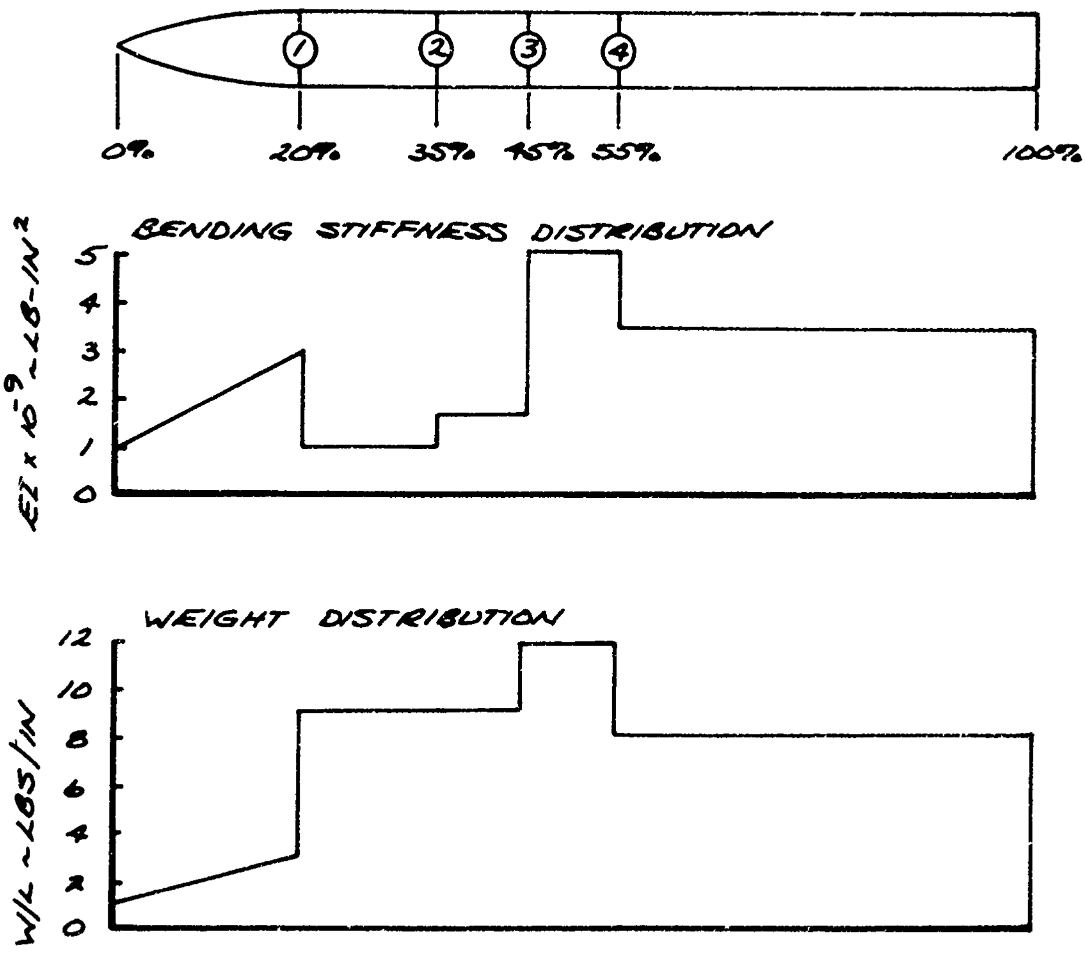

MODE NO.	FREQUENCY WITH JOINTS (HZ)	FREQUENCY W/O JOINTS (HZ)
1	35.9	50.4
2	100.7	118.3

JOINT NO.	COMPLIANCE RAD/IN-LB
1	.1 -7
2	.1 -7
3	.1 -7
4	.1 -7

FIGURE 4-2
NON-UNIFORM BENDING BEAM
SOLUTION FOR THREE JOINT COMPLIANCES
USING TWO MODES, r = 25%

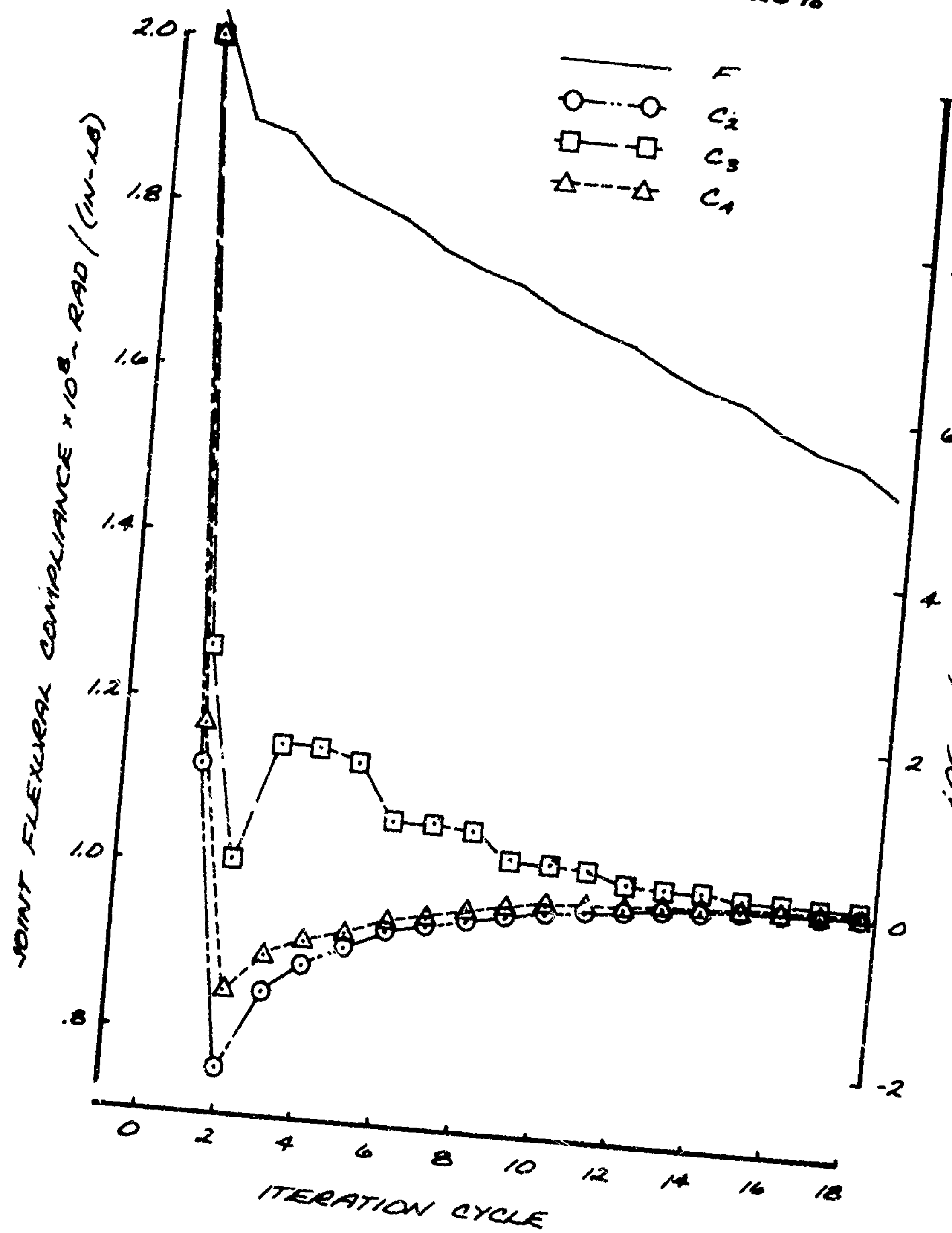

FIGURE 4-3

NON-UNIFORM BENDING BEAM
SOLUTION FOR THREE JOINT COMPLIANCES
USING TWO MODES, r = 1%

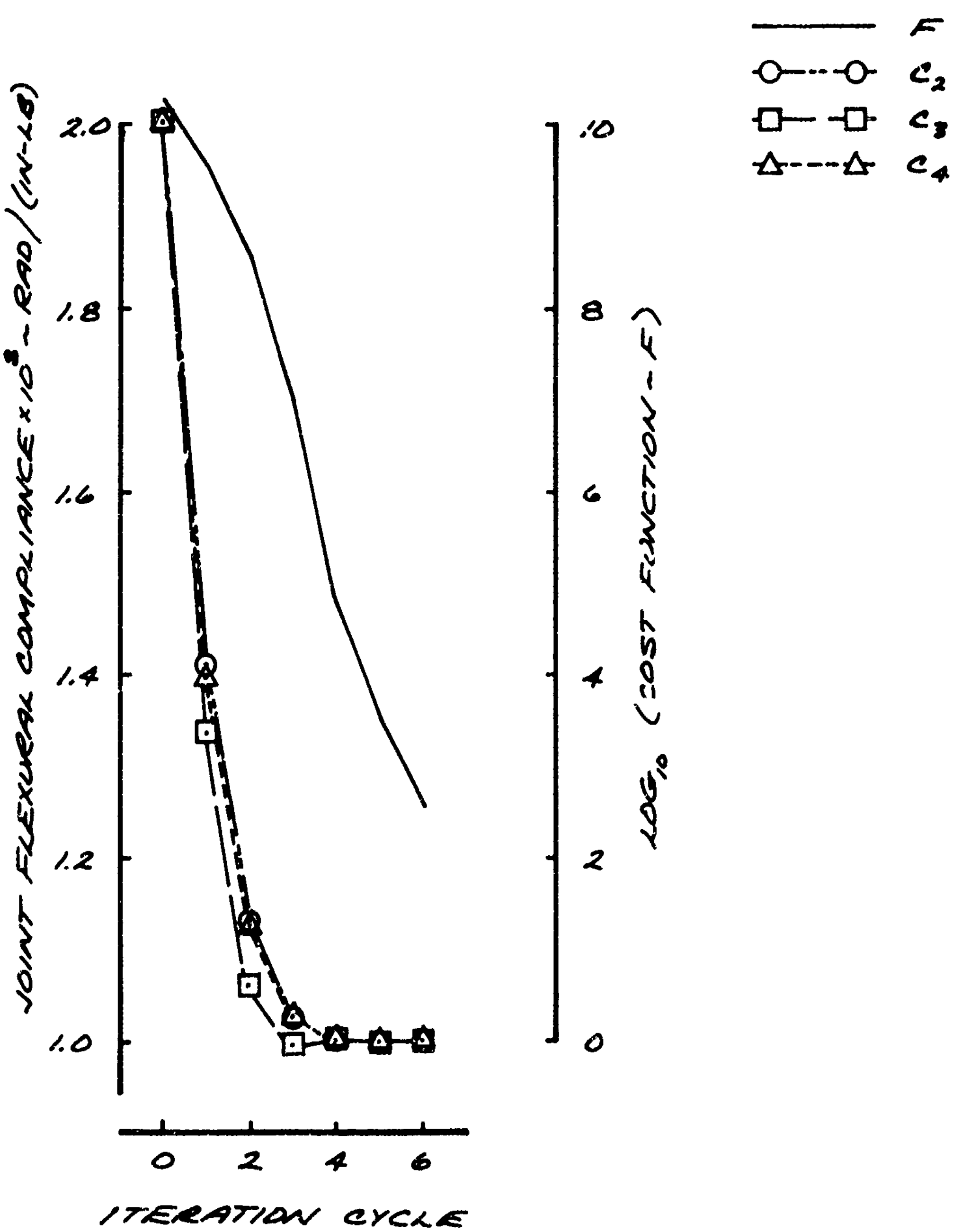

FIGURE 4-4

NON-UNIFORM BENDING BEAM
CONVERGENCE VS. INTERMEDIATE STEP SIZE - r
SOLVING FOR THREE JOINT COMPLIANCES
USING TWO MODES

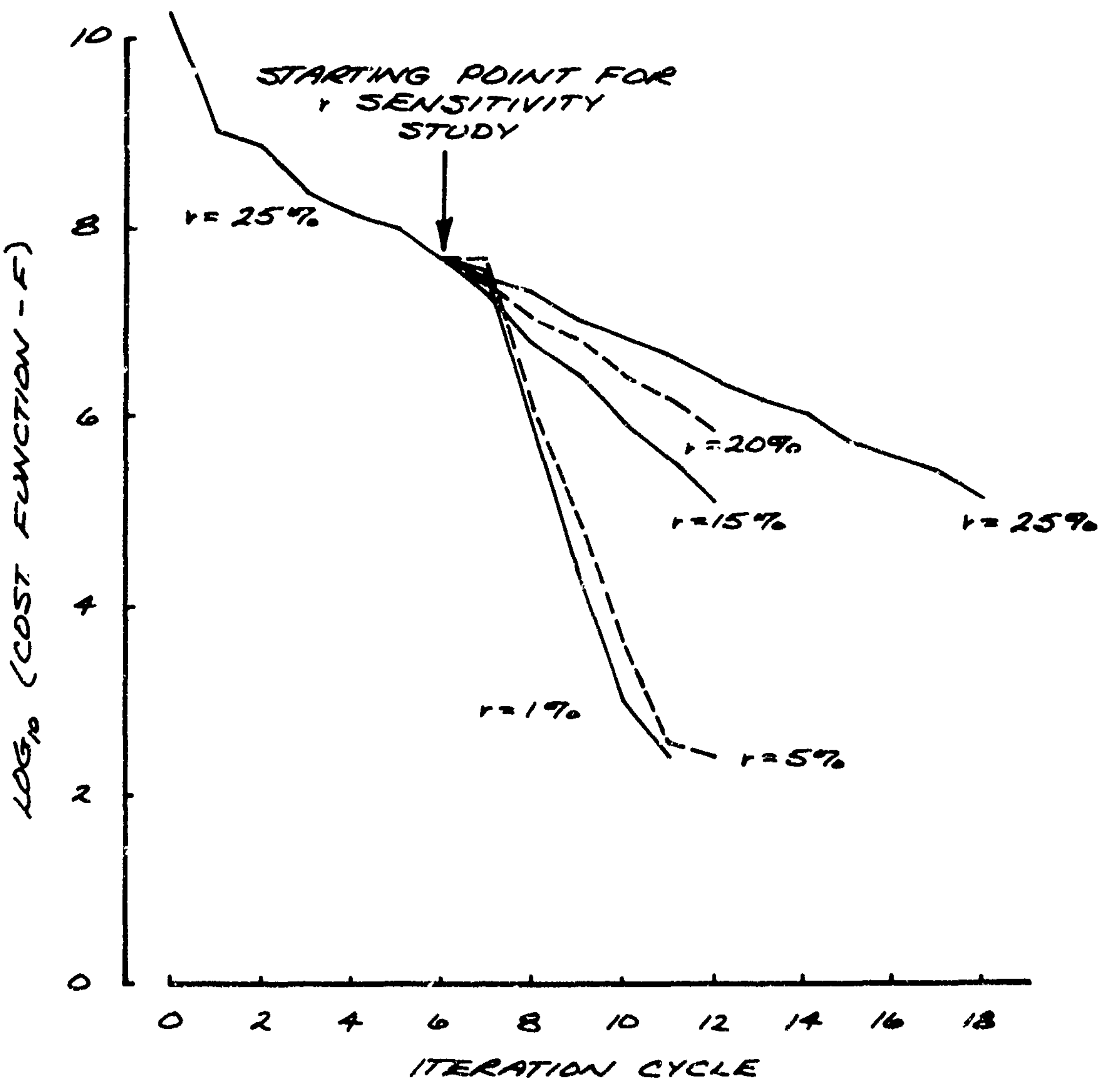

FIGURE 4-5

TACTICAL MISSILE MEASURED BENDING MODES

FIRST MODE $f_E = 59.3$ Hz

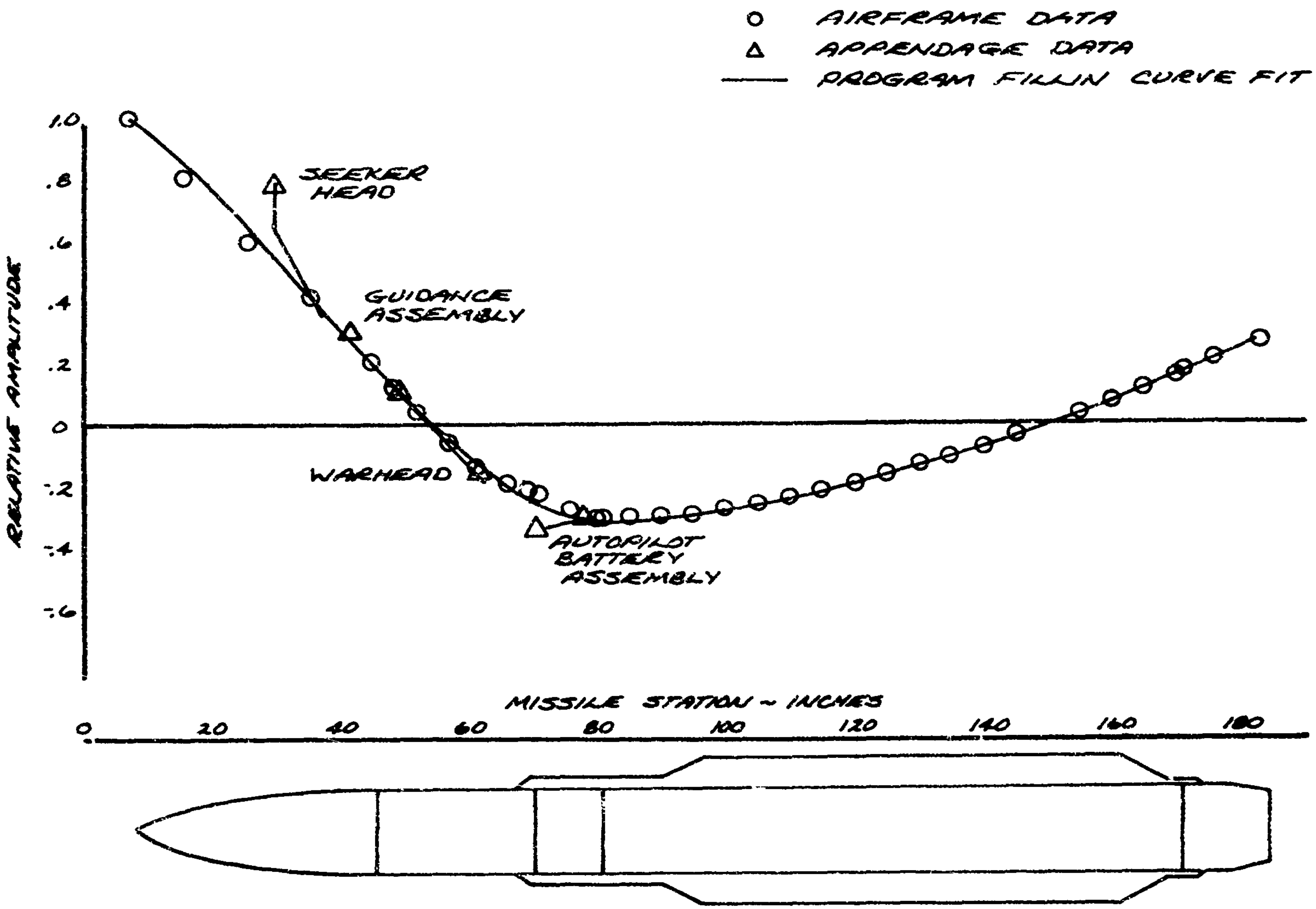

FIGURE 4-6

TACTICAL MISSILE MEASURED BENDING MODES
SECOND MODE f_E = 116 HZ

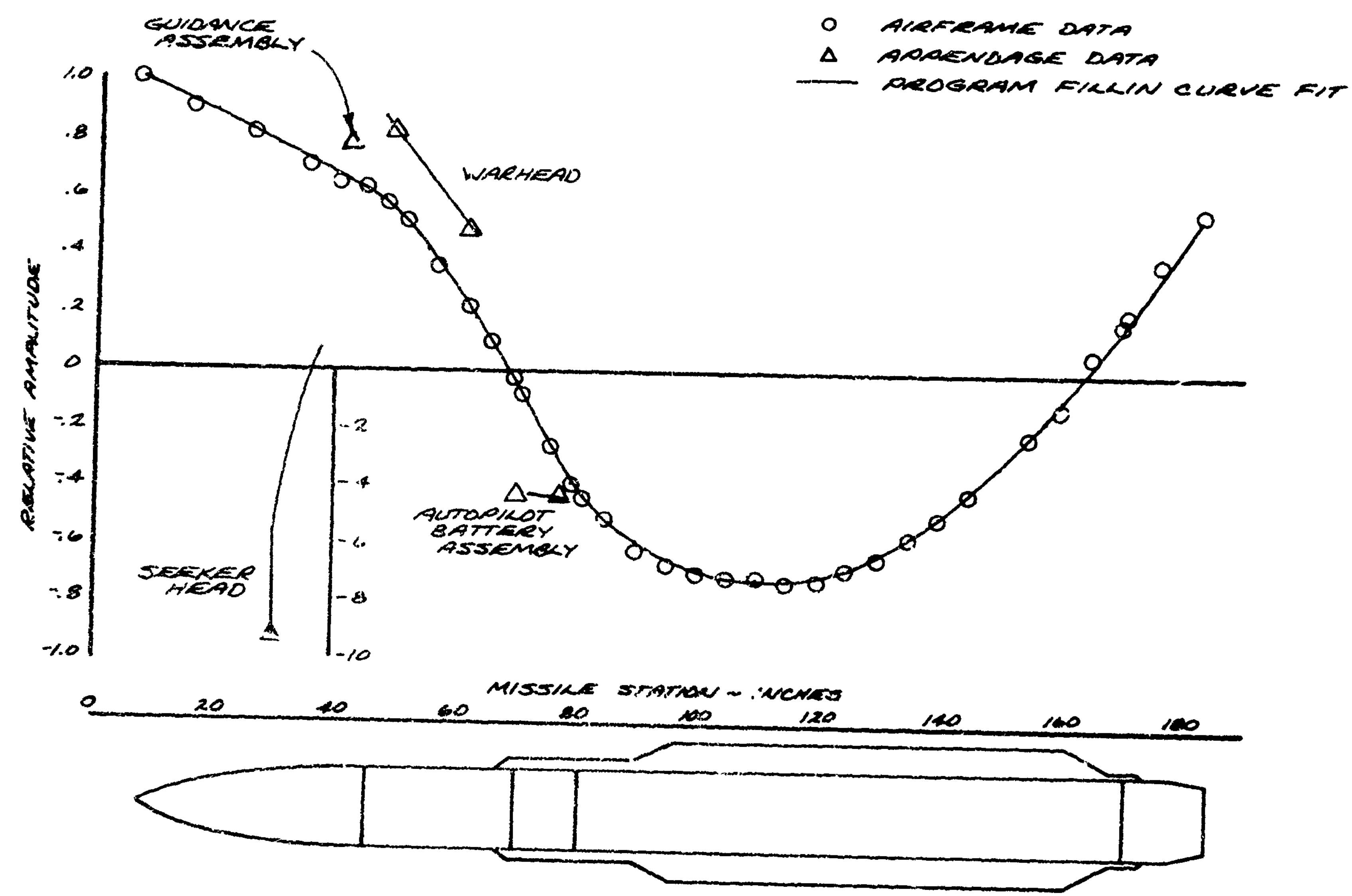

FIGURE 4-7

TACTICAL MISSILE MEASURED BENDING MODES
THIRD MODE f_E = 153 Hz

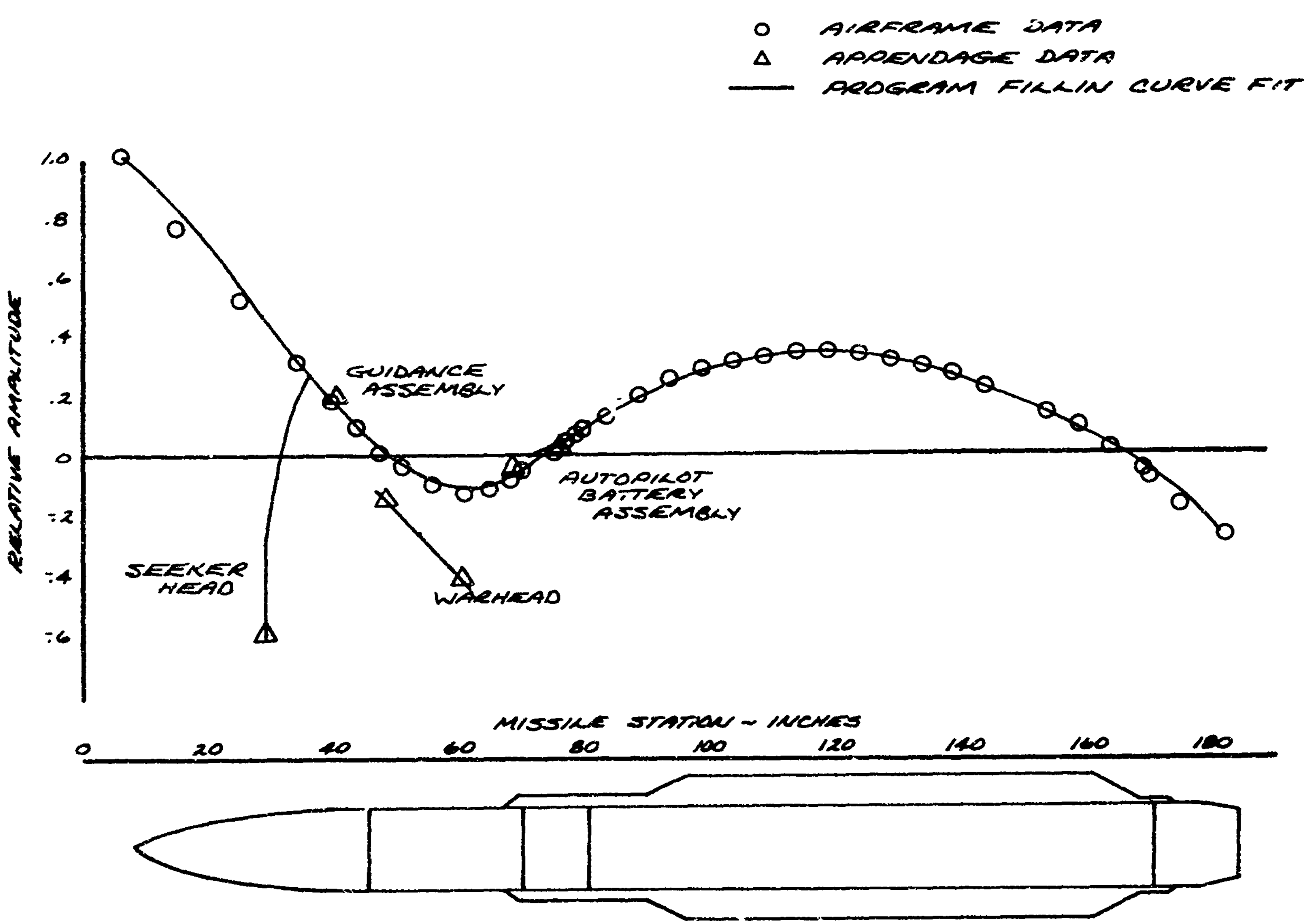

FIGURE 4-8

TACTICAL MISSILE APPLICATION

SOLUTION NO. 1

EQUAL WEIGHTING FACTORS

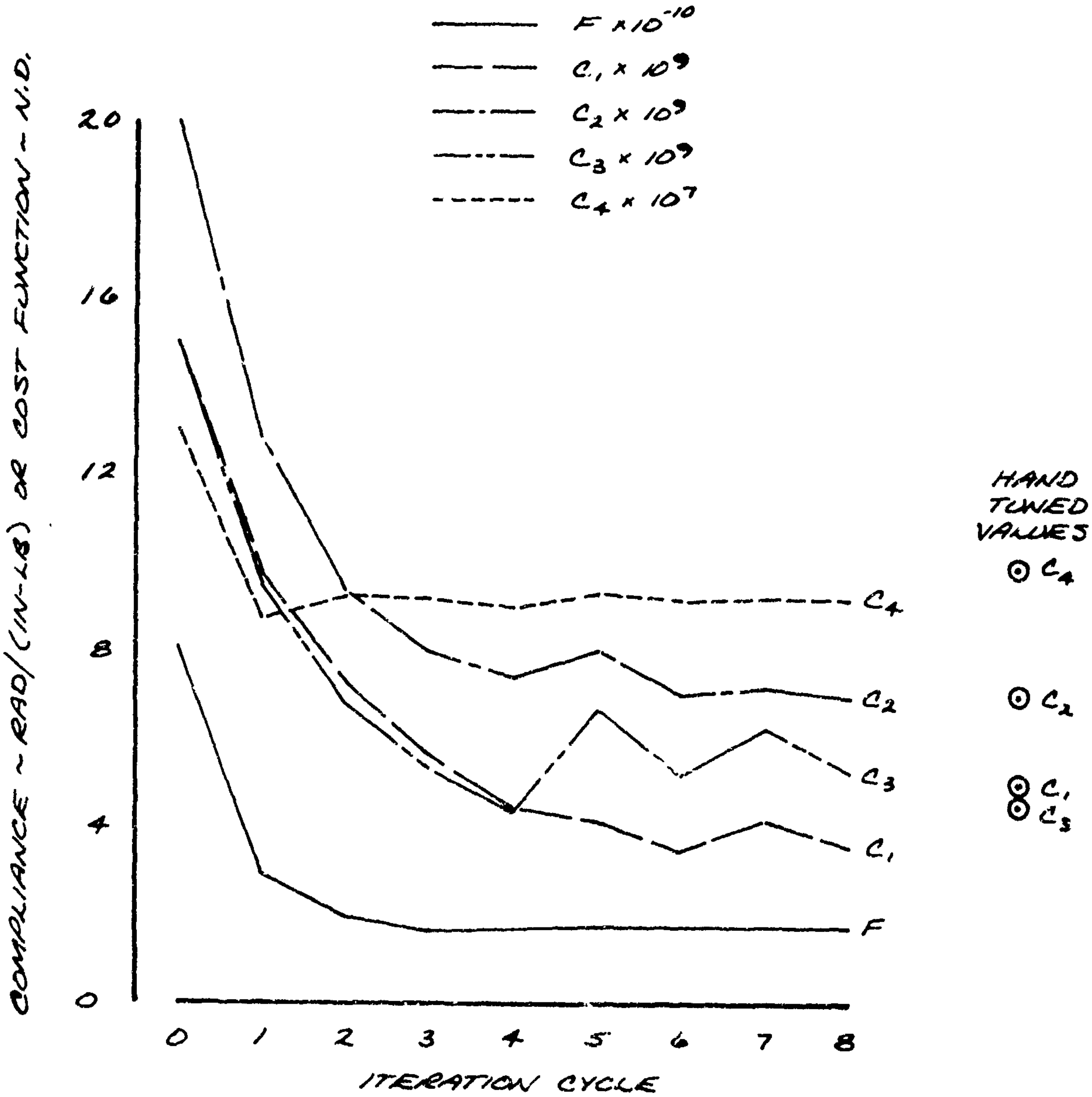

FIGURE 4-9

TACTICAL MISSILE APPLICATION
COMPARISON OF EXPERIMENTAL AND THEORETICAL FIRST MODES

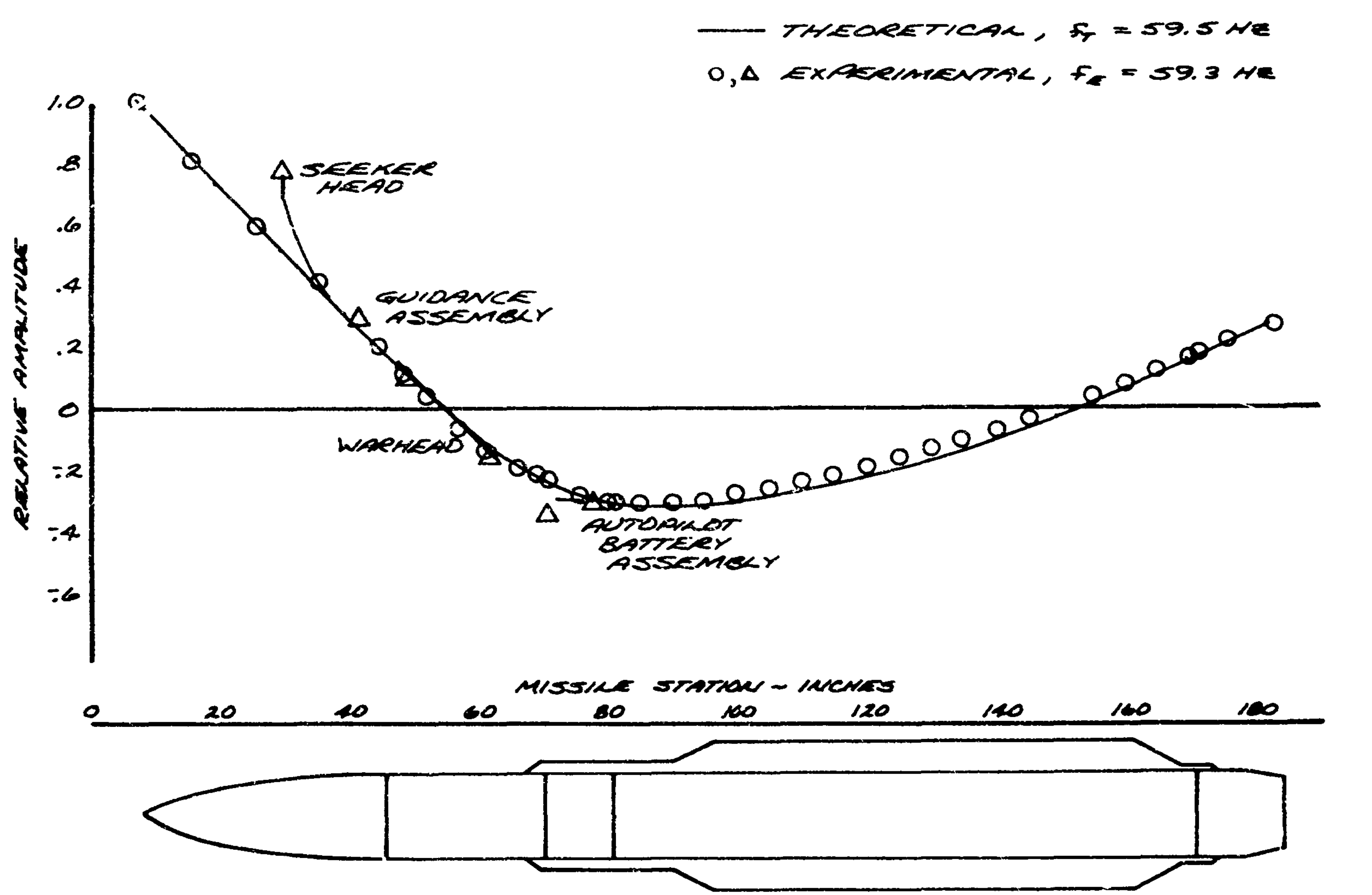

FIGURE 4-10

TACTICAL MISSILE APPLICATION

COMPARISON OF EXPERIMENTAL AND THEORETICAL SECOND MODES

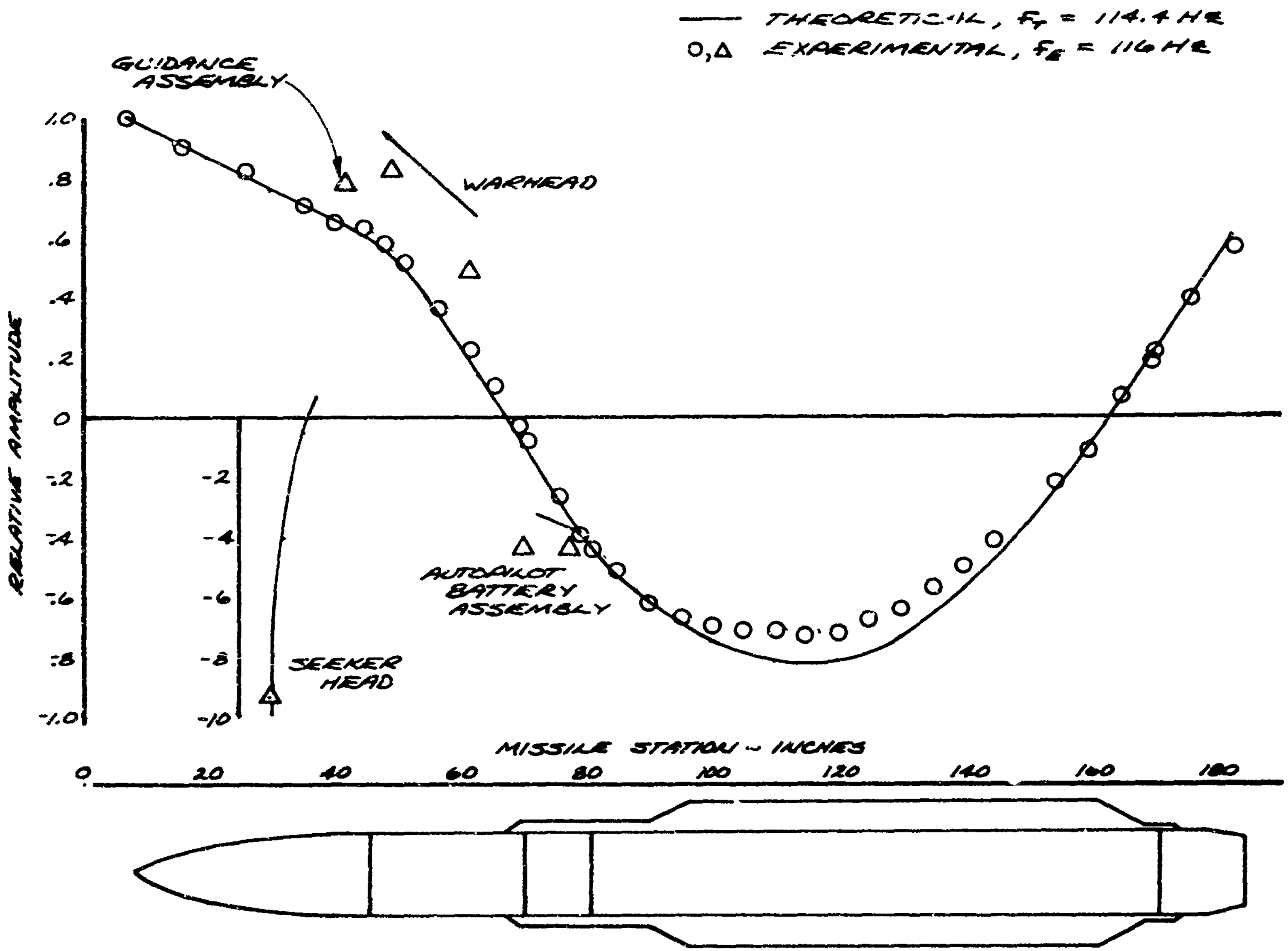

FIGURE 4-11

TACTICAL MISSILE APPLICATION

COMPARISON OF EXPERIMENTAL AND THEORETICAL THIRD MODES

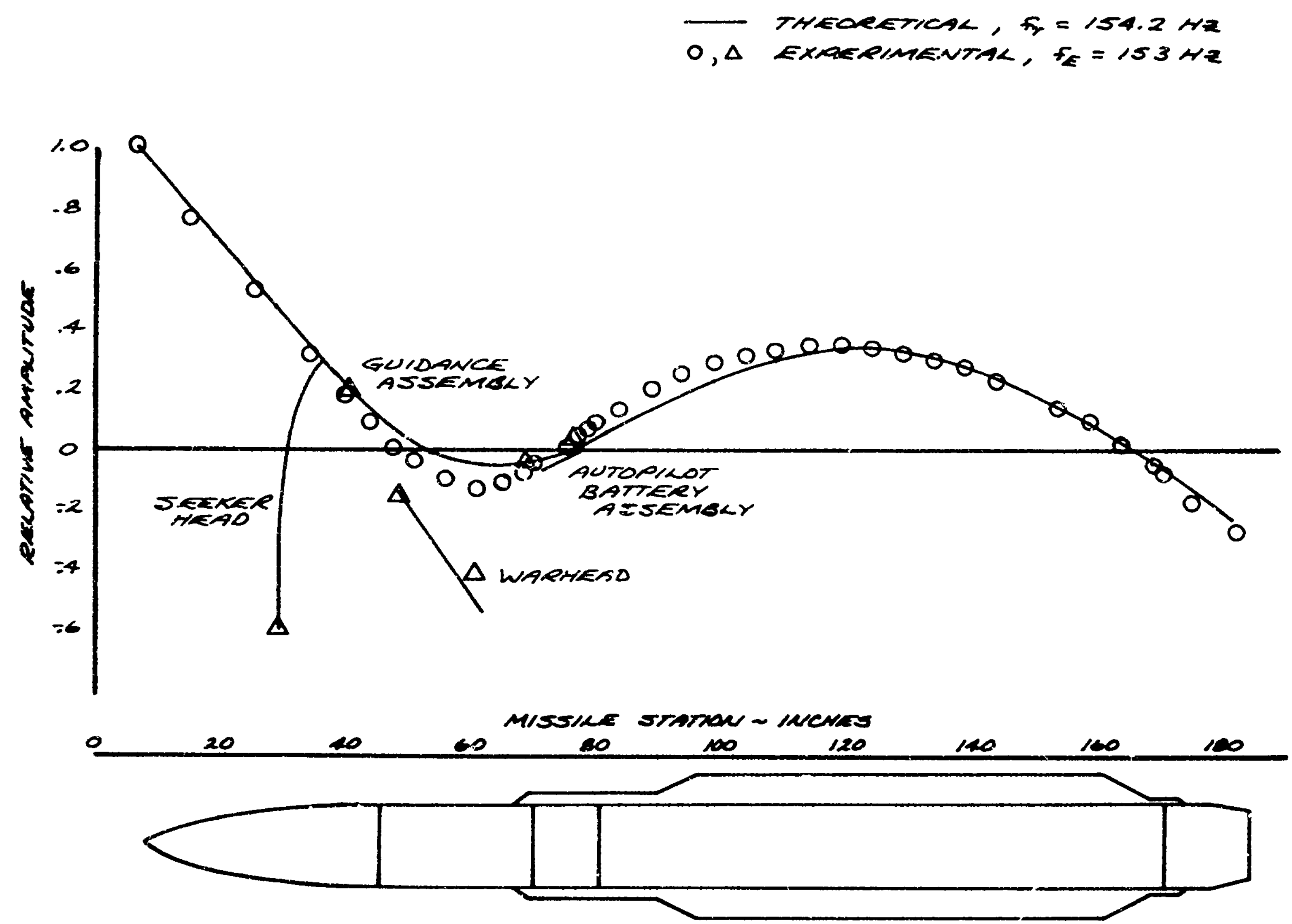

FIGURE 4-12

TACTICAL MISSILE APPLICATION

SOLUTION NO. 2

UNEQUAL WEIGHTING FACTORS

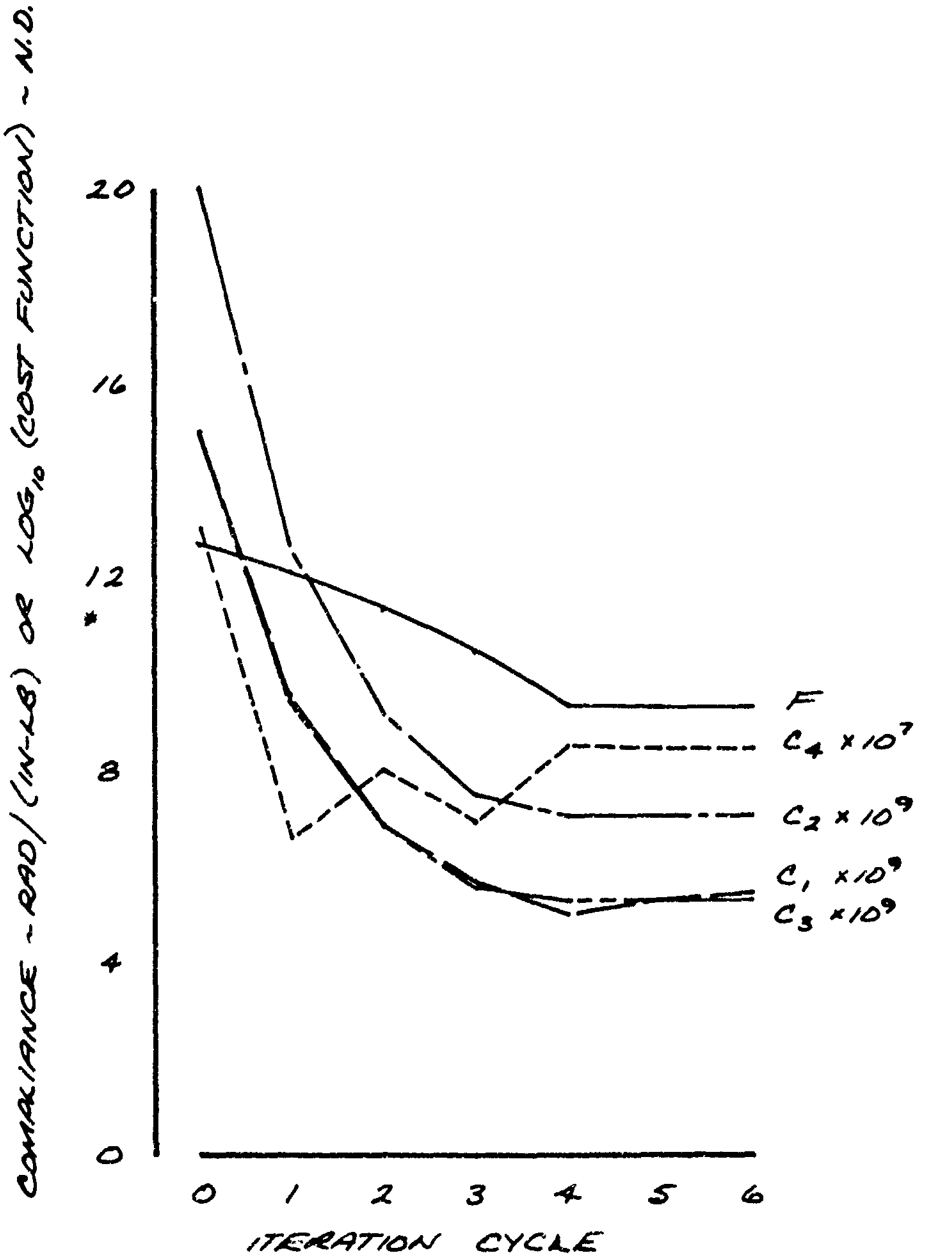

Section 5.0

MISSILE JOINT SELF INDUCED VIBRATION

Tactical missile airframe joints can become significant sources of mechanical shock and vibration under transient loading conditions which exceed mating surface interface preloads. If mating surface separation and impact occurs, shock transients generated at the interface will propagate from the airframe joints throughout the missile structure. Under oscillatory loading conditions, the repetitive shock transients - modified by strain wave reflections - often assume the appearance of broadband vibration when monitored at missile components.

One obvious potential problem area with noisy joints can occur in laboratory sinusoidal vibration testing where the test conditions are specified in terms of displacement or acceleration input at the test fixture/specimen interface. Since only the fundamental input levels at the excitation frequency are usually controlled, a significant overtest can result from uncontrolled broadband vibration induced by mechanical joint interface impact.

The vibration environment source characteristic can also be of concern in the case of air launched missiles which are often exposed to many captive flight hours. Excitation of comparatively low frequency aircraft and missile modes by aerodynamic turbulence and/or buffet may result in the secondary generation of high frequency vibration due to mechanical interface impact within missile airframe joints and in some instances at aircraft interface contact points such as sway brace pads and lugs.

Recent tactical missile flight vibration measurements, furthermore, provide suspicious evidence that for some current missile designs the joints may be a prime contributor to missile flight vibration and shock environments. If this premise is valid, then improvements in missile joint design may yield significant reductions in environmental exposure and support cost saving relaxations in environmental specifications.

This section presents the results of an exploratory investigation of the mechanism of joint self induced vibration and an initial evaluation of possible methods for control and suppression. The scope of the investigation has included tests of both full scale actual missile joints and an idealized subscale joint model. A design concept for a joint interface treatment to suppress self induced vibration involving flame deposited teflon was developed in missile section level testing with sufficient promise to warrant missile round level flight test evaluation. Test results from both laboratory section level (encouraging) and flight missile level (inconclusive) are reviewed and discussed. Due to the inconclusive results obtained in the missile level testing, a sub-scale idealized joint model was designed with the objective of isolating and controlling some of the more elusive full scale test parameters. The model test results, while exhibiting some scatter, do show consistent trends and a significant improvement in joint preload, damping, and mechanical noise reduction when a teflon coating is present at the model joint interfaces.

More work clearly remains to be done in this area. The investigation thus far has shown that joint interface impact can be a powerful source of broadband vibration and that interface coatings can effect a substantial improvement in joints exhibiting these characteristics.

5.1 FULL SCALE LAB TESTS

The full scale joint designs selected for consideration in this study include a discontinuous land ring joint shown in Figure 5-1 and a continuous split ring joint shown in Figure 5-2. Both of these joints are highly compliant (rated about "moderate' under the classification basis discussed in Section 2.0) with comparatively low interface contact preload (estimated to be approximately 12 pounds/inch) under design assembly torques. The low preload is best illustrated by the fact that in one tactical missile application, with the discontinuous land ring joint, the assembly preload is well exceeded in a one g environment; i.e. the static moment produced by the missile structure forward of the joint is nearly twice the preload induced moment.

Ring joints of this type have consistently demonstrated a capacity for generating joint interface impact vibration in section level vibration testing. In one instance of sinusoidal vibration testing of a missile guidance section, a 3g sweep was observed to produce 20g broadband when the fundamental passed through a joint impact resonance.

The initial hypothesis in searching for a fix for this behavior was that compliant material placed on the contacting surfaces of the joint would inhibit metal to metal impact and thus materially reduce the resulting vibration. It was further conjectured that any adverse effect of this compliant material on joint stiffness could be offset by a general improvement in load distribution resulting from filling voids and irregularities in the mating surfaces. Each of the ring joint designs has 3 contacting surfaces - two associated with the ring nut and subject to abrasion as the surfaces slide in contact during assembly, and one where the missile shroud sections butt together. With practical manufacturing tolerances, a perfect fit on the mating surfaces is virtually never achieved. The uncertain and variable load paths due to this feature are viewed as a major contributing factor to both high compliance and noise generation characteristics. Another obviously important parameter is the joint preload, with any increase achieved either through higher assembly torques or reduced friction in the sliding surfaces (threads) being beneficial.

A variety of candidate joint interface materials including epoxy, RTV, plastics, elastomers, and soft metals such as lead and aluminum were selected for evaluation. These materials, in general, were only introduced on the non-sliding surfaces of the joint. Epoxy and RTV were applied also to the sliding surfaces with the expectation that most of the coating would be wiped off points of contact but that some of the voids in the mating surfaces might be filled. The test set-up used to determine the effect on joint self induced vibration, shown in Figure 5-3, consisted of a missile nose section cantilevered from a discontinuous ring joint attached through a test fixture to an oil slide table. The basic test specimen when driven at resonance would exhibit an abrupt increase in broadband vibration when the joint preload was exceeded with the ratio of broadband to fundamental response at the joint exceeding a factor of 8 for one test point. The test was then repeated with each of the joint interface materials using a constant assembly torque and recording broadband (20 5000 Hz) response at the joint for several reference fundamental response levels. Table 5-1 presents the results obtained with the different interface coatings for two dynamic bending moment levels at the ring joint interface. These data should be considered qualitative at best with the test results generally showing poor repeatability with large variations for small changes in test conditions. The exception to this was the Teflon configuration which showed not only the best performance from the standpoint of minimum impact noise but also good repeatability and consistency in subsequent re-tests.

It should be noted that the teflon configuration represented the first effort to coat the sliding surfaces of the joint. Flame deposited teflon has sufficient bond strength on the coupling ring and low friction on the sliding surfaces to remain intact and not be wiped off the contacting surfaces during joint assembly. The low friction on the sliding surfaces in fact undoubtedly accounts for a major portion of the substantial improvement shown for this configuration by producing a large increase in joint interface preload for the same torque. The teflon coating was applied only to the coupling ring, rather than all joint contacting surfaces, not by choice but by expedience since the coating process was performed out of plant. One other potentially important characteristic of the teflon was observed to be an apparent significant increase in effective structural damping for the test specimen, with larger shaker output required for the same bending moment response. Based on these admittedly limited but encouraging results, the use of teflon on ring joint interfaces was concluded to have shown sufficient promise to warrant missile level evaluation.

5.2 MISSILE LEVEL QUALIFICATION AND FLIGHT TEST

A continuing series of test firings for an advanced version of a surface launched missile planned for the Spring of 1973 offered an opportunity for missile level flight evaluation of the effect of teflon coated joints on missile flight vibration. Environmental data obtained on earlier flights of essentially the same missile airframe with unmodified joints provided a direct basis for comparison. The missile configuration in question employs six primary joints. Three of which are ring joints, two being of the discontinuous land type and one of the continuous split ring type. The remaining three joints are of the tension bolt type, considered to be very stiff and sufficiently preloaded under assembly torques to preclude any separation under flight loads. The missile profile and joint locations are shown in Figure 5-4.

A decision was made to treat only the ring joints and furthermore to confine the teflon coating to the coupling rings, recognizing that one of the interfaces for each joint, as was the case in the lab test configuration, would not be teflon coated. Prior to design release and acceptance for flight of this missile joint modification, several possible issues needed to be resolved in securing a design requalification. This effort included:

1. Proof load tests of the modified joints to demonstrate that the teflon coating had not compromised structural integrity.

2. Creep tests to provide assurance that missile assembly preloads (albeit low in the case of the ring joints) would not be seriously degraded.

3. Further lab evaluation to confirm the expected noise suppression characteristics of the teflon.

One facet of this phase of the investigation was a concerted attempt to devise a means for measuring the interface preload - both for the basic and teflon coated joints. This effort, unfortunately, was largely unsuccessful, precluding definition of this important parameter which would have been particularly useful in interpreting dynamic response and creep characteristics. Proof loads were successfully applied to the joints in question without incident, and the creep issue was qualitatively resolved by retorqueing control joints after suitable aging and noting that no relative motion of the joint coupling ring occurred.

Joint impact noise suppression tests were carried out using essentially the same test set-up shown in Figure 5-3. In this case, however, three different test fixtures were required to represent the three different joint locations on the missile airframe. The test results for the three joints are plotted in Figure 5-5 in terms of noise suppression achieved by the teflon coating versus the basic joint noise factor, with these parameters defined as follows:

g_F = in-plane fundamental response at the joint

g_{BB} = in-plane broadband response at the joint (20-5000 Hz)

$g_N = \vec{g}_{BB} - \vec{g}_F$ = in-plane noise at the joint

(g_N/g_F) = joint noise factor

$(g_N/g_F)_T/(g_N/g_F)_B$ = joint noise suppression factor - a ratio of teflon coated joint noise factor to basic joint noise factor.

The test results obtained in this series showed considerably less improvement in joint noise characteristics with teflon coated coupling rings than had been observed in the earlier testing. Previous lab data for Joint 1 are shown for comparison. Joint 3 at low response levels was "quieter" in the basic configuration than with teflon for the one specimen tested, although the performance of the teflon configuration improved rapidly as the excitation level was increased. Data points connected by straight lines in Figure 5-5 reflect the two different response levels for the same joint. These data would appear to indicate that "quiet" joints do not admit much improvement while considerable benefit from the teflon coating might be expected with "noisy" joints.

Since the teflon coated rings had satisfactorily passed all design qualification requirements, the configuration was released for flight test evaluation. A total of four instrumented test flights were made with complete data acquisition. From the standpoint of showing an improvement attributable to the teflon coated coupling rings, however, the flights were uniformly disappointing being virtually indistinguishable from the earlier flight series with the basic unmodified joints.

Possible interpretations of this test outcome include:

1. The importance of coating all three joint interface surfaces rather than just two may have been underestimated. Lab testing could have been misleading in this respect if excitation levels relative to joint preloads were not representative of the flight conditions.

2. Joint impact may not be a significant contributor to the flight vibration environment for this missile configuration. In this case, improvements in the joint response characteristics would not have been noticed.

In hopes of answering some of the questions associated with joint self induced vibration, an idealized ring joint model which would admit more precise measurements of the critical parameters was designed and tested.

5.3 JOINT IMPACT MODEL DESIGN AND TEST

The ideal test specimen for joint impact modeling was visualized (as in previous joint investigations) as a simple uniform structure with a single ring joint replica at the mid-span. Free-free boundary conditions would be used to avoid uncertainties in support constraints. As a result, the primary joint characteristics of interest (compliance, damping, impact noise generation) would dominate and be deducible from the test specimen dynamic response. The model joint replica design, while permitting considerable simplification, was required to simulate all of the important properties of a typical full scale missile ring joint including compliance, low interface preload, and similar assembly and interface contact characteristics. Additionally, the joint replica design approach must provide accurate and reliable means for measuring joint interface preload versus applied torque during assembly and as a function of time during creep investigations.

The joint replica designed to satisfy these requirements is illustrated in Figure 5-6. Joint preload is accomplished through a single strain gaged bolt on the center line of the aluminum test specimen, with this preload reacted circumferentially through a separate joint ring representing multiple joint interface contact surfaces. Interchangeable stainless steel "joint rings" provide a convenient means for investigating the effects of various joint interface materials. The model joint compliance is assumed to be provided primarily by the extensional elasticity of the center axis bolt estimated as follows:

$$C_{\theta} = \frac{\ell}{r^2 AE} \qquad (5.1)$$

where: ℓ = effective spring length, 3".

r = effective radius, 1.265 inches.

E = modulus of elasticity, 30 $(10)^6$ #/in^2.

A = cross sectional area of spring elements, in^2.

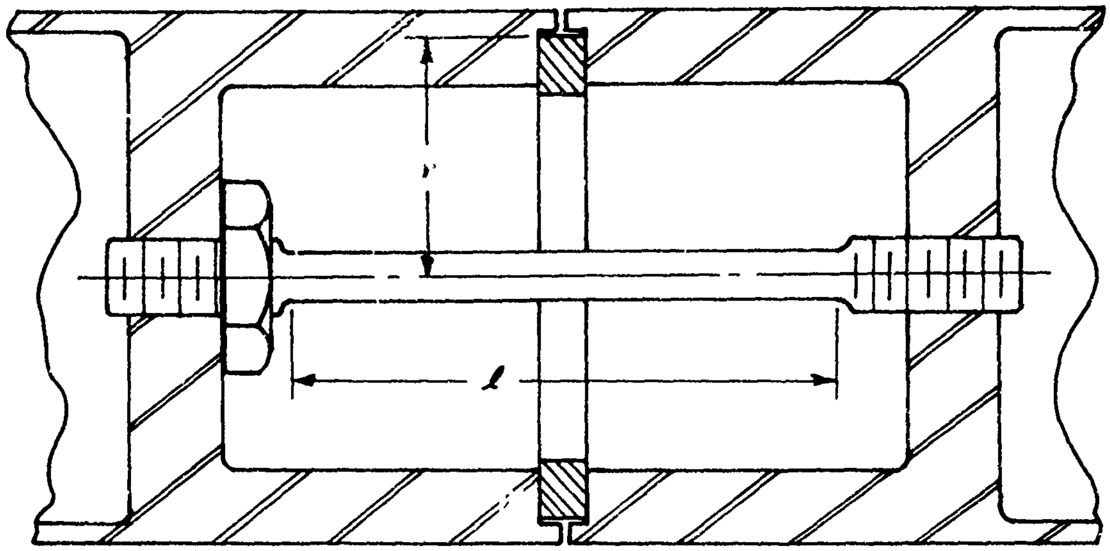

The center axis bolt is locked to one half of the model with a locking nut and the model assembled by applying preselected torques to the other half of the test specimen. The threads on the center axis bolt are lubricated to insure that the primary frictional torques in the joint assembly are associated with the contacting surfaces on the interface ring. The full scale ring joints described in Section 5.2 have estimated compliances ranging from $0.75(10)^{-8}$ to $2.7(10)^{-8}$ rad/in # and fall in the moderate to good joint compliance classification scale. A corresponding range for the model joint compliance was provided by making three center axis couplers with diameters from 1/8 to 3/8 inches. A direct comparison between model and full scale joint compliance is obtained by multiplying the full scale values by the cube of the full scale to model diameter ratio as follows:

CONFIGURATION	$C_\theta(10)^6$ Rad/In #
Full Scale X $(D_F/D_M)^3$	.88 - 3.2
Model	.57 - 5.1

Where: D_F = Full scale Missile Diameter, 13.5 inches

D_M = Model Diameter, 2.75 inches

5.3.1 Model Joint Preload. The relationship between joint preload - measured by strain gages on the center axis tension bolt - and applied torque was investigated for three joint interface coatings in addition to the basic clean dry joint. The results of these measurements are shown in Figure 5-7. The teflon coating, approximately 3 mils thick, was flame deposited by an application process identical to that used on the full scale rings discussed in Section 5.2. The Molybdenum Disulfide (MDS) Dry Film was applied using an aerosol spray; and the Silicon Grease, DC-4, was directly wiped on the joint interface surfaces. A thorough cleaning of the joint interfaces with solvent was performed between each test of a different coating material.

Both of the lubricants, MDS and DC-4, resulted, as might be expected, in a fairly significant increase in joint preload, ranging from 60 to 100 percent. The teflon coating, however, produced the largest increase in joint preload with a consistent and repeatable gain of greater than 5 over the basic unlubricated joint.

Teflon has a well recognized tendency to cold flow under load. To assess the implications of this behavior on the preload of a joint with teflon on the interface surfaces, a preload of 600 pounds was applied to the model joint and found to have been maintained with virtually no change after 64 hours. The estimated loading on the teflon for this condition was 318 psi, assuming uniform distribution over the joint interface.

5.3.2 Model Vibration Test Setup and Results. A sketch of the test setup used to evaluate the dynamic response characteristics of the ring joint model is shown in Figure 5-8. A free-free suspension was employed with the model oriented vertically to avoid any gravity moment bias on the joint. Force excitation was provided by an MB Electrodynamic Shaker, rated at 50 pounds peak force capability, monitored by a force gage at the input station on the test specimen. Triaxial response (acceleration) was monitored at the top end of the specimen to establish a total response reference, and both force and in-plane acceleration at the input station were monitored to provide a basis for estimating system damping. Although vibration induced by joint interface impact is propagated in all response coordinates, the longitudinal response ($\ddot{z}$) was concluded to provide the primary and most sensitive measure of joint impact induced response. The impact forcing function is assumed to be impulsive in nature with primary excitation at twice the transverse mode frequency with the response distributed over a broad frequency spectrum. Total impact induced noise was interpreted as the rms vibration over a 20-5000 κ hz bandwidth measured in thelongitudinal coordinate ($\ddot{z}$) at the response station on the test specimen. This broadband vibration level was then normalized by the vector sum of the inplane and crossplane transverse response at the excitation frequency to establish a noise ratio for the particular test condition.

Table 5-2 presents response data for the basic configuration with uncoated metalic surfaces at the joint interface. Test parameters include variations in both joint preload and excitation level. Estimates of system damping shown are based on calculated generalized mass and generalized force in the model response. The general trend is for frequency to increase with response level. Corresponding data for the test specimen with teflon at the joint interface is presented in Table 5-3. Considerable scatter in the response parameters is shown for both configurations at the lower preload and excitation levels, reflecting the nonlinearities and cross coupling in the test specimen response. The two higher values for joint preload used with the teflon configuration (200 and 400 pounds) are intended to represent a conservative estimate of the preload increase which would be realized over the basic configuration (50 to 100 pounds) for the same assembly torque. Particularly noteworthy is the fact that the teflon configuration at the higher preload levels exhibits pronounced decreases in impact noise ratio accompanied by significant increases in resonant frequency. The predicted relationship between test specimen 1st mode frequency and effective joint compliance is shown in Figure 5-9. Upper bound frequency test points are shown for the basic configuration assembled with 50 to 100 pounds for comparison with the teflon configuration assembled first with equal preload (50 to 100 pounds) and then with "equal" torque (200 to 400 pounds preload). Table 5-4 presents a comparison of the basic and teflon configuration response based on an arithmetic average of all test data with the following conclusions:

1. For comparable preloads, the teflon coating on the model joint interface reduced joint impact vibration by an average factor of greater than 2 while increasing mode damping by an average factor of greater than 2.

2. For comparable assembly torques, the teflon configuration reduced joint impact vibration by an average factor of nearly ten while maintaining and slightly increasing the improved damping attributed to the teflon. Additionally, the effective joint stiffness was found to be nearly a factor of 3 greater than the basic joint for the same torque, presumably because of the significantly higher joint preload realized with teflon.

5.4 FULL SCALE IMPLICATIONS OF MODEL TEST RESULTS

1. Joint interface impact can be a significant source of self-induced vibration.

2. The vibration generation mechanism requires physical separation at the joint interface for impact to occur.

3. Corrective measures would appear to include increasing preload to avoid interface separation and/or coating the impacting surfaces with a compliant material to attenuate the response.

4. Teflon as a candidate material for joint interface treatment has been shown in idealized model tests to produce a

substantial improvement in joint preload, reduction in self-induced vibration, and increase in joint contribution to structural damping.

5. Conflicting and mixed results obtained with partial teflon treatment of full scale noise susceptible joints are suspected to have been caused by neglecting to coat all of the primary joint interface surfaces.

6. The results to date in exploring joint interface coatings have shown some encouraging trends. Many questions remain unanswered, however, and more work is clearly needed before practical applications can be considered in actual missile structure.

Table 5-1
Measured Noise Ratios for Discontinuous Land Joint with Different Surface Treatments
Constant Assembly Torque 4500 in #

Config.	Application	Response Level (1)	Noise Ratio (2)
Basic	Dry Film Lube (MDS) on All Surfaces	1 2	3.37 8.30
Epoxy	All Surfaces (with parting agent) to Fill Voids	1 2	1.36 5.45
RTV	All Surfaces	1 2	1.19 2.62
Lead	Foil Tape on Non-Sliding Surfaces Only	1 2	1.35 2.52
Aluminum	Foil Tape on Non-Sliding Surfaces Only	1 2	1.70 1.98
Silicone	Thin Sheet Non-Sliding Surfaces Only	1 2	2.10 2.01
Teflon	Flame Deposited on Coupling Ring Only	1 2	1.12 1.14

(1)

Response Level	Dynamic Bending Moment Induced at Joint
1	3000 in #
2	5000 in #

(2) Noise ratio defined as ratio of broadband response to fundamental response (g_{BB}/g_F)

Table 5-2
Basic Joint Model Dynamic Response

Preload #	Freq f_1 hz	$\ddot{n}_T$ g's	% Cross Plane	Noise Ratio	Damping ζ
50	101	9.9	110	.19	.0078
50	106	16.7	117	.66	.0077
50	103	22.2	119	72	.0049
75	107	7.4	93	.11	.022
75	108	18.6	124	.78	.0095
75	108	24.7	116	.63	.0079
100	110	9.9	108	1.42	.046
100	113	11.5	86	.45	.017
100	109	20.3	109	.84	.0098

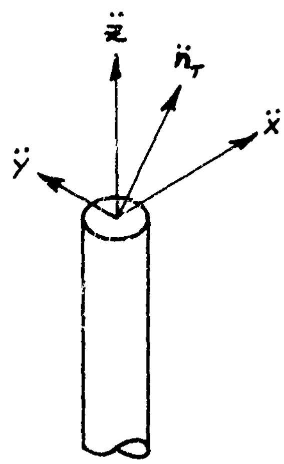

Where:

$\ddot{x}$ = inplane response at f_i

$\ddot{y}$ = crossplane response at f_i

$\ddot{n}_T$ = vector sum $\vec{\ddot{x}} + \vec{\ddot{y}}$

$\ddot{z}$ = broadband (20-5000 hz) response

Noise Ratio = $\ddot{z} / \ddot{n}_T$

Table 5-3
Teflon Coated Joint Model Dynamic Response

Preload Comparable to Basic Joint

Preload #	Freq. Hz	g's	% Cross Plane	Noise Ratio	Damping
50	111	8.5	138	.088	.094
	110	18.7	124	.69	.0072
	111	21.0	107	.86	.0055
75	137	7.7	116	.072	.014
	134	8.1	127	.11	.013
	97	11.8	30	.13	.073
	101	18.8	20	.38	.060
100	94	6.1	35	.033	.042
	122	16.3	129	.41	.007
	101	13.5	27	.096	.059
	104	20.4	19	.27	.058

"Torque" Comparable to Basic Joint

Preload #	Freq. Hz	g's	% Cross Plane	Noise Ratio	Damping
200	114	7.9	51	.026	.031
	150	15.2	114	.19	.013
	119	12.4	45	.039	.037
	120	18.5	43	.092	.048
400	153	8.1	19	.031	.034
	151	15.9	22	.063	.053
	143	33.2	27	.048	.049

Table 5-4
Basic/Teflon Joint Model
Dynamic Response Comparison

Configuration	Comparison Basis	Preload Range #	Average Noise Factor	Average Damping ζ
Basic	Reference	50-100	.644	.015
Teflon	Equal Preload	50-100	.285	.032
Teflon	Equal Torque	200-400	.070	.038

Noise Factor Reduction:

Equal Preload .285/.644 = .44

Equal Torque .070/.644 = .11

Damping Increase:

Equal Preload .032/.015 = 2.1

Equal Torque .038/.015 = 2.5

FIGURE 5-1

DISCONTINUOUS LAND RING JOINT

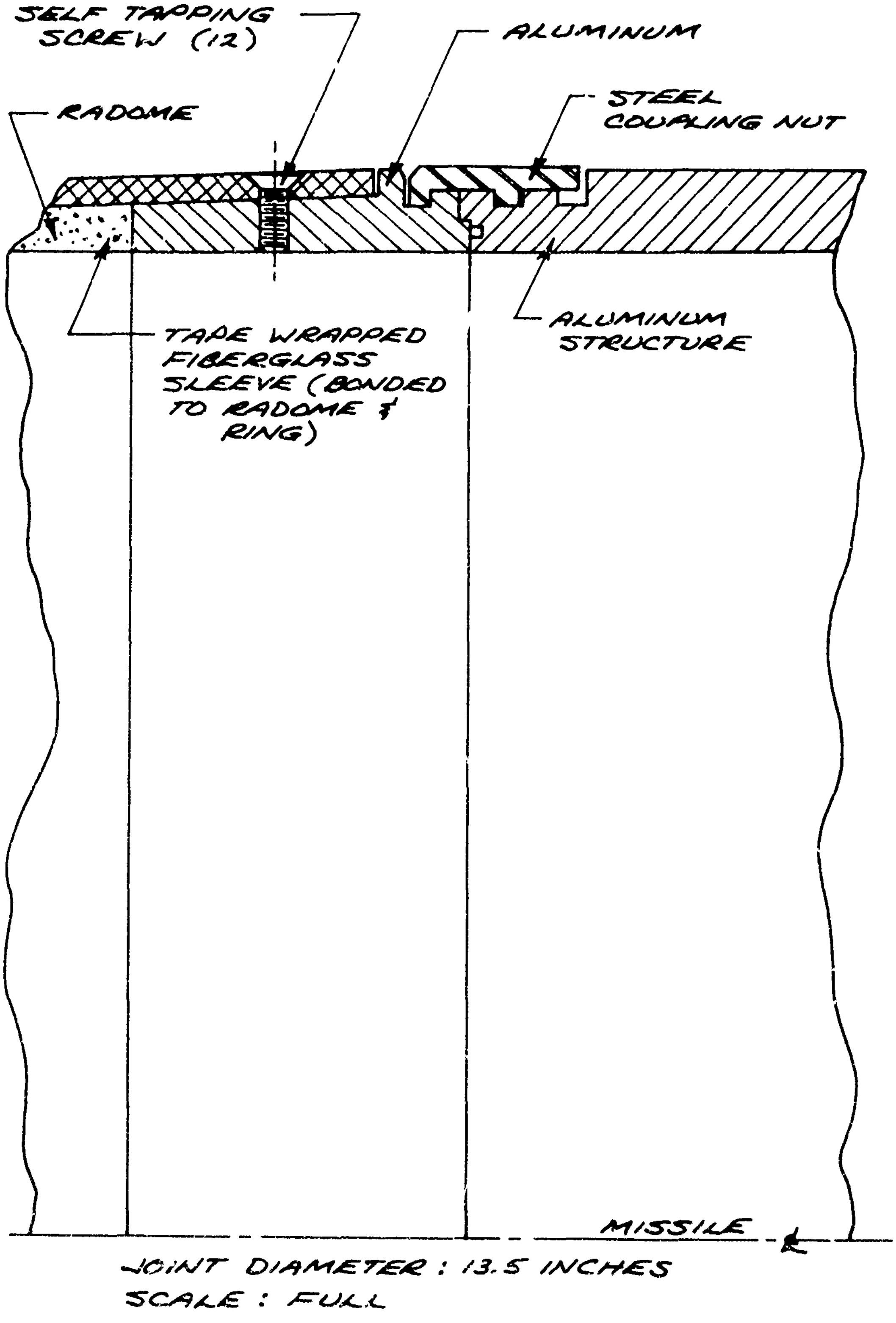

JOINT DIAMETER : 13.5 INCHES

SCALE : FULL

FIGURE 5-2

CONTINUOUS LAND RING JOINT

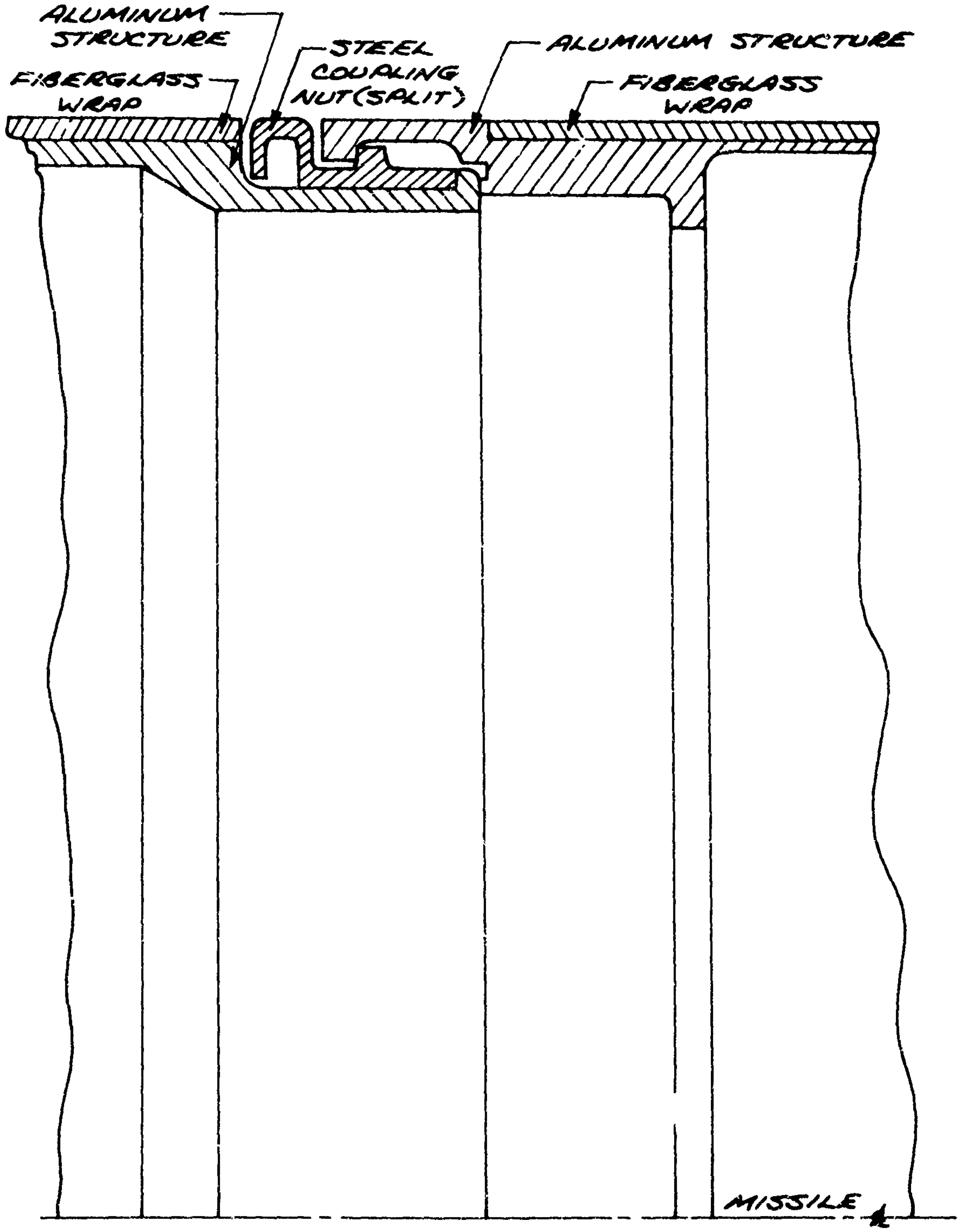

JOINT DIAMETER : 13.5 INCHES

SCALE : FULL

FIGURE 5-3

MISSILE JOINT INDUCED VIBRATION TEST SET-UP

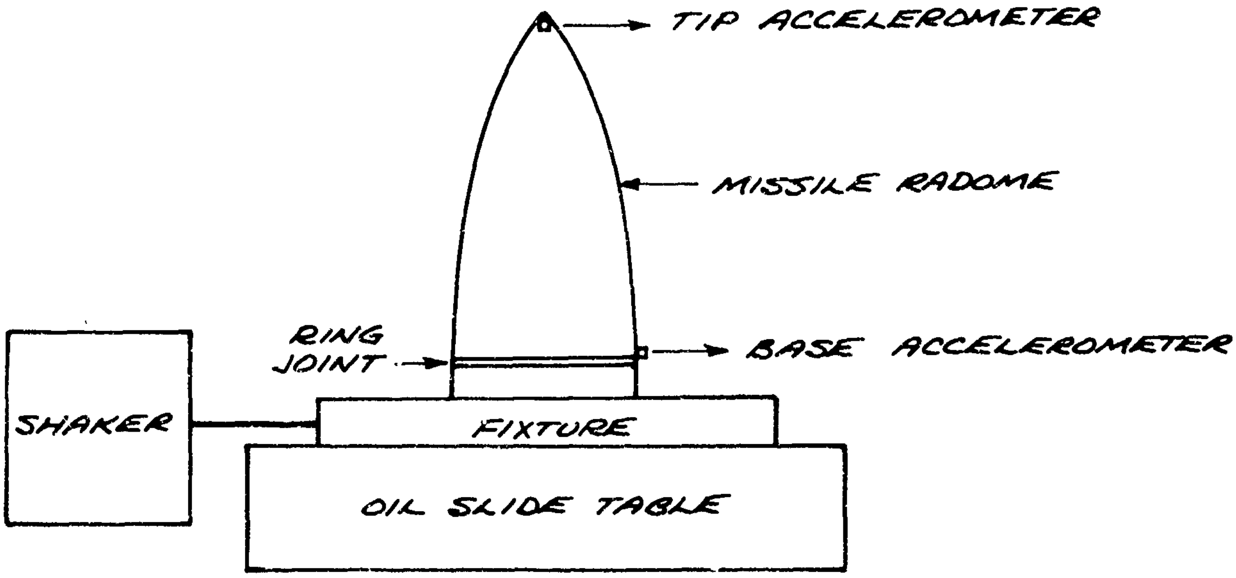

FIGURE 5-4

FLIGHT TEST MISSILE JOINT LOCATIONS

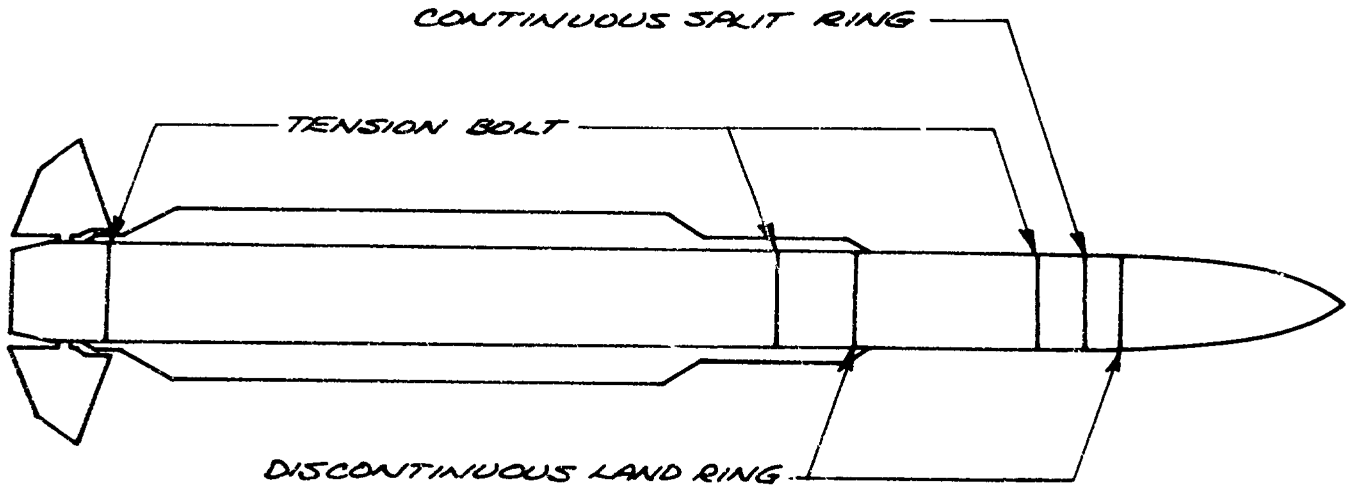

FIGURE 5-5

TEFLON COUPLING RING
JOINT IMPACT NOISE SUPPRESSION
VERSUS BASIC JOINT NOISE FACTOR

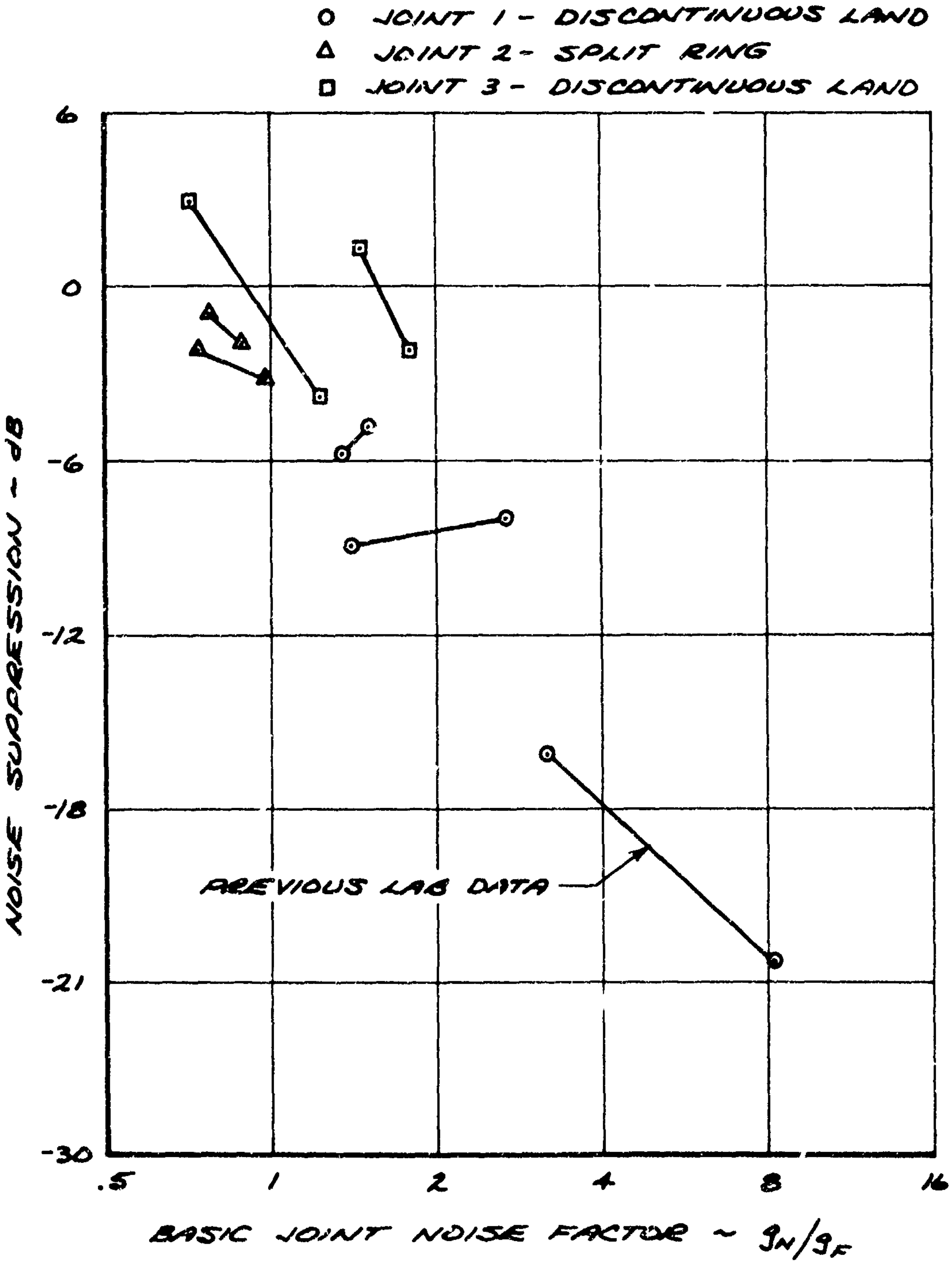

FIGURE 5-6

IDEALIZED RING JOINT MODEL

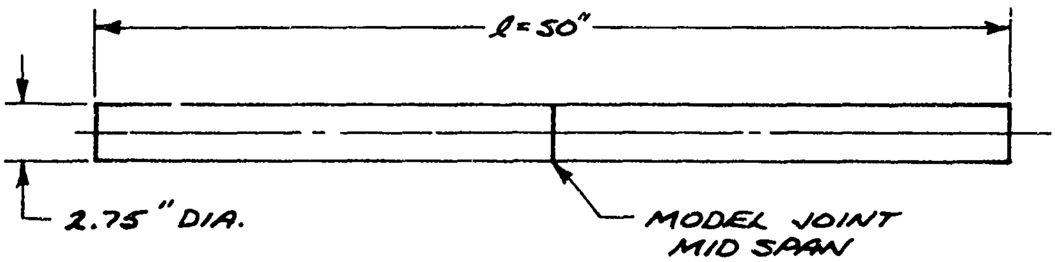

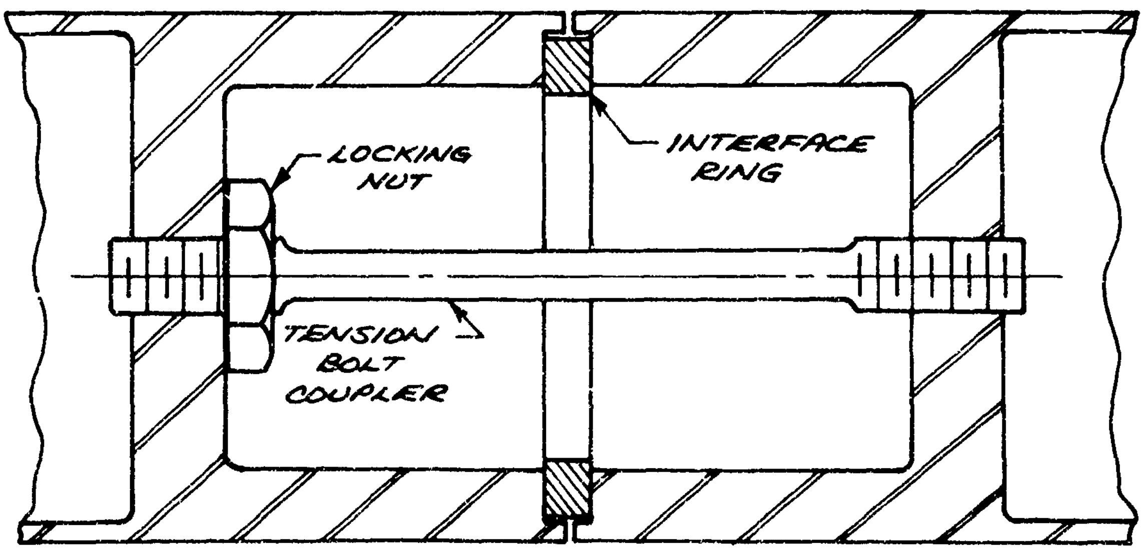

JOINT CROSS SECTION DETAIL

FIGURE 5-7

SCALE MODEL RING JOINT
PRELOAD VERSUS TORQUE

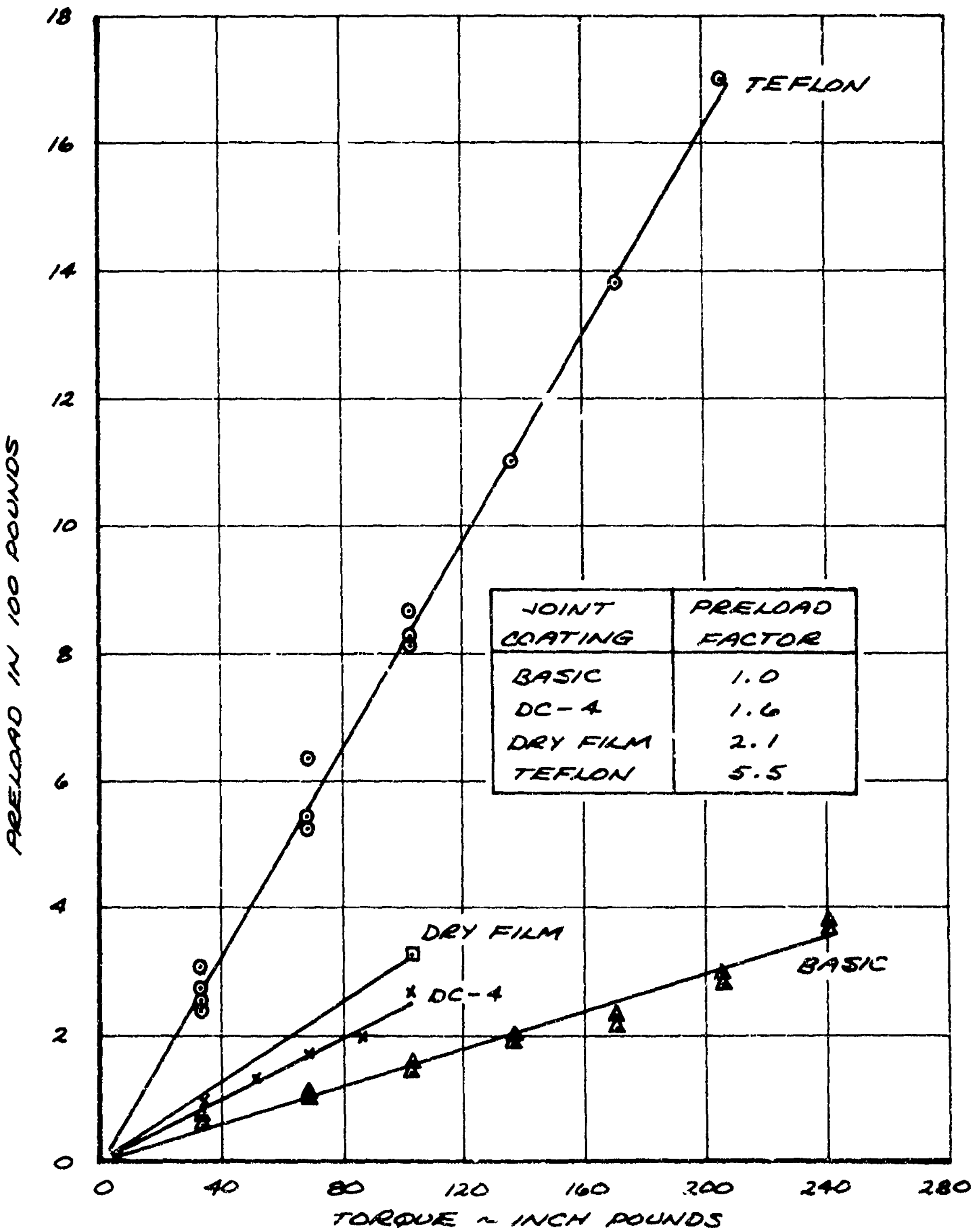

FIGURE 5-8

RING JOINT MODEL TEST SET-UP
(FREE-FREE SUSPENSION)

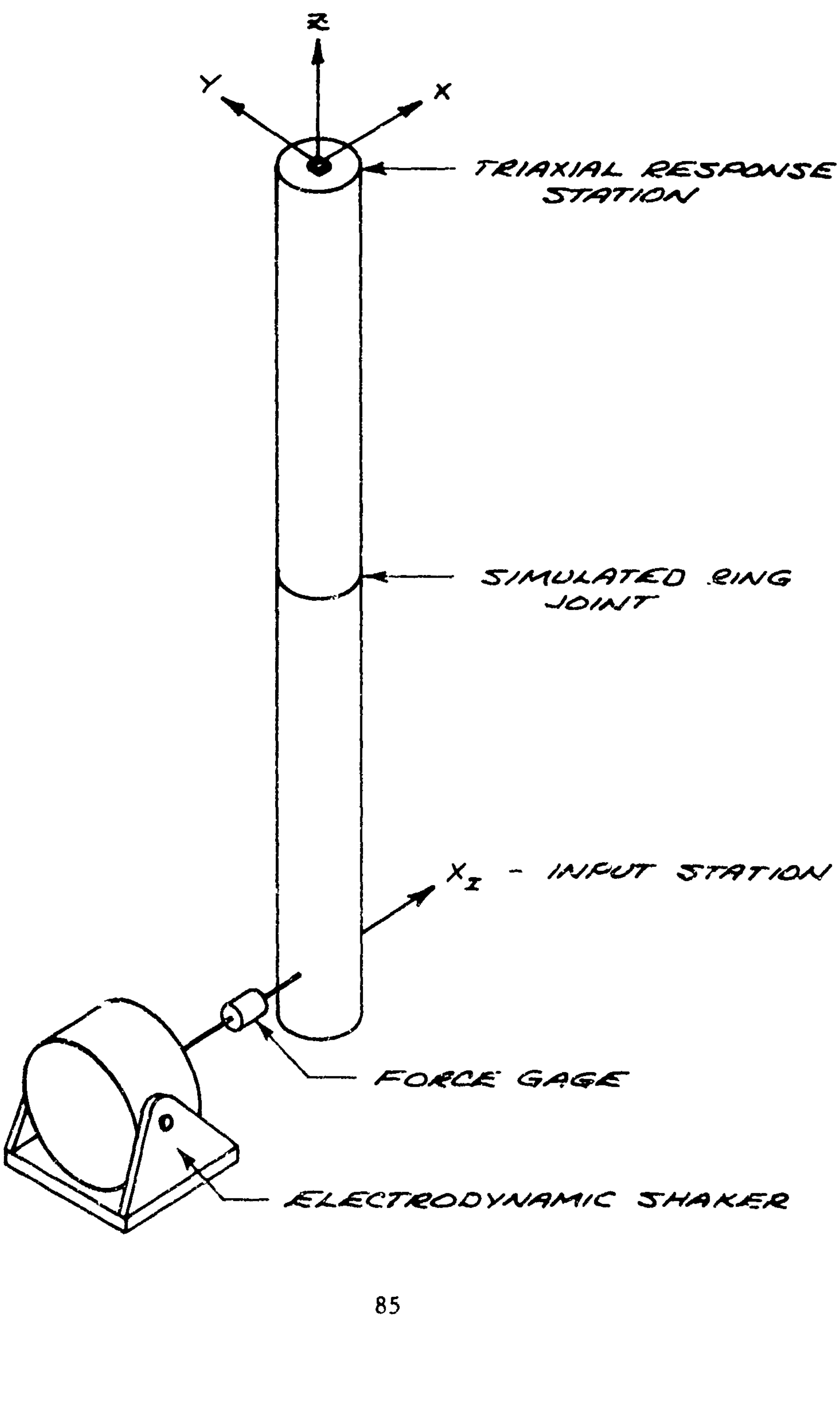

FIGURE 5-9

MODEL 1ST MODE FREQUENCY VERSUS EFFECTIVE JOINT COMPLIANCE

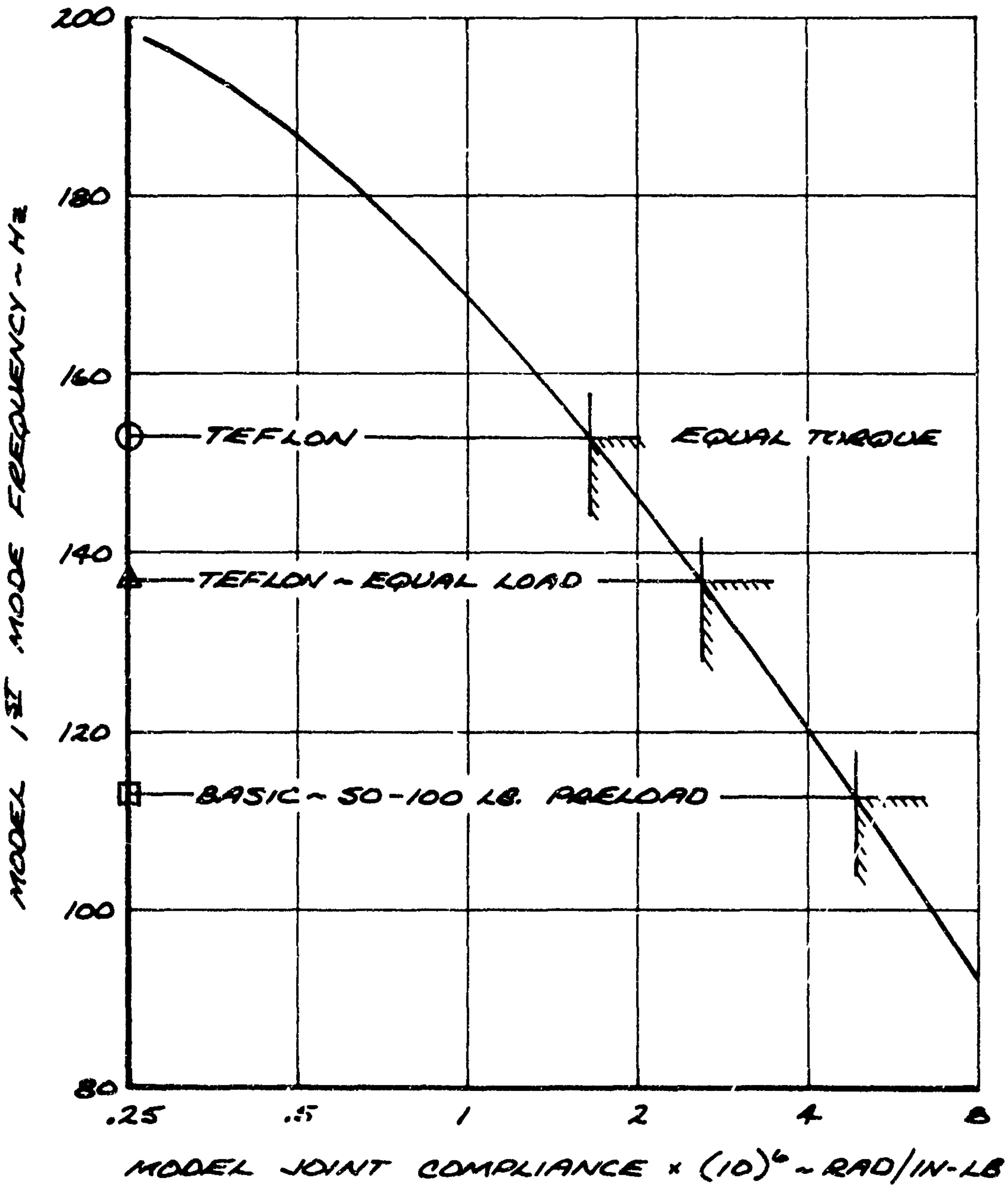

Section 6.0

INTEGRATION INTO OVERALL SYSTEM REQUIREMENTS

The study thus far has been concerned with structural dynamic characteristics of joints such as stiffness, tightness and damping. There are a number of other characteristics that influence the design of tactical missile airframe joints. These include strength, weight, volumetric efficiency, degree of enclosure, producibility and maintainability. A brief discussion of each of these topics is now presented to provide an overview of airframe joint characteristics.

A rating scheme is then developed which is intended to facilitate the integration of these various characteristics into the overall system requirements. The rating scheme will then be applied to three different joints as an illustration. The three joints, which are used in the Medium Range Standard Missile (RIM-66), are shown in Figures 6-1 thru 6-3.

6.1 SYSTEM CONSIDERATIONS

The airframe joints of a tactical missile possess attributes which must satisfy a number of requirements. The dominant requirements which will be considered here are strength, weight, volumetric efficiency, degree of enclosure, producibility and missile maintainability.

6.1.1 Strength

The static load carrying capability of the airframe of a typical tactical missile is often determined by the airframe joints rather than the shell structure between joints. The fatigue capability of the airframe is also frequently determined by the joints. The reason that airframe joints are relatively inefficient load carrying members when compared to the adjacent shell structure is associated with the distortion of the load path created by the presence of the joint.

The critical static strength requirements for airframe joints are frequently the bending moments that arise from lateral loading conditions such as handling of the assembled missile or free flight steering maneuvers. There are of course shear, torque and longitudinal load requirements imposed on airframe joints. However, the strength requirement that drives the design of tactical missile airframe joints is usually the bending moment.

The strength of a joint can be quite sensitive to design details that are sometimes quite subtle. Since stress concentrations play an important role in the strength of joints, considerations such as ductility of the material and avoidance of sharp or rapid transitions are important. The static strength of the three airframe joints that are studied in this section of the report provide an indication of the variation in strength. The strengths are listed below.

Joint Type	Illustration (Figure No.)	Strength (Inch-Pounds)
Continuous Land	6-1	104,000 to 209,000
Four Bolt Tension	6-2	231,000 to 347,000
Eight Bolt Tension	6-3	345,000 to 425,000

The variation in the strength for the first and third joints represent the effect of minor design changes that were implemented to improve the strength of the joint. The variation in the strength of the second joint is due to a combination of material property and dimensional differences.

A measure of the strength efficiency of a joint can be developed by rationing the strength of the joint to the flexural strength of the adjacent shell structure.

Joint Type	Strength Efficiency - (%)
Continuous Land	28 to 57
Four Bolt Tension	41 to 62
Eight Bolt Tension	62 to 76

6.1.2 Weight

The weight of a joint is defined as the weight of the airframe in the vicinity of the joint less the weight of the thin shell sections if they were extended to the joint interface. Thus it is seen that the build-up in the shell adjacent to a joint is included as part of the weight of the joint. The weight of the fasteners, covers and fairings associated with the joint are also included in the weight figure. The weight of each of the three joints was calculated using the approach outlined above. The weight of the three joints is listed below.

Joint Type	Weight (Pounds)
Continuous Land	3.83
Four Bolt Tension	8.81
Eight Bolt Tension	8.80

A measure of the weight efficiency of a joint can be developed by ratioing the weight of the thin shell sections over half a body diameter if no joint were present to the weight of the same region of the structure with the joint present. This efficiency is of course referenced to the thin shell section which may not have been designed for minimum weight.

Joint Type	Weight Efficiency - (%)
Continuous Land	37
Four Bolt Tension	26
Fight Bolt Tension	48

6.1.3 Volumetric Efficiency

The presence of joints in an airframe influence the volume available to package the electronics, propulsion and ordnance. A measure of volumetric efficiency that reflects the influence that joints have on packaging volume is the open cross sectional area of the joint. The volumetric efficiency of the three joints are tabulated below.

Joint Type	Volumetric Efficiency
Continuous Land	86%
Four Bolt Tension	91%
Eight Bolt Tension	54%

The first and second joints are quite efficient with respect to volume required while the third joint is inefficient in that it occupies almost one half of the cross sectional area.

The significance of volumetric efficiency is dependent upon the design application. If the design is such that the packaged volume must pass thru the inside diameter of the joint, the volume penalty is experienced over the entire length of the packaged item. Thus a substantial volume penalty would be incurred for such an application. However, if the packaged volume need not pass thru the inside diameter of the joint, the volume penalty is experienced only over the relatively short length of the joint. Applications in which the packaged volume need not pass thru the inside diameter of the joint are usually those in which the entire packaged volume is loaded from the opposite end of the airframe section. The volume constraint of the joint on the opposite end is then of course the governing factor.

6.1.4 Degree of Enclosure

The sealing or degree of enclosure characteristics of joints are a consideration in most tactical missile applications. It is generally preferable to provide sealing at the airframe joints for the entire interior of the missile rather than for selected sensitive components. The purpose of the seal is to preclude the entrance of moisture, sand and dust.

Sealing of airframe joints is generally accomplished by using elastomeric O-rings in the joint interface. Typically an annular groove is machined in one of the mating surfaces and the O-ring is sized such that it is stretched when installed in the groove. The tension in the installed O-ring provides for the retention of it during assembly of the joint.

The O-ring provides sealing of the primary potential leakage path to the interior of the airframe. There are however, a number of secondary leakage paths that must be sealed with certain joint designs. The eight bolt tension joint shown in Figure 6-3 is an example of a design that has potential secondary leakage paths. The eight fasteners pass from the exterior to the sealed interior of the airframe. This provides eight potential leakage paths. Sealing of the fastener assembly is accomplished by providing a spotfaced surface on the casting under the washer. The machined surfaces and the contact stresses generated on assembly of the joint provide sealing of the fastener areas. Other joint designs such as the discontinuous land shown in Figure 6-1 and the four bolt tension shown in Figure 6-2 preclude the existence of secondary leakage paths by keeping the fastener totally external to sealed interior.

6.1.5 Producibility

The producibility attribute of a joint design is concerned with the cost of manufacturing the joint hardware. Since costs are highly dependent upon production quantities, no attempt will be made here to generate quantitative cost figures. Rather the producibility of the joint will be based upon the complexity of the machining involved in fabrication of the hardware.

The continuous land joint shown in Figure 6-1 has three machined elements. Two of the machined elements are complex in that a large acme thread surface and tight tolerances are involved. The two elements are the split coupling nut and the mating female surface. Thus the producibility of this joint design is rated low.

The four bolt tension joint shown in Figure 6-2 has six machined elements, four of which are simply bolts. The two major elements require only straight forward machining to moderate tolerances. Thus the producibility of this joint design is rated high.

The eight bolt tension joint shown in Figure 6-3 has two major machined elements plus eight fastener assemblies. The tolerances involved are moderate, but the geometry of the assembly is such that an elaborate casting is required for one member and considerable machining is required on the other member to minimize weight. Thus the producibility of this joint design is rated low.

6.1.6 Maintainability

The ease of assembly and disassembly of a joint design effects both the producibility and maintainability of tactical missiles. Extensive functional testing of the missile electronics is performed during both manufacturing and deployment. All repair work and certain types of functional testing require disassembly of the airframe joints. Logistic policies also commonly require periodic disassembly of the joints. The time and equipment required to assemble and disassemble as well as the opportunity for human error or damage to the hardware become important considerations when large quantities of hardware or frequent testing are involved.

The maintainability of the joint hardware itself is limited to inspection of the hardware such as the machined surfaces at disassembly and replacement of the O-rings and possibly certain of the fasteners at reassembly.

The ease of assembly and reassembly of the continuous land joint is somewhat greater than that of the four and eight bolt tension joints. Although the continuous land joint has a single fastener that requires roughly only one full turn to engage or disengage, it is difficult to position to start the thread engagement. The tension bolt joints are easier to position but the need to individually torque each fastener on assembly is time consuming.

6.2 INTEGRATION METHOD

The various attributes of airframe joints that were discussed in section 6.1 plus the structural dynamic attributes must be considered in an integrated fashion to produce an overall rating of different joint designs. This is accomplished by assigning a figure of merit to the individual joint attributes, a relative weighting among the attributes, and finally summing the ratings over the attributes.

The three joints shown in Figures 6-1 thru 6-3 will be rated as an illustration. Equal weightings among the attributes are used, although unequal weightings can of course be used to emphasize or deemphasize certain attributes relative to the others. The four ratings of excellent, good, fair and poor are used for the attributes based on the quantitative and qualitative factors proposed in Table 6-1. In addition to the joint attributes discussed in Section 6.1, the structural dynamic attributes of stiffness and tightness are included in Table 6-1. The stiffness rating is the NASA rating discussed in Reference 3. The tightness attribute refers to self induced noise characteristics that are discussed in Section 5 of the present report.

The illustrative rating comparison for the three joints (Figures 6-1 thru 6-3) is presented in Table 6-2. Using equal weightings for each of the eight joint attributes results in the best overall rating for the four bolt tension joint. The overall rating using equal weighting factors, does not reveal large differences between the three joints. However, the use of unequal weighting factors in which certain attributes are assigned very high or very low emphasis would produce more dramatic differences in the overall ratings.

Table 6-1
Proposed Joint Attribute Rating Basis

Attribute	Measure or Units	Rating			
		Excellent	Good	Fair	Poor
Stiffness[1]	Inch-Pounds/Radian	$(10)^{10}/C$	$(10)^{9}/C$	$(10)^{8}/C$	$(10)^{7}/C$
Tightness	Noise generation	Low			High
Strength Efficiency	Per cent	>75	75 to 50	50 to 25	<25
Weight Efficiency	Per cent	>60	60 to 40	40 to 20	<20
Volumetric Efficiency	Per cent	>90	90 to 70	70 to 50	<50
Degree of Enclosure	No. of locations requiring sealing	1	2 to 5	>5	Unsealable
Producibility	Manufacturing cost	Low			High
Maintainability	Ease of assembly and disassembly	Simple			Difficult

(1) NASA stiffness rating as defined on page 16 of Reference 1, $C = (20/D)^3$, D = body diameter in inches.

Table 6-2
Illustrative Rating Comparison for Three Joints

Attribute	Ratings (1)		
	Continuous Land	Four Bolt Tension	Eight Bolt Tension
Stiffness	F	G	F
Tightness	P	G	G
Strength	G	G	E
Weight	G	F	G
Volume	G	E	F
Degree of Enclosure	E	E	F
Producibility	F	E	F
Maintainability	E	G	F
Overall	G(-)	G	F(+)

(1) E = Excellent, G = Good, F = Fair, P = Poor

FIGURE 6-1

CONTINUOUS LAND RING JOINT

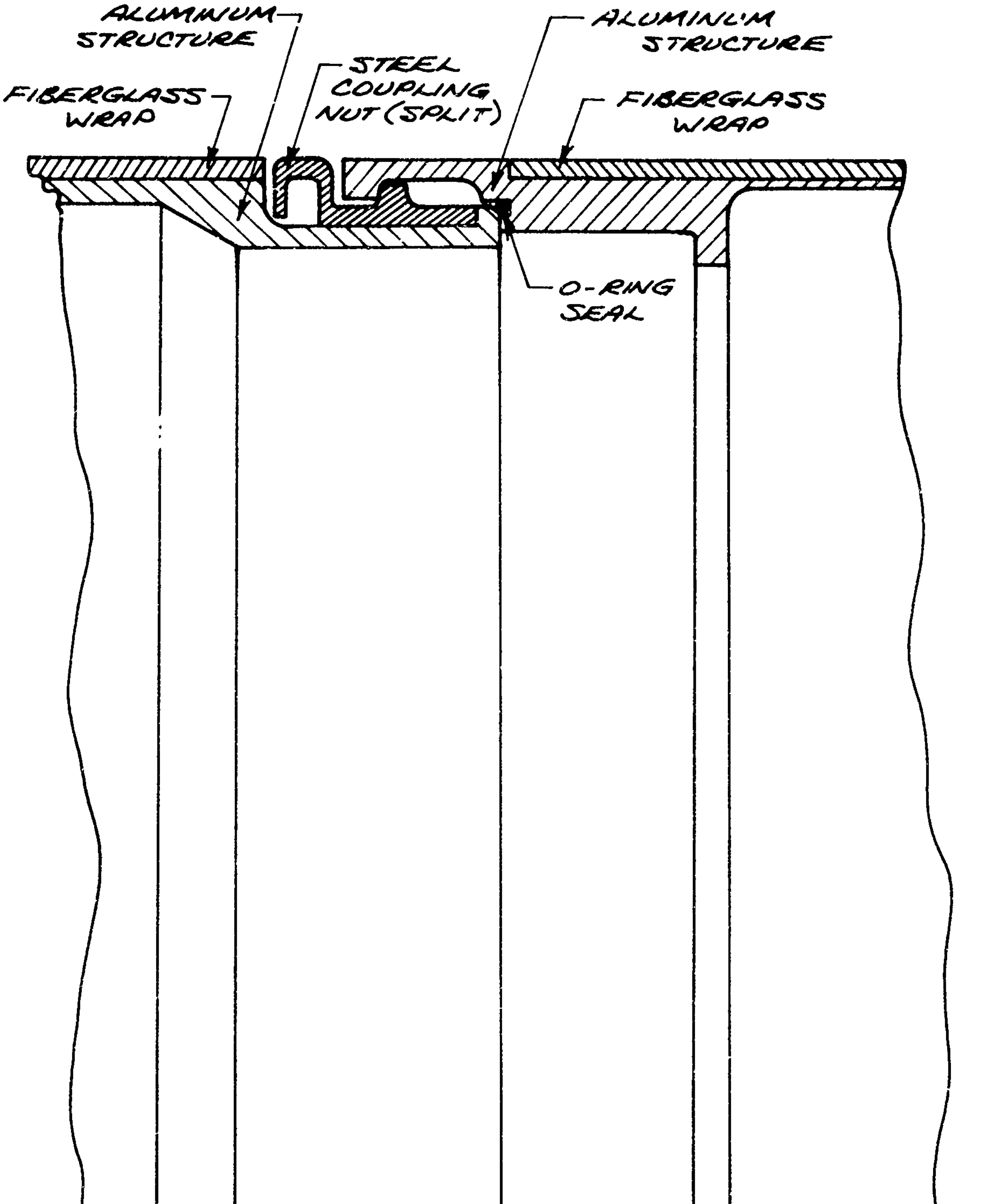

JOINT LOCATION: 22% AIRFRAME LENGTH

JOINT DIAMETER: 13.5 INCHES

SCALE: FULL

FIGURE 6-2

FOUR BOLT TENSION JOINT

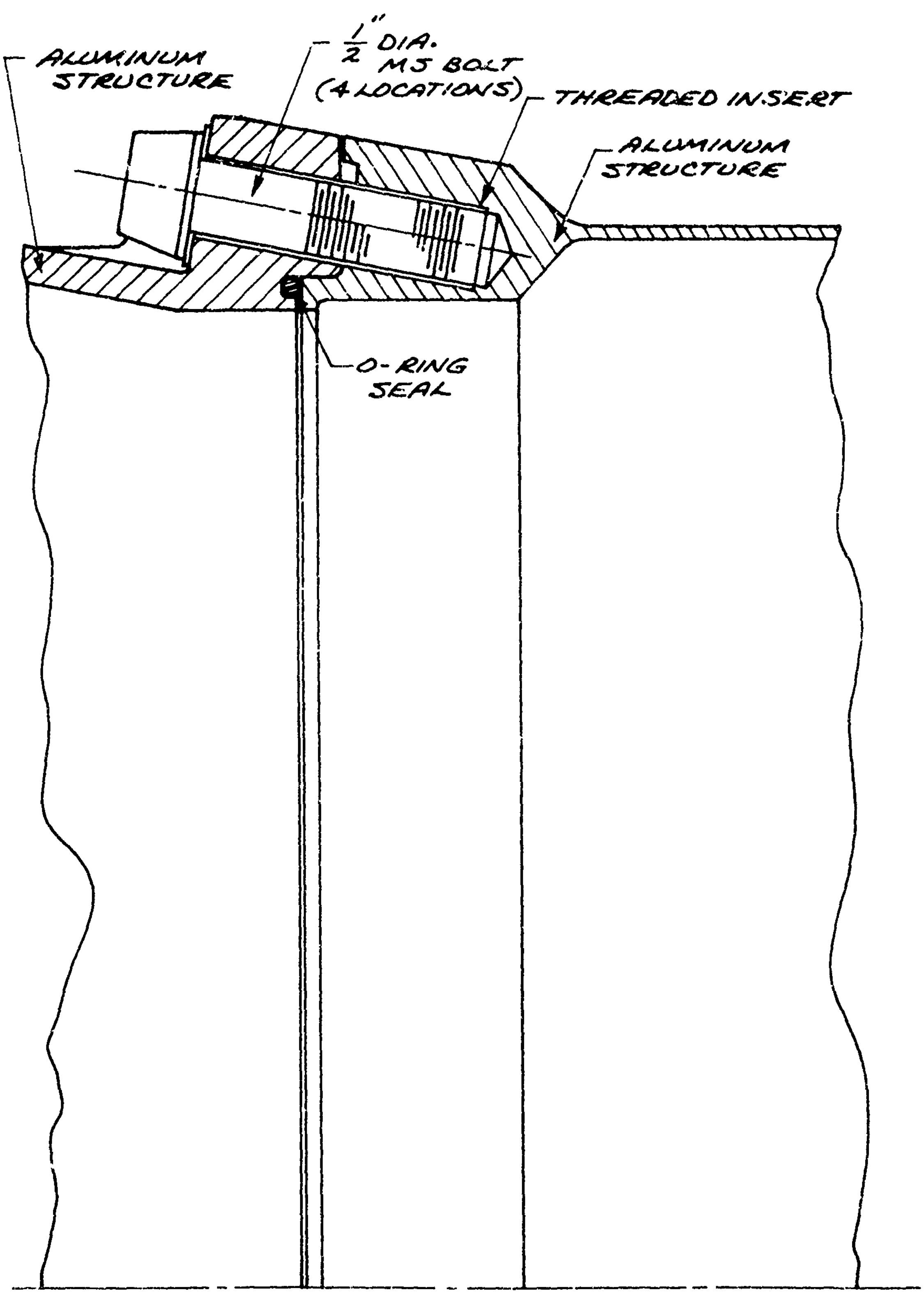

JOINT LOCATION : 35 % AIRFRAME LENGTH

JOINT DIAMETER : 13.5 INCHES

SCALE : FULL

FIGURE 6-3

EIGHT BOLT TENSION JOINT

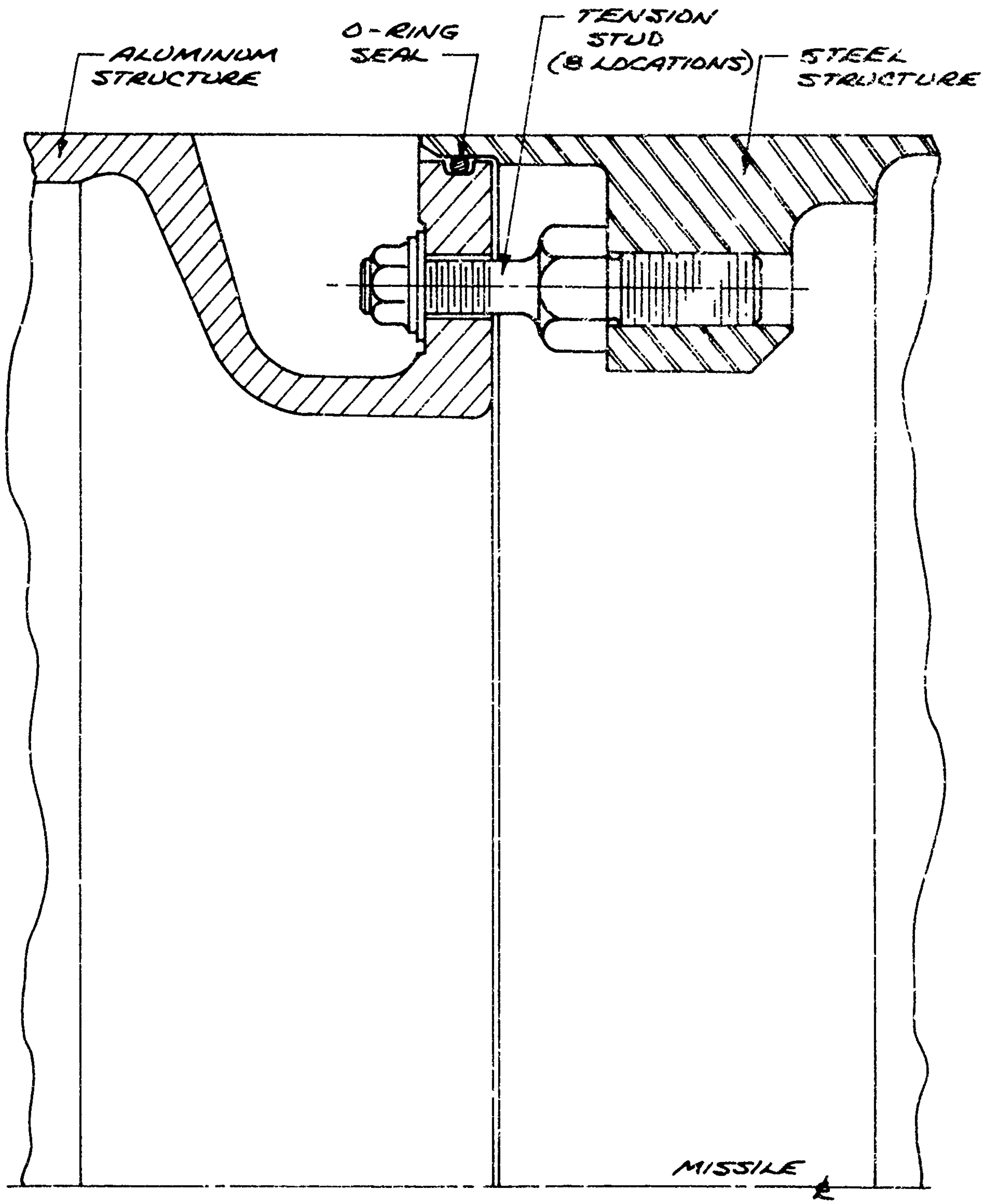

JOINT LOCATION : 41 % AIRFRAME LENGTH

JOINT DIAMETER : 13.5 INCHES

SCALE : FULL

REFERENCES

1. Maloney, J. G., Shelton, M. T., and Underhill, D. A., "Structural Dynamic Properties of Tactical Missile Joints - Phase I", General Dynamics, Pomona Division Report No. CR-6-348-945-001, June 1970.

2. Maloney, J. G. and Shelton, M. T., "Structural Dynamic Properties of Tactical Missile Joints - Phase 2", General Dynamics, Pomona Division Report No. CR-6-348-945-002, September 1971.

3. Alley, Jr., V. L. and Leadbetter, S. A., "The Prediction and Measurement of Natural Vibrations on Multistage Launch Vehicles", American Rocket Society Launch Vehicles: Structures and Materials Conference Report, April 1962.

4. Hall, B. M., Calkin, E. D. and Sholar, M. S., "Linear Estimation of Structural Parameters from Dynamic Test Data", AIAA/ASME 11th Structures, Structural Dynamics, and Materials Conference, Denver, Colorado, April 22-24, 1970.

5. McIntyre, K. L., "Modified Holzer-Myklestad Modal Analysis Final Report - CWA 245", General Dynamics/Pomona TM-348-15.1-3, July 24, 1961.

6. Householder, A. S., Principles of Numerical Analysis, McGraw Hill; New York, 1953.

7. Fox, R. L. and Kapoor, M. P., "Rates of Change of Eigenvalues and Eigenvectors", AIAA Journal, Vol. 6, Number 12, December 1968, p. 2426.

APPENDIX

JOINT COMPLIANCE EXTRACTION CODE

USER'S MANUAL

LIST OF TABLES AND FIGURES

INTRODUCTION

The computational system used for implementing the method of analysis described in Section 4 is composed of the following two digital computer programs:

1) Program FILLIN
2) Program JOINTS

Computer program FILLIN is a small prelude program that accepts measured modal data obtained at a set of test missile stations and interpolates these data to provide "measured" modal data at a set of missile stations consistent with theoretical modal data calculated within computer program JOINTS. This preliminary step is needed so that a comparison of experimental and theoretical modal data at identical missile stations can be made within computer program JOINTS.

Within the Appendix input data instructions, data output and program limitations are discussed for both computer programs FILLIN and JOINTS. Computer program FORTRAN listings and a sample application data deck listing are also presented.

PROGRAM FILLIN

Because comparisons between experimental and theoretical modal data are made at all modal analysis stations, within computer program JOINTS, computer program FILLIN was written to provide interpolated measured modal data for the modal analysis stations. The resulting interpolated measured mode shape deflections and slopes are punched on cards for the complete set of modal analysis missile stations in a format acceptable for subsequent input to computer program JOINTS.

Usually, only mode shape deflections are measured in the laboratory while both mode shape deflections and slopes are computed. Therefore, an added feature of computer program FILLIN is the computation of mode shape slopes from the measured mode shape deflection data.

Computer program FILLIN has the following restrictions:

1) There must be at least two experimental points on each appendage (to establish slope).

2) There must be at least two experimental points on either side of a joint (to establish shear discontinuity).

Computer program FILLIN and JOINTS were written to be run on the CDC 6400 digital computer with 32K words of memory storage, under control of the CDC 6000 Series Scope Monitor System (Version 3.3), at General

Dynamics, Pomona Division. All programs and subroutines are written in the CDC 6400 FORTRAN Extended Language (Version 3.0) and should be easily implemented on any machine having a FORTRAN IV compiler. Input/output devices required are the card reader (logical unit 60), the line printer (logical unit 6) and the card punch.

Computer program FILLIN is composed of the following routines:

1) Program FILLIN

2) Subroutine SQUARE

3) Subroutine PARAB

4) Subroutine LINFIT

In addition, FORTRAN library routines EOF (end of file) and EXIT are called. FORTRAN listings of these four routines comprising computer program FILLIN are presented in Tables A-4 through A-7.

The input data instructions showing card formats for computer program FILLIN are presented in Table A-1. A listing of a sample data deck is presented in Table A-15. Data output consists of a listing of the input data and the interpolated experimental data (mode shape deflections and slopes) computed at all modal analysis stations. It is suggested that the results obtained from computer program FILLIN be checked before using the punched output as input to program JOINTS.

PROGRAM JOINTS

A simplified flow diagram of computer program JOINTS is presented in Table A-2. The procedure for joint compliance extraction is described as follows:

1) A starting value of joint compliance is assumed for each joint at which the compliance is unknown (initially from the input data).

2) Modes and the resulting cost function and first order gradients are computed for this initial configuration.

3) Each unknown joint compliance is varied independently from the trial configuration.

4) Modes and the resulting cost function and first order gradients are computed for each of these configurations obtained in Step 3.

5) Second order gradients are computed from the finite differences of the results obtained in Step 4.

6) A new trial set of joint compliances is calculated using the first and second order gradients terms.

7) If the trial set of compliances has converged within a specified tolerance, the analysis stops. Otherwise Step 2 is reentered and the analysis continues.

These seven steps comprise a cycle of iterations (a configuration for each of the unknown springs plus the nominal configuration). A detailed description of the computational procedure for first and second order gradients and the new trial spring rates is presented in Section 4.

A brief description of the mathematical model of a missile is presented here to aid in understanding the input data to program JOINTS. A missile is modeled using a lumped parameter representation. A typical model is shown below.

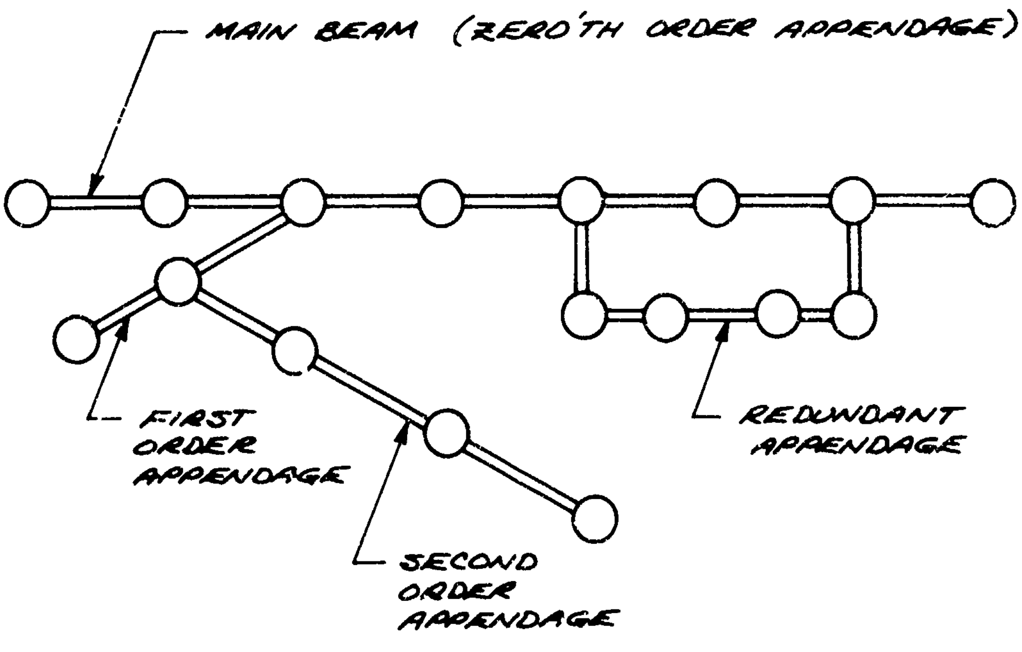

Appendage attachment angles are defined by the following diagram.

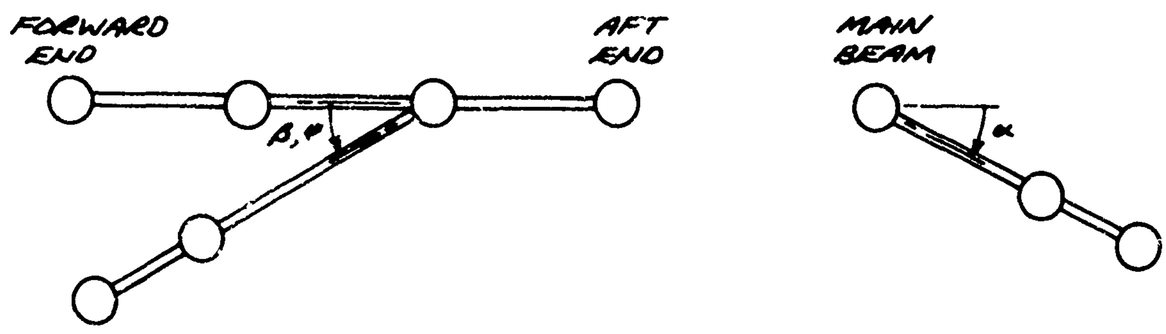

If this is the top view, the marked angle is φ. If this is the side view, the marked angle is β.

End view of main beam looking aft.

The following five types of stations are available for modeling missile system:

1) mass

2) spring

3) appendage attachment

4) forward redundant appendage attachment

5) aft redundant appendage attachment

When modeling a system for input to the computer, each station input can perform only one function, that is, a mass station cannot have a spring associated with it or be an appendage attachment station.

The main beam or zero order appendage must be input first. The first station on the main beam must be labeled one. After that, any other positive integer may be used as a station identification number. As a general practice, station identification numbers should be unique since appendage attachment designations are made using these identification numbers. Simple appendages are entered next starting from their free end. Redundant appendages are entered last starting from their forward attachment end. Within the main beam or any appendages, station location values must be entered in increasing order (consecutive stations may have equal station locations). Redundant appendages must lie along the main beam and have the same type of motion (bending, torsion or longitudinal) as the main beam. Redundant appendages may not overlap but simple appendages may be attached to redundant appendages.

Complications arise due to the manner in which the Myklestad subroutine in Computer Program JOINTS functions. The number of stations in the actual mathematical model of a missile (input stations) is added to by the Myklestad subroutine for the following reasons:

1) A joint is represented by a single input station. However, for computations, a second station (at the same location) is needed to define the displacement and slope discontinuities at the joint.

2) At appendage attachment stations, an additional station is added (at the same location) to show the shear and moment discontinuities at the attachment station.

3) For each appendage and for the main beam, an additional station is added at the end of each beam system (at the same location as the last station) to allow for imposition of the boundary conditions.

Computer Program JOINTS is composed of the following routines.

1) Program JOINTS

2) Subroutine STEEP

3) Subroutine ALTER

4) Subroutine RENORM

5) Subroutine MYKL

6) Subroutine MEMSET

7) Subroutine MATNF5

In addition, FORTRAN library routines EOF (end of file), EXIT, SQRT, ABS, LABS, LOCF (storage address of variable in machine), SIN and COS are called. FORTRAN listings of these seven routines comprising computer program JOINTS are presented in Tables A-8 through A-14.

Computer program JOINTS and FILLIN have the following size limitations:

1) A maximum of 100 theoretical missile stations

2) A maximum of 10 experimental and theoretical modes

3) A maximum of 10 redundant appendages

The input data instructions showing card formats for computer program JOINTS are presented in Table A-3. A FORTRAN listing of the program and its subroutines is presented in Table A-8 thru A-14. A listing of a sample data deck is presented in Table A-16.

Data output from the program consists of a listing of the input data, the input configuration for each iteration, a comparison of experimental and theoretical modes (deflections and slopes) and frequencies and cost function data for each iteration.

SAMPLE APPLICATION

A sample application is included to assist the user in checkout of the codes. Assume three experimental modes for a missile have been measured in the laboratory. A 59 station mathematical model has been developed, which includes two simple appendages and one redundant appendage. Three theoretical modes are to be computed and four joint compliances are to be extracted from the measured data using computer program JOINTS.

First, computer program FILLIN is run to determine the experimental mode shape deflections and slopes at the modal analysis stations. The data deck listing for computer program FILLIN is presented in Table A-15.

With the experimental mode shape deflections and slopes defined at the desired stations, computer program JOINTS is then run. The data deck listing for computer program JOINTS is presented in Table A-16. The entire output listing from the computer program is not presented because of the large quantity of output. Key output data are given in Table A-17. Certain of the results are plotted in Figure A-1. Other application examples are presented in Section 4 of this report.

GENERAL DYNAMICS
Electro Dynamic Division
POMONA OPERATION

TABLE A-1

INPUT DATA INSTRUCTIONS FOR COMPUTER PROGRAM FILLIN

~~FORTRAN CODING AND DATA FORM~~

PROBLEM: PROGRAM FILLIN

PROGRAMMER: D.O. RIFE

ONE GENERAL TITLE CARD

MYKLESTAD FORMAT BEAM DESCRIPTIONS OF STATIONS AT WHICH MODE SHAPE DEFLECTIONS AND SLOPES ARE DESIRED (CARD FORMAT - 2I4, 3I2, 2X, 7E8.0)

```
ID(1) IA(1) IT(1) ... XSTA(1) ... COMP1(1) COMP2(1)
ID(2) IA(2) IT(2) ... XSTA(2) ... COMP1(2) COMP2(2)
  :     :     :         :           :        :
ID(K) IA(K) IT(K) ... XSTA(K) ... COMP1(K) COMP2(K)
  :     :     :         :           :        :
```

ID(I) - STATION IDENTIFICATION COUNTER FOR STATION I. ID(I) > 0

NOTE: THE FIRST STATION OF THE MAIN BEAM MUST BE LABELED 1, I.E. ID(1) = 1

AS A GENERAL PRACTICE, STATION IDENTIFICATION COUNTERS SHOULD BE UNIQUE SINCE APPENDAGE ATTACHMENT STATION NUMBERS REFER TO THESE IDENTIFICATION COUNTERS.

IA(I) - APPENDAGE ATTACHMENT STATION IDENTIFICATION NUMBER FOR STATION I. IA(I) ≥ 0

NOTE: EXCEPT FOR MAIN BEAM IN WHICH IA(I) = 0, THE APPENDAGE ATTACHMENT STATION IDENTIFICATION NUMBER MUST REFER TO A STATION ID. COUNTER, I.E., IA(I) = ID(J) FOR A STATION J IN WHICH IT(J) = 2

(WITHIN AN APPENDAGE, ALL APPENDAGE ATTACHMENT NUMBERS ARE EQUAL)

IT(I) - DESIGNATION OF STATION TYPE FOR STATION I

0 - MASS STATION

1 - SPRING STATION

2 - APPENDAGE ATTACHMENT STATION

3 - FORWARD REDUNDANT APPENDAGE ATTACHMENT STATION

4 - AFT REDUNDANT APPENDAGE ATTACHMENT STATION

NOTE: ENTER ALL REDUNDANT APPENDAGES LAST STARTING FROM THE FORWARD END.

GENERAL DYNAMICS
Electro Dynamic Division
POMONA OPERATION

TABLE A-1 (CONT'D)

~~FORTRAN CODING AND DATA FORM~~

PROBLEM

PROGRAMMER

```
XSTA(I)  - STATION LOCATION OF STATION I - INCHES
           NOTE: WITHIN THE MAIN BEAM OR ANY APPENDAGE, XSTA(I+1)≥XSTA(I)
                 (A STATION LOCATION IS NEEDED FOR EACH CARD INPUT, CAN BE ZERO)

COMP1(I) - SHEAR COMPLIANCE FOR STATION I - IN/LB                COMP1(I)>0.0
           NOTE: ENTER A VALUE HERE ONLY IF IT(I)=1

COMP2(I) - FLEXURAL COMPLIANCE FOR STATION I - RAD/IN*LB         COMP2(I)>0.0
           NOTE: ENTER A VALUE HERE ONLY IF IT(I)=1


NOTE: ENTER ALL MAIN BEAM CARDS FIRST, THEN APPENDAGE CARDS - MAIN BEAM AND
      APPENDAGE CARDS MUST BE IN ORDER AS PROGRAM DOES NO SORTING.
      ENTER SIMPLE APPENDAGES STARTING AT FREE END, ENDING AT ATTACHED END.
      ID(I)=0 ENDS THE READING OF THE BEAM DESCRIPTION CARDS - READ A MAXIMUM
      OF 100 OF THESE CARDS (COUNTING THE ID(I)=0 CARD)


OPTION CARD (CARD FORMAT - 3I5)

 NSTA NESTA NEXP

NSTA  - NUMBER OF INTERNAL THEORETICAL STATIONS AT WHICH INTERPOLATED
        EXPERIMENTAL MODE SHAPE DEFLECTIONS AND SLOPES WILL BE PUNCHED.
        (100 IS MAXIMUM BECAUSE OF PROGRAM JOINTS)              3≤NSTA≤100

NESTA - NUMBER OF STATIONS AT WHICH EXPERIMENTAL MODES WERE MEASURED.
        NOTE: NSTA>NESTA                                        2≤NESTA≤99

NEXP  - NUMBER OF EXPERIMENTAL MODES                            1≤NEXP≤10
```

GENERAL DYNAMICS
Electro Dynamic Division
POMONA OPERATION

TABLE A-1 (CONT'D)

~~FORTRAN CODING AND DATA FORM~~

PAGE 3 OF 3

PROBLEM | ~~AND~~ | ~~EWO~~ | ~~WAP~~
PROGRAMMER | ~~PHONE EXT~~ | ~~DATE~~

```
APPENDAGE INDICATORS AND STATIONS AT WHICH EXPERIMENTAL MODES WERE MEASURED
          (CARD FORMAT - 4(I10,E10.0))

    JA(1) | XESTA(1) |   JA(2) | XESTA(2) |   ..   |   ..   | JA(NESTA) | XESTA(NESTA)

JA(I)    - APPENDAGE ATTACHMENT STATION IDENTIFICATION NUMBER FOR
          MEASUREMENT STATION I
          NOTE: JA(I)=IA(J) WHERE IA(J) APPEARS IN THE BEAM DESCRIPTION ABOVE
                (ENTER APPENDAGES IN THE SAME ORDER AS IN THE BEAM DESCRIPTION)

XESTA(I) - STATION LOCATION OF MEASUREMENT STATION I - INCHES
          NOTE: WITHIN THE MAIN BEAM OR ANY APPENDAGE, XESTA(I+1)>XESTA(I)

EXPERIMENTAL MODE SHAPE DEFLECTIONS (CARD FORMAT - 6X,2I3,5E12.5)

  X  |     1|  1|  PHI(1,1)   |  PHI(1,2)   |  PHI(1,3)   |  PHI(1,4)    |  PHI(1,5)   |  X
     |     2|  1|  PHI(2,1)   |  PHI(2,2)   |  PHI(2,3)   |  PHI(2,4)    |  PHI(2,5)   |
     |     :|  :|     :       |     :       |     :       |     :        |     :       |
     | NESTA|  1|PHI(NESTA,1) |PHI(NESTA,2) |PHI(NESTA,3) |PHI(NESTA,4)  |PHI(NESTA,5) |
     |     1|  6|  PHI(1,6)   |  PHI(1,7)   |     :       | PHI(1,NEXP)  |
     |     2|  6|  PHI(2,6)   |  PHI(2,7)   |     :       | PHI(2,NEXP)  |
     |     :|  :|     :       |     :       |     :       |     :        |
  X  | NESTA|  6|PHI(NESTA,6) |PHI(NESTA,7) |     :       |PHI(NESTA,NEXP)|            X

PHI(I,J) - EXPERIMENTAL MODE SHAPE DEFLECTION (IN/IN) AT MEASUREMENT STATION I
          FOR EXPERIMENTAL MODE J

NOTE: THERE MUST BE AT LEAST TWO MEASUREMENT POINTS ON AN APPENDAGE AND
      AT LEAST TWO MEASUREMENT POINTS ON EITHER SIDE OF EACH JOINT.
      ADDITIONAL DATA DECKS MAY BE SUBMITTED, STARTING WITH A NEW TITLE CARD, ETC.
```

TABLE A-2

FLOW DIAGRAM OF COMPUTER PROGRAM JOINTS

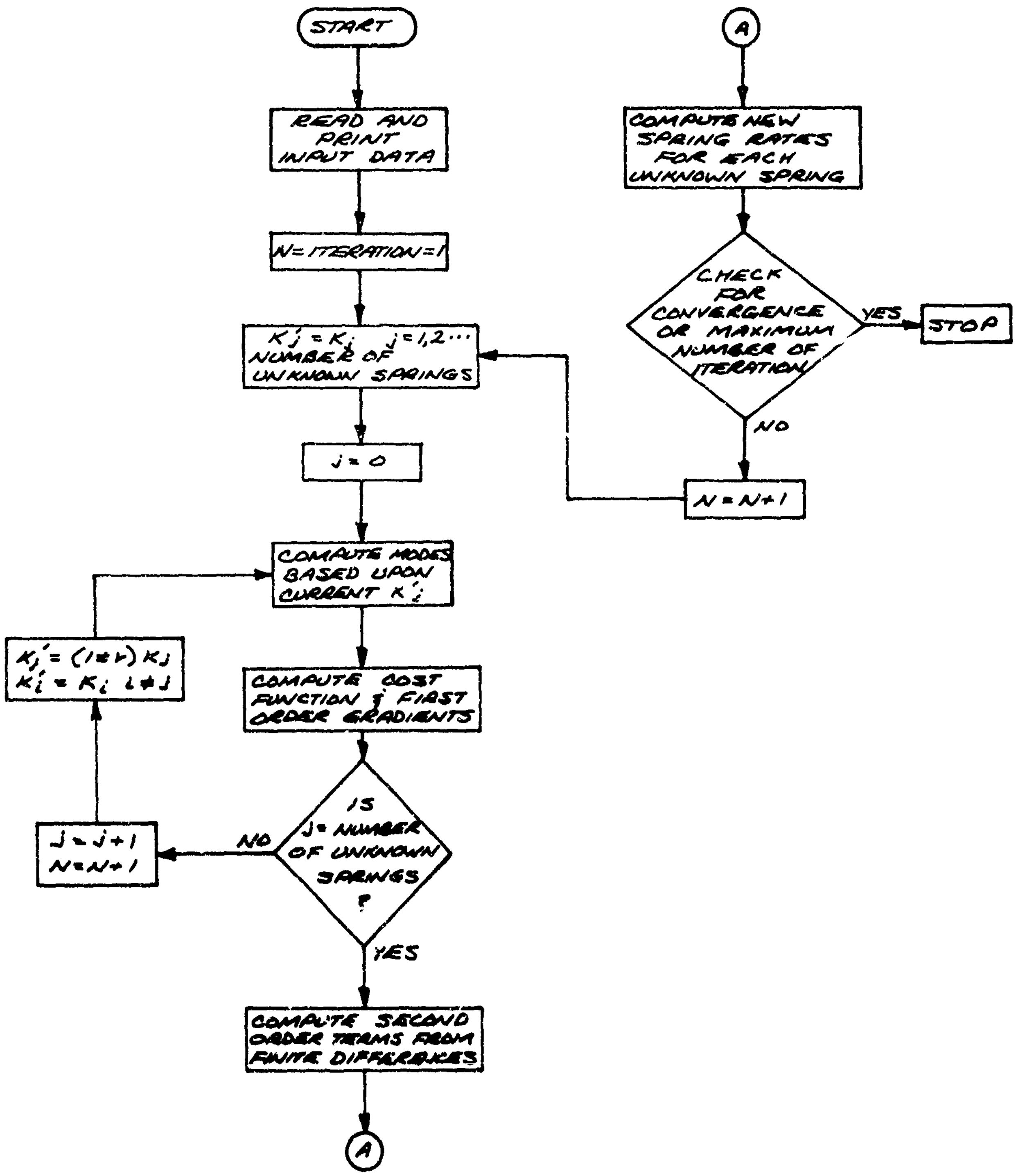

GENERAL DYNAMICS
Electro Dynamic Division
POMONA OPERATION

TABLE A-3

INPUT DATA INSTRUCTIONS FOR COMPUTER PROGRAM JOINTS

~~FORTRAN CODING AND DATA FORM~~

PROBLEM: PROGRAM JOINTS

PROGRAMMER: M.T. SHELTON, D.O. RIFE

```
          ONE GENERAL TITLE CARD

OPTION CARDS (CARD FORMAT - 8I5, 4E10.0)

KNORM   NT  NEXP  NWT ITMAX NVSPR NSTA NESTA   STEP   TOL   CLOSE   XRATIO
KCHECK  XMASS

KNORM  - CARD NUMBER (NOT A STATION IDENTIFICATION COUNTER) AT WHICH
         THEORETICAL MODES WILL BE NORMALIZED.                 0≤KNORM≤NSTA
         NOTE: THIS IS AN INTERNAL STATION CARD NUMBER, NOT AN INPUT CARD NUMBER
               IF KNORM IS BLANK OR ZERO, PROGRAM SETS KNORM=1

NT     - NUMBER OF THEORETICAL MODES TO BE COMPUTED             1≤NT≤10

NEXP   - NUMBER OF EXPERIMENTAL MODES BEING INPUT             1≤NEXP≤10
         NOTE: SAME VALUE AS IN PROGRAM FILLIN

NWT    - MODE SHAPE AND MODE FREQUENCY WEIGHTING FACTOR OPTION
         IF BLANK OR ZERO, PROGRAM COMPUTES WEIGHTING FACTORS.
         OTHERWISE, WEIGHTING FACTORS ARE INPUT.

ITMAX  - MAXIMUM NUMBER OF ITERATIONS FOR ANALYSIS             ITMAX≥1
         NOTE: THE PROGRAM COMPUTES ITERATIONS IN THE FOLLOWING MANNER:
               THE NOMINAL CONFIGURATION OF A CYCLE OF ITERATIONS IS DESIGNATED
               AS ITERATION NUMBER 1. EACH SPRING WHICH CAN VARY IS COUNTED AS
               ANOTHER ITERATION. THEREFORE, TO COMPLETE ONE FULL CYCLE OF
               ITERATIONS REQUIRES NVSPR+1 ITERATIONS. AFTER EACH CYCLE OF
               ITERATIONS, THE PROGRAM COMPUTES A NEW NOMINAL CONFIGURATION
               AND THE PROCESS OF ITERATION COUNTING CONTINUES AS BEFORE. THE
               PROGRAM ALWAYS COMPLETES A CYCLE OF ITERATIONS BEFORE STOPPING.
```

GENERAL DYNAMICS
Electro Dynamic Division
POMONA OPERATION

TABLE A-3 (CONT'D.)

~~FORTRAN CODING AND DATA FORM~~

PAGE 2 OF 8

PROBLEM | PROGRAMMER

```
NVSPR  - NUMBER OF SPRINGS WHOSE COMPLIANCES CAN BE VARIED.           1≤NVSPR≤10

NSTA   - NUMBER OF INTERNAL THEORETICAL STATIONS.                     3≤NSTA≤100
         NOTE: SAME VALUE AS IN PROGRAM FILLIN.

NESTA  - NUMBER OF STATIONS AT WHICH EXPERIMENTAL MODES WERE MEASURED
                                                                      2≤NESTA≤99
         NOTE: THIS PARAMETER HAS BEEN INCLUDED FOR USE WHEN PROGRAMS FILLIN
               AND JOINTS ARE COMBINED. SINCE THIS HAS NOT OCCURRED, SET NESTA=NSTA

STEP   - PARAMETER USED IN DETERMINING CHANGE IN SPRING RATES FOR VARYING
         SPRINGS. A VALUE OF STEP ≈ 0.15 IS RECOMMENDED.              0.0<STEP<1.0
         NOTE: K_NEW=(1±STEP)*K_OLD

TOL    - PARAMETER USED IN DETERMINING SOLUTION TOLERANCE FOR SPRING RATES.
         A VALUE OF TOL ≈ 0.01 IS RECOMMENDED.                        0.0<TOL<1.0
         NOTE: IF ABS(K_CURRENT/K_PREVIOUS CYCLE -1.0)<TOL FOR ALL VARYING SPRINGS,
               ANALYSIS IS STOPPED.

CLOSE  - PARAMETER USED IN DETERMINING STARTING FREQUENCY FOR MYKLESTAD MODE
         SEARCH. A VALUE OF CLOSE ≈ 0.90 IS RECOMMENDED.              0.0≤CLOSE≤1.0
         NOTE: IF BLANK OR ZERO, PROGRAM MAKES A CONTINUOUS SEARCH STARTING
               FROM PREVIOUS MODE FREQUENCY. FOR STARTING FREQUENCY FOR MODE 1,
               SEE LAST CARD INPUT IN DATA DECK.
               IF CLOSE≠0.0, f_START(I)=CLOSE*EFREQ(I) WHERE I IS THE MODE COUNTER.
               OTHERWISE, f_START(I)=f_MODE(I-1).

XRATIO - PARAMETER USED IN DETERMINING NEXT CYCLE INITIAL SPRING RATE VALUES
         WHEN COST FUNCTION HAS INCREASED.                            0.0≤XRATIO≤1.0
         NOTE: IF XRATIO IS BLANK OR ZERO, PROGRAM SETS XRATIO=0.5
```

TABLE A-3 (CONT'D.)

~~FORTRAN CODING AND DATA FORM~~

PROBLEM
PROGRAMMER

```
KCHECK  -  OPTION FOR ASKING PROGRAM TO SEE IF A MODE MAY HAVE BEEN MISSED
           DURING THE MYKLESTAD MODE SEARCH PHASE OF THE ANALYSIS.
           NOTE: IF KCHECK≠2, PROGRAM WILL CHECK TO SEE IF MODE HAS BEEN MISSED.
                 OTHERWISE, NO CHECK WILL BE MADE.
                 THIS OPTION SHOULD NOT BE EXERCISED IF MYKLESTAD MODEL CONTAINS
                 REDUNDANT APPENDAGES.

XMASS   -  TOTAL SYSTEM MASS (REQUIRED)                               LB-SEC²/IN

WEIGHTING FACTORS - DO NOT READ IF NWT=0 (CARD FORMAT - 8E10.0)

  PWMAT(1) | PWMAT(2) |   ..   | PWMAT(K) |   ..   |   ..   | PWMAT(NEXP)
  FWMAT(1) | FWMAT(2) |   ..   | FWMAT(K) |   ..   |   ..   | FWMAT(NEXP)

PWMAT(I) - RELATIVE MODE SHAPE DEFLECTION AND SLOPE WEIGHTING FACTOR FOR MODE I.
                                                                  0.0<PWMAT(I)

FWMAT(I) - RELATIVE MODE FREQUENCY WEIGHTING FACTOR FOR MODE I.   0.0<FWMAT(I)


EXPERIMENTAL FREQUENCIES (CARD FORMAT - 8E10.0)

  EFREQ(1) | EFREQ(2) |   ..   | EFREQ(K) |   ..   |   ..   | EFREQ(NT)

EFREQ(I) - EXPERIMENTAL MODE FREQUENCY FOR MODE I - HZ.  0.0<EFREQ(I)<EFREQ(I+1)
           NOTE: WHERE MODES HAVE BEEN MEASURED, ENTER MEASURED MODE FREQUENCIES
                 OTHERWISE, ESTIMATE WHERE MODES MAY BE FOUND.
```

GENERAL DYNAMICS
Electro Dynamic Division
POMONA OPERATION

TABLE A-3 (CONT'D.)

~~FORTRAN CODING AND DATA FORM~~

PROBLEM

PROGRAMMER

```
VARIABLE SPRINGS (CARD FORMAT - 2I4, 2E8.0, I4)

KSTA(1)  KVAR(1)  SPRINGL(1)  SPRINGU(1)  KTYPE(1)
KSTA(2)  KVAR(2)  SPRINGL(2)  SPRINGU(2)  KTYPE(2)
   :        :         :           :          :
KSTA(K)  KVAR(K)  SPRINGL(K)  SPRINGU(K)  KTYPE(K)
   :        :         :           :          :
KSTA     KVAR     SPRINGL     SPRINGU     KTYPE
(NVSPR)  (NVSPR)  (NVSPR)     (NVSPR)     (NVSPR)

KSTA(I)      - CARD NUMBER (NOT A STATION IDENTIFICATION COUNTER) FROM INPUT
               MYKLESTAD BEAM DESCRIPTION OF VARYING SPRING NUMBER I
                                                          1≤KSTA(I)≤NESTA

KVAR(I)      - CARD NUMBER (NOT A STATION IDENTIFICATION COUNTER) FROM INTERVAL
               MYKLESTAD BEAM DESCRIPTION OF VARYING SPRING NUMBER I
               NOTE: KVAR(I)≥KSTA(I)                       1≤KVAR(I)≤NSTA

SPRINGL(I)   - LOWER LIMIT TO WHICH SPRING RATE MAY BE CHANGED FOR VARYING
               SPRING NUMBER I - LB/IN OR IN-LB/RAD        0.0<SPRINGL(I)

SPRINGU(I)   - UPPER LIMIT TO WHICH SPRING RATE MAY BE CHANGED FOR VARYING
               SPRING NUMBER I - LB/IN OR IN-LB/RAD        0.0<SPRINGU(I)
               NOTE: SPRINGU(I)>SPRINGL(I)

KTYPE(I)     - TYPE OF SPRING OPTION COUNTER FOR VARYING SPRING NUMBER I
                                                             1≤KTYPE(I)≤2
               IF KTYPE(I)=1, A SHEAR SPRING HAS BEEN INDICATED AND SPRINGL(I)
                              AND SPRINGU(I) ARE INPUT IN UNITS OF LB/IN.
               IF KTYPE(I)=2, A FLEXURAL SPRING HAS BEEN INDICATED AND SPRINGL(I)
                              AND SPRINGU(I) ARE INPUT IN UNITS OF IN-LB/RAD.
```

GENERAL DYNAMICS
Electro Dynamic Division
POMONA OPERATION

TABLE A-3 (CONT'D.)

~~FORTRAN CODING AND DATA FORM~~

PROBLEM

PROGRAMMER

EXPERIMENTAL MODE SHAPE DEFLECTIONS AND SLOPES (CARD FORMAT - 6X, 2I3, 5E12.5)

Cols 7–9	Cols 10–12	Cols 13–24	Cols 25–36	Cols 37–48	Cols 49–60	Cols 61–72
1	1	EPHI(1,1)	EPHI(1,2)	EPHI(1,3)	EPHI(1,4)	EPHI(1,5)
2	1	EPHI(2,1)	EPHI(2,2)	EPHI(2,3)	EPHI(2,4)	EPHI(2,5)
:	:	:	:	:	:	:
NESTA	1	EPHI(NESTA,1)	EPHI(NESTA,2)	EPHI(NESTA,3)	EPHI(NESTA,4)	EPHI(NESTA,5)
1	6	EPHI(1,6)	EPHI(1,7)	:	EPHI(1,NEXP)	
2	6	EPHI(2,6)	EPHI(2,7)	:	EPHI(2,NEXP)	
:	:	:	:	:	:	
NESTA	6	EPHI(NESTA,6)	EPHI(NESTA,7)	:	EPHI(NESTA,NEXP)	
1	1	EPHIP(1,1)	EPHIP(1,2)	EPHIP(1,3)	EPHIP(1,4)	EPHIP(1,5)
2	1	EPHIP(2,1)	EPHIP(2,2)	EPHIP(2,3)	EPHIP(2,4)	EPHIP(2,5)
:	:	:	:	:	:	:
NESTA	1	EPHIP(NESTA,1)	EPHIP(NESTA,2)	EPHIP(NESTA,3)	EPHIP(NESTA,4)	EPHIP(NESTA,5)
1	6	EPHIP(1,6)	EPHIP(1,7)	:	EPHIP(1,NEXP)	
2	6	EPHIP(2,6)	EPHIP(2,7)	:	EPHIP(2,NEXP)	
:	:	:	:	:	:	
NESTA	6	EPHIP(NESTA,6)	EPHIP(NESTA,7)	:	EPHIP(NESTA,NEXP)	

EPHI(I,J) - EXPERIMENTAL MODE SHAPE DEFLECTION AT INTERNAL MYKLESTAD BEAM STATION I FOR EXPERIMENTAL MODE NUMBER J - IN/IN

EPHIP(I,J) - EXPERIMENTAL MODE SHAPE SLOPES AT INTERNAL MYKLESTAD BEAM STATION I FOR EXPERIMENTAL MODE NUMBER J - RAD/IN

NOTE: THESE CARDS ARE PUNCHED BY PROGRAM FILLIN.

TABLE 19-3 (CONT'D.)

~~FORTRAN CODING AND DATA FORM~~

PROBLEM

PROGRAMMER

```
MYKLESTAD FORMAT BEAM DESCRIPTIONS OF STATIONS (CARD FORMAT - 2I4, 3I2, 2X, 7E8.0)

ITEM1(1) ITEM2(1) (1) (1) (1)  DATA1(1) DATA2(1) DATA3(1) DATA4(1) DATA5(1) DATA6(1) DATA7(1)
ITEM1(2) ITEM2(2) (2) (2) (2)  DATA1(2) DATA2(2) DATA3(2) DATA4(2) DATA5(2) DATA6(2) DATA7(2)
   :        :      :   :   :      :        :        :        :        :        :        :
ITEM1(K) ITEM2(K) (K) (K) (K)  DATA1(K) DATA2(K) DATA3(K) DATA4(K) DATA5(K) DATA6(K) DATA7(K)
   :        :      :   :   :      :        :        :        :        :        :        :

ITEM1(I) - STATION IDENTIFICATION COUNTER FOR STATION I                   ITEM1(I)>0
           NOTE: THE FIRST STATION OF THE MAIN BEAM MUST BE LABELED 1,
                 I.E., ITEM1(1)=1. AS A GENERAL PRACTICE, STATION IDENTIFICATION
                 COUNTERS SHOULD BE UNIQUE SINCE APPENDAGE ATTACHMENT STATION
                 NUMBERS REFER TO THESE IDENTIFICATION COUNTERS.

ITEM2(I) - APPENDAGE ATTACHMENT STATION IDENTIFICATION NUMBER FOR STATION I
                                                                          ITEM2(I)≥0
           NOTE: EXCEPT FOR THE MAIN BEAM IN WHICH ITEM2(I)=0, THE APPENDAGE
                 ATTACHMENT STATION IDENTIFICATION NUMBER MUST REFER TO A
                 STATION ID. COUNTER, I.E. ITEM2(I)=ITEM1(J) FOR A STATION J
                 IN WHICH ITEM4(J)=2
                 (WITHIN AN APPENDAGE, ALL ATTACHMENT NUMBERS ARE EQUAL)

ITEM3(I) - DESIGNATION OF APPENDAGE ORDER FOR STATION I                  ITEM3(I)≥-1
           NOTE: IF MAIN BEAM, ITEM3(I)=0
                 IF APPENDAGE ATTACHES TO MAIN BEAM, ITEM3(I)=1
                 IF APPENDAGE ATTACHES TO A FIRST ORDER APPENDAGE, ITEM3(I)=2
                 ETC.
                 FOR A REDUNDANT APPENDAGE, ITEM3(I)=-1
```

GENERAL DYNAMICS
Electro Dynamic Division
POMONA OPERATION

TABLE A-3 (CONT'D.)

~~FORTRAN CODING AND DATA FORM~~

PAGE 7 OF 8

PROBLEM	AND	EXT	MAP
PROGRAMMER		PHONE EXT	DATE

```
ITEM4(I)  -  DESIGNATION OF STATION TYPE FOR STATION I              0≤ITEM4(I)≤4
                    0 - MASS STATION
                    1 - SPRING STATION
                    2 - APPENDAGE ATTACHMENT STATION
                    3 - FORWARD REDUNDANT APPENDAGE ATTACHMENT STATION
                    4 - AFT REDUNDANT APPENDAGE ATTACHMENT STATION
             NOTE: ENTER ALL REDUNDANT APPENDAGES LAST STARTING FROM FORWARD END

ITEMS(I)  -  DESIGNATION OF TYPE OF MOTION FOR STATION I            0≤ITEMS(I)≤2
                    0 - BENDING
                    1 - TORSION
                    2 - COMPRESSIVE

             BENDING(ITEMS(I)=0)       TORSION(ITEMS(I)=1)        COMPRESSIVE(ITEMS(I)=2)

DATA1(I)     EI - LB*IN²               GJ - LB*IN²                EA - LB
DATA2(I)     WEIGHT - LB
DATA3(I)     X - IN                    X - IN                     X - IN
DATA4(I)     Jα - LB*IN²               Iκ - LB*IN²                WEIGHT - LB
DATA5(I)     Kα - IN/LB OR α - DEG     α - DEG                    α - DEG
DATA6(I)     Kαk - RAD/IN*LB OR β - DEG  β-DEG OR Kθ-RAD/IN*LB    β - DEG OR Kε - IN*LB
DATA7(I)                  φ - DEG      φ - DEG                    φ - DEG

NOTE: ENTER ALL MAIN BEAM CARDS FIRST, THEN APPENDAGE CARDS - MAIN BEAM AND
      APPENDAGE CARDS MUST BE IN ORDER AS PROGRAM DOES NO SORTING.
      ENTER APPENDAGES STARTING AT FREE END, ENDING AT ATTACHED END.
      EVERY STATION EXCEPT LAST SHOULD HAVE A VALUE IN DATA1(I). THIS IS THE
      STIFFNESS FROM X(I) TO X(I+1).
      WEIGHT AND INERTIA VALUES ARE ASSUMED TO BE LUMPED AT X(I)
      WEIGHTS AND INERTIA SHOULD ONLY BE ENTERED IF ITEM4(I)=0
```

GENERAL DYNAMICS
Electro Dynamic Division
POMONA OPERATION

TABLE A-3 (CONT'D.)

~~FORTRAN CODING AND DATA FORM~~

PAGE 8 OF 8

PROBLEM

PROGRAMMER

```
      WITHIN THE MAIN BEAM OR ANY APPENDAGE, X(I+1) ≥ X(I)
      (A STATION LOCATION IS NEEDED FOR EACH CARD INPUT, CAN BE ZERO)
      PARAMETERS SHOULD ONLY BE ENTERED IN DATA5(I), DATA6(I) AND DATA7(I)
      IF ITEM4(I)=1 OR 2
      ITEM1(I)=0 ENDS THE READING OF THE BEAM DESCRIPTION CARDS - READ A
      MAXIMUM OF 100 OF THESE CARDS (COUNTING THE ITEM1(I)=0 CARD)

ALSO CONTAINED ON THE ITEM1(I)=0 CARD ARE THE FOLLOWING PARAMETERS:

ITEM2(I) - DESIGNATION OF BOUNDARY CONDITIONS FOR MAIN BEAM       1≤ITEM2(I)≤6
            1 - FREE FORWARD END, FREE AFT END
            2 - FREE FORWARD END, CLAMPED AFT END
            3 - CLAMPED FORWARD END, CLAMPED AFT END
            4 - FREE FORWARD END, PINNED AFT END
            5 - PINNED FORWARD END, CLAMPED AFT END
            6 - PINNED FORWARD END, PINNED AFT END

DATA1(I) - STARTING FREQUENCY FOR MYKLESTAD MODE SEARCH FOR MODE 1 - HZ
                                                                  DATA1(I)≥0.0
            NOTE: IF DATA1(I) IS BLANK OR ZERO, PROGRAM SETS DATA1(I)=2.5 HZ

DATA2(I) - TOLERANCE ON FREQUENCY FOR MODE DETERMINATION          DATA2(I)≥0.0
            NOTE: IF DATA2(I) IS BLANK OR ZERO, PROGRAM SETS DATA2(I)=1.0x10^-5

DATA3(I) - FREQUENCY CHANGE BITE SIZE PARAMETER                   DATA3(I)≥0.0
            (FREQnew=FREQold*DATA3(I))
            NOTE: IF DATA3(I) IS BLANK OR ZERO, PROGRAM SETS DATA3(I)=1.10

DATA4(I) - UPPER MODE SEARCH FREQUENCY - HZ                       DATA4(I)≥0.0
            NOTE: IF DATA4(I) IS BLANK OR ZERO, PROGRAM SETS DATA4(I)=250.0
```

NOTE: ADDITIONAL DATA DECKS MAY BE SUBMITTED, STARTING WITH A NEW TITLE CARD, ETC.

Table A-4
FORTRAN Listing of Program FILLIN

```
      PROGRAM FILLIN(INPUT=65,OUTPUT=65,TAPE 60=INPUT,PUNCH=65)
      DIMENSION XSTA(200),XESTA(200),EPHI(200,10),EPHIP(200,10),PHI(200,
     110),NAEND(11),NAAS(200),ITME(5,201),DAAT(7,201),TITLE(8),NAONE(11)
     2,LABEL(200),ITYPE(200),PSAVE(10),NAS(200),
     3SHEL(5),LAONE(11),LAEND(11)
      COMMON Y(4),PH(4) A(3),X,P,PP,D,YSQ(4)
   10 READ20,TITLE
   20 FORMAT(8A10)
      IF(EOF(60))30,40
   30 CALL EXIT
   40 PRINT 50,TITLE
   50 FORMAT(1H1,15X,8A10)
C
C     READ BEAM DESCRIPTION
C
      NX=0
   60 NX=NX+1
      READ70,(ITME(LL,NX),LL=1,5),(DAAT(KK,NX),KK=1,7)
   70 FORMAT(2I4,3I2,2X,7E8.0)
      IF(ITME(1,NX).NE.0)GO TO 60
C     READ CONTROL CARD
C
      READ80,NSTA,NESTA,NEXP
   80 FORMAT(3I5)
      PRINT 90,NSTA,NESTA
   90 FORMAT(///20X,*NUMBER OF MYKLESTAD STATIONS=*,I5,10X,*NUMBER OF EX
     1PERIMENTAL POINTS=*,I5)
      NCARD=NX
C
C     PRINT BEAM DESCRIPTION
C
      PRINT 100
  100 FORMAT(///,20X,*MYKLESTAD INPUT*,///)
      DO 110 I=1,NCARD
  110 PRINT 120,I,(ITME(J,I),J=1,5),(DAAT(JJ,I),JJ=1,7)
  120 FORMAT (6I4,4X,7E13.5)
C
C     READ IN AND PRINT MEASUREMENT STATIONS AND APPENDAGE INDICATORS
C
      READ130,(NAAS(I),XESTA(I),I=1,NESTA)
  130 FORMAT((4(I10,E10.0)))
      PRINT 140,(I,NAAS(I),XESTA(I),I=1,NESTA)
  140 FORMAT(1H1,10X,*MODAL MEASUREMENT STATIONS AND APPENDAGE ATTACHMEN
     1T STATION NUMBERS*,/(20X,2I10,10X,E13.5))
      L=1
      LAONE(1)=1
      DO 150 I=2,NESTA
      IF(NAAS(I).EQ.NAAS(I-1))GO TO 150
      LAEND(L)=I-1
      L=L+1
```

Table A-4
(Cont'd.)

```
      LAONE(L)=I
  150 CONTINUE
      LAEND(L)=NESTA
C
C     READ AND PRINT EXPERIMENTAL MODE SHAPES OR SLOPES
C
      PRINT 160
  160 FORMAT(1H1,20X,*EXPERIMENTAL MODE SHAPES*,//)
      MSTA=NESTA
      IF(NEXP.GT.5)MSTA=2*NESTA
      DO 180 IT=1,MSTA
      READ190,J,K,(SHEL(L),L=1,5)
      PRINT 200,J,NAAS(IT),K,(SHEL(L),L=1,5)
      DO 170 L=1,5
  170 PHI(J,(K+L-1))=SHEL(L)
  180 CONTINUE
  190 FORMAT(6X,2I3,5E12.5)
  200 FORMAT(6X,3I6,5X,5E12.5)
C
C     DEFINE MYKLESTAD OUTPUT STATIONS
C     DEFINE APPENDAGE END POINTS
C     INITIALIZE NAT=NUMBER OF APPENDAGES, NA=APPENDAGE NUMBER,
C     NAONE(NA),NAEND(NA)=NUMBERS OF FIRST AND LAST STATIONS,
C     DEFINE STATION TYPE,ITYPE(J)=0(NO JOINT),1(LEFT SIDE ROTATIONAL
C     SPRING), 2 (LEFT SIDE SHEAR SPRING), 3 (LEFT SIDE ROTATIONAL AND
C     SHEAR SPRINGS), 4 (RIGHT SIDE ROTATIONAL SPRING), 5 (RIGHT SIDE
C     SHEAR SPRING), 6 (RIGHT SIDE ROTATIONAL AND SHEAR SPRINGS)
C
      NAT=NA=NAONE(1)=1
      NN=1
      K=0
      DO 270 J=1,NSTA
      XSTA(J)=DAAT(3,NN)
      LABEL(J)=ITME(1,NN)
      NAS(J)=ITME(2,NN)
      ITYPE(J)=0
      IF(K.NE.0)GO TO 210
      IF(ITME(4,NN).EQ.0)GO TO 230
      IF(ITME(4,NN).NE.1)GO TO 260
      IF(DAAT(6,NN).NE.0)ITYPE(J)=1
      IF(DAAT(5,NN).NE.0)ITYPE(J)=2
      IF(DAAT(5,NN).NE.0.AND.DAAT(6,NN).NE.0)ITYPE(J)=3
      GO TO 260
  210 K=0
      IF(ITME(4,NN).NE.1)GO TO 220
      IF(DAAT(6,NN).NE.0)ITYPE(J)=4
      IF(DAAT(5,NN).NE.0)ITYPE(J)=5
      IF(DAAT(5,NN).NE.0.AND.DAAT(6,NN).NE.0)ITYPE(J)=6
      GO TO 230
  220 NN=1+NN
```

Table A-4
(Cont'd.)

```
      GO TO 270
  230 IF(ITME(1,NN+1).EQ.0)GO TO 240
      IF(ITME(2,NN).NE.ITME(2,NN+1))GO TO 240
      NN=1+NN
      K=0
      GO TO 270
  240 NAEND(NA)=1+J
      IF(ITME(1,NN+1).EQ.0)GO TO 250
      NA=1+NA
      NAONE(NA)=2+J
      GO TO 260
  250 NAT=NA
  260 K=1
  270 CONTINUE
      NAEND(NAT)=NSTA
C
      PRINT 280,NAT
  280 FORMAT(//10X,*NUMBER OF APPENDAGES INCLUDING MAIN BEAM=*,I3)
      PRINT 290
  290 FORMAT(//10X*APPENDAGE NUMBER*,5X*FIRST STATION*,5X*END STATION*)
      PRINT 300,(J,NAONE(J),NAEND(J),J=1,NAT)
  300 FORMAT(20X,I3,12X,I3,12X,I3)
      PRINT 310
  310 FORMAT(1H1,T10*STATION NUMBER*T30*STATION*T50*LABEL*T70*TYPE*T90*A
     1PPENDAGE LABEL*/)
      PRINT 320,(J,XSTA(J),LABEL(J),ITYPE(J),NAS(J),J=1,NSTA)
  320 FORMAT(I20,15XE13.5,I7,I18,I20)
C
      DO 840 L=1,NAT
      II=NAONE(L)
      IFN=NAEND(L)
      JI=LAONE(L)
      JFN=LAEND(L)
      JN=JFN-JI+1
      DO 830 I=II,IFN
       X=XSTA(I)
      IT=ITYPE(I)+1
      GO TO (330,450,540,630,690,760,790)IT
C     PLAIN STATION
  330 IF(X.LE.XESTA(JI+1))GO TO 390
      IF(X.GE.XESTA(JFN-1))GO TO 400
      IF(JN.GT.4)GO TO 360
      IF(JN.EQ.4)GO TO 410
      JO=JI
      JE=JI+1
      Y(1)=XESTA(JO)
      Y(2)=XESTA(JE)
  340 D=1.0/(Y(2)-Y(1))
      DO 350 M=1,NEXP
      PH(1)=PHI(JO,M)
```

Table A-4
(Cont'd.)

```
      PH(2)=PHI(JE,M)                                                    FIL1510
      CALL LINFIT                                                        FIL1520
      EPHI(I,M)=P                                                        FIL1530
  350 EPHIP(I,M)=PP                                                      FIL1540
      GO TO (830,460,550,680,700,770,820)IT                              FIL1550
  360 JJ=JI+1                                                            FIL1560
      JM=JFN-2                                                           FIL1570
      DO 370 J=JJ,JM                                                     FIL1580
      IF(X.GT.XESTA(J).AND.X.LE.XESTA(J+1))GO TO 380                     FIL1590
  370 CONTINUE                                                           FIL1600
  380 JONE=J-1                                                           FIL1610
      GO TO 420                                                          FIL1620
  390 Y(1)=XESTA(JI)                                                     FIL1630
      Y(2)=XESTA(JI+1)                                                   FIL1640
      JO=JI                                                              FIL1650
      JE=JI+1                                                            FIL1660
      GO TO 340                                                          FIL1670
  400 Y(1)=XESTA(JFN-1)                                                  FIL1680
      Y(2)=XESTA(JFN)                                                    FIL1690
      JO=JFN-1                                                           FIL1700
      JE=JFN                                                             FIL1710
      GO TO 340                                                          FIL1720
  410 JONE=JI                                                            FIL1730
  420 CONTINUE                                                           FIL1740
      DO 440 M=1,NEXP                                                    FIL1750
      DO 430 K=1,4                                                       FIL1760
      Y(K)=XESTA(K+JONE-1)                                               FIL1770
  430 PH(K)=PHI(K+JONE-1,M)                                              FIL1780
      CALL SQUARE                                                        FIL1790
      CALL PARAB                                                         FIL1800
      EPHI(I,M)=P                                                        FIL1810
  440 EPHIP(I,M)=PP                                                      FIL1820
      GO TO (830,460,550,680,700,770,820)IT                              FIL1830
  450 KSAVE=1                                                            FIL1840
      GO TO 330                                                          FIL1850
  460 KSAVE=KSAVE+1                                                      FIL1860
      IF(KSAVE.EQ.3) GO TO 520                                           FIL1870
      DO 470 M=1,NEXP                                                    FIL1880
  470 PSAVE(M)=EPHI(I,M)                                                 FIL1890
      DO 480 J=JI,JFN                                                    FIL1900
      JJ=J                                                               FIL1910
      IF(X.EQ.XESTA(J))GO TO 500                                         FIL1920
      IF(X.LT.XESTA(J))GO TO 490                                         FIL1930
  480 CONTINUE                                                           FIL1940
      GO TO 510                                                          FIL1950
  490 JFN=JJ-1                                                           FIL1960
      GO TO 510                                                          FIL1970
  500 JFN=JJ                                                             FIL1980
  510 JL=JJ-JI                                                           FIL1990
      IF(JL.GT.3)JI=JJ-3                                                 FIL2000
```

Table A-4

(Cont'd.)

```
      JN=JFN-JI+1
      GO TO 330
  520 DO 530 M=1,NEXP
  530 EPHI(I,M)=PSAVE(M)
      JI=LAONE(L)
      JFN=LAEND(L)
      JN=JFN-JI+1
      GO TO 830
  540 KSAVE=1
      GO TO 630
  550 KSAVE=1+KSAVE
      IF(KSAVE.EQ.3) GO TO 610
      DO 560 M=1,NEXP
  560 PSAVE(M)=EPHIP(I,M)
      DO 570 J=JI,JFN
      JJ=J
      IF(X.EQ.XESTA(J))GO TO 590
      IF(X.LT.XESTA(J))GO TO 580
  570 CONTINUE
      GO TO 600
  580 JFN=JJ-1
      GO TO 600
  590 JFN=JJ
  600 JL=JJ-JI
      IF(JL.GT.3)JI=JJ-3
      JN=JFN-JI+1
      GO TO 330
  610 DO 620 M=1,NEXP
  620 EPHIP(I,M)=PSAVE(M)
      JI=LAONE(L)
      JFN=LAEND(L)
      JN=JFN+1-JI
      GO TO 830
C
C     STATION TO LEFT OF A ROTATIONAL AND A SHEAR SPRING
C
  630 DO 640 J=JI,JFN
      JJ=J
      IF(X.EQ.XESTA(J))GO TO 660
      IF(X.LT.XESTA(J))GO TO 650
  640 CONTINUE
      GO TO 670
  650 JFN=JJ-1
      GO TO 670
  660 JFN=JJ
  670 JL=JJ-JI
      IF(JL.GT.3)JI=JJ-3
      JN=JFN-JI+1
      GO TO 330
  680 JFN=LAEND(L)
```

Table A-4
(Cont'd.)

```
      JI=LAONE(L)
      JN=JFN+1-JI
      GO TO 830
C
C     STATION TO RIGHT OF A ROTATIONAL SPRING
C
  690 KSAVE=1
      GO TO 330
  700 KSAVE=1+KSAVE
      IF(KSAVE.EQ.3)GO TO 740
      DO 710 M=1,NEXP
  710 PSAVE(M)=EPHI(I,M)
      DO 720 J=JI,JFN
      JJ=J
      IF(X.LE.XESTA(J))GO TO 730
  720 CONTINUE
      GO TO 830
  730 JI=JJ
      IF(JI+3.LE.JFN)JFN=JI+3
      JN=JFN-JI+1
      GO TO 330
  740 DO 750 M=1,NEXP
  750 EPHI(I,M)=PSAVE(M)
      JI=LAONE(L)
      JFN=LAEND(L)
      JN=JFN-JI+1
      GO TO 830
C
C     STATION TO RIGHT OF A SHEAR SPRING
C
  760 KSAVE=1
      GO TO 790
  770 DO 780 M=1,NEXP
      EPHIP(I,M)=0.5*(EPHIP(I-1,M)+EPHIP(I,M))
  780 EPHIP(I-1,M)=EPHIP(I,M)
      GO TO 830
C
C     STATION TO THE RIGHT OF A ROTATIONAL SPRING AND A SHEAR SPRING
C
  790 DO 800 J=JI,JFN
      JJ=J
      IF(X.LE.XESTA(J))GO TO 810
  800 CONTINUE
      GO TO 830
  810 JI=JJ
      IF(JI+3.LE.JFN)JFN=JI+3
      JN=JFN-JI+1
      GO TO 330
  820 JFN=LAEND(L)
      JI=LAONE(L)
```

Table A-4
(Cont'd.)

```
      JN=JFN+1-JI
      IF(IT.EQ.6)GO TO 770
  830 CONTINUE
  840 CONTINUE
      DO 880 I=1,NEXP
      PRINT 850,I
  850 FORMAT(1H1,20X*COMPLETE EXPERIMENTAL MODE*,I4,//,T15,*STATION NUMB
     1ER*,T30,*STATION LABEL*,T45,*APPENDAGE LABEL*,T70,*STATION TYPE*,T
     285,*STATION*,T98,*DISPLACEMENT*,T118,*SLOPE*,//)
      DO 860 J=1,NSTA
  860 PRINT 870,J,LABEL(J),NAS(J),ITYPE(J),XSTA(J),EPHI(J,I),EPHIP(J,I)
  870 FORMAT(20X,I5,I10,2I20,5X,3E15.5)
  880 CONTINUE
      NP=1
  890 IT=1
      NE=NEXP
      IF(NEXP.GT.5)NE=5
  900 DO 920 J=1,NSTA
      PUNCH 910,J,IT,(EPHI(J,L),L=IT,NE)
  910 FORMAT(6X,2I3,5E12.5)
  920 CONTINUE
      IF(NEXP.GT.NE)GO TO 930
      GO TO 940
  930 IT=6
      NE=NEXP
      GO TO 900
  940 NP=NP+1
      IF(NP.EQ.3)GO TO 960
      DO 950 L=1,NEXP
      DO 950 J=1,NSTA
  950 EPHI(J,L)=EPHIP(J,L)
      GO TO 890
  960 CONTINUE
      GO TO 10
      END
```

Table A-5
FORTRAN Listing of Subroutine SQUARE

```
      SUBROUTINE SQUARE
      COMMON Y(4),PH(4),A(3),X,P,PP,D,YSQ(4)
      DIMENSION Z(4),F(4)
      DO 10 I=1,4
      Z(I)=Y(I)
      F(I)=PH(I)
      Y(I)=0.0
      YSQ(I)=0.0
   10 PH(I)=0.0
      DO 20 I=1,4
      PH(1)=PH(1)+F(I)
      Y(1)=Y(1)+Z(I)
      YSQ(1)=YSQ(1)+Z(I)*Z(I)
      PH(2)=PH(2)+F(I)*Z(I)
      YSQ(2)=YSQ(2)+Z(I)*Z(I)*Z(I)
      PH(3)=PH(3)+F(I)*Z(I)*Z(I)
   20 YSQ(3)=YSQ(3)+Z(I)**4
      PH(1)=0.25*PH(1)
      Y(1)=0.25*Y(1)
      YSQ(1)=0.25*YSQ(1)
      Y(2)=YSQ(1)/Y(1)
      PH(2)=0.25*PH(2)/Y(1)
      YSQ(2)=0.25*YSQ(2)/Y(1)
      PH(3)=0.25*PH(3)/YSQ(1)
      Y(3)=0.25*Y(3)/YSQ(1)
      YSQ(3)=0.25*YSQ(3)/YSQ(1)
      D=1.0/(Y(2)*YSQ(3)+Y(1)*YSQ(2)+Y(3)*YSQ(1)-Y(2)*YSQ(1)-Y(1)*YSQ(3)
     1-Y(3)*YSQ(2))
      END
```

Table A-6
FORTRAN Listing of Subroutine PARAB

```
      SUBROUTINE PARAB
      COMMON Y(4),PH(4),A(3),X,P,PP,D,YSQ(4)
      A(1)=D*(PH(1)*(Y(2)*YSQ(3)-Y(3)*YSQ(2))+PH(2)*
     1(Y(3)*YSQ(1)-Y(1)*YSQ(3))-PH(3)*(Y(2)*YSQ(1)-Y(1)*YSQ(2)))
      A(2)=D*(PH(1)*(YSQ(2)-YSQ(3))+PH(2)*(YSQ(3)-YSQ(1))+PH(3)*(YSQ(1)-
     1YSQ(2)))
      A(3)=D*(PH(1)*(Y(3)-Y(2))+PH(2)*(Y(1)-Y(3))+PH(3)*(Y(2)-Y(1)))
      P=A(1)+A(2)*X+A(3)*X*X
      PP=A(2)+2*A(3)*X
      END
```

Table A-7
FORTRAN Listing of Subroutine LINFIT

```
SUBROUTINE LINFIT
COMMON Y(4),PH(4),A(3),X,P,PP,D,YSQ(4)
A(1)=D*(Y(2)*PH(1)-Y(1)*PH(2))
A(2)=D*(PH(2)-PH(1))
P=A(1)+A(2)*X
PP=A(2)
END
```

Table A-8
FORTRAN Listing of Program JOINTS

```
      PROGRAM JOINTS (INPUT,OUTPUT,TAPE60=INPUT,TAPE6=OUTPUT)
C
C     PROGRAM JOINTS - PROBLEM 2049   02/26/71   VARIABLE DELTAK
C                      WITH SHEAR SPRINGS
C
      DIMENSION MAXSIGN(10),NSMAXPH(10),NAONE(10),NAEND(10)
      DIMENSION TITLE(8),          GM(10),SHFL(5),BB(10,10),CC(10,10)
      DIMENSION STFREQ(10),XFSTA(100)
C
C     STORAGE COMMON TO SUBROUTINE MYKL
C
      COMMON    FINK(300)
      COMMON    A(4,4,101),SAP(4,4),AP(4,4),VINV(4,4),ALV(4,4),T(4,4),AL
     1VT(4,4),TAP(4,4,100),VEC(4,101),ITEM(6,101),DATA(8,101),I1(300),IR
     2(300),OM(300),FUNC(300),R(3),KKK(100),MODE(100),JOINT(101),AL(4,4)
     3,I6(101),PRNT(4),HOL(12)
      COMMON    ICON(10),ICB(10),FPM(10,4,4),FOM(10,4,4),VSAVE(4),ARSTAR
     1(10,6,4),           ARPB(4,4),ARPA(4,4),APR(4,4),CANV(2,2),DENV(2,2
     2),THMAN(6,6),BMAN(6,6),BINV(6,6),RMUL(6,4)
      COMMON    I4(101)
      COMMON    ITMF(5,101),DAAT(7,101),IETM(5),DTAA(7)
C
C     STORAGE COMMON TO SUBROUTINE STEEP
C
      COMMON/1/ MWH, ISTOP,NSTA,NT,NEXP,STEP,ITMAX,TOL,ITER
      COMMON/2/      KKKK,ALPHA,F,PFK(20),INTEG(20)
      COMMON/3/PWMAT(10),FWMAT(10),EOMEGS(10),KVAR(20),SPRINGL(20),SPRIN
     1GU(20),EPHI(100,10),EPHIP(100,10),EFREQ(10),TFREQ(10)
      COMMON/4/TOMEGS(10),TPHI(100,10),TPHIP(100,10)
      COMMON/5/JA,JB,JD,FF,     SPFK(10),AA(10,10),ASPRING(20)
      COMMON/6/NVSPR,SPRING(10),SSPRING(10),KSTA(10),KTYPE(10),COMP(10)
      COMMON/7/XRATIO,OLDSPR(10)
      COMMON/8/KNORM,XSTA(100)
      CALL MEMSET (FINK(1),DTAA(7))
C
C     READ AND PRINT TITLE
C
   10 READ20,TITLE
   20 FORMAT(8A10)
      IF(EOF(60))30,40
   30 CALL EXIT
   40 PRINT 50,TITLE
   50 FORMAT(1H1,20X*EXTRACTION OF JOINT COMPLIANCES FROM ELASTIC MODE T
     1EST DATA*//20X,8A10///)
C
C     INITIALIZATION PASS
C
      ISTOP=0
      ITER=1
C
```

Table A-8
(Cont'd.)

```
C       READING OPTIONS, WEIGHTING MATRICES, AND LIMITS                    JTS 510
C                                                                          JTS 520
        READ60,KNORM,NT,NEXP,NWT,ITMAX,NVSPR,NSTA,NESTA,STEP,TOL,CLOSE,  X JTS 530
       1RATIO                                                              JTS 540
   60 FORMAT(4I5,4I5,4E10.0)                                               JTS 550
        IF(KNORM.EQ.0) KNORM=1                                             JTS 560
        NOTM=NT                                                            JTS 570
        PRINT 70,    NT,NEXP,ITMAX,NVSPR,NSTA,STEP,CLOSE,NWT,NESTA         JTS 580
   70 FORMAT(//40X,* NT      = *,I13,/40X,* NEXP    = *,I13,/40X,* ITMAX   JTS 590
       1= *,I13,/40X,* NVSPR  = *,I13,/40X,* NSTA   = *,I13,/40X,* STEP    JTS 600
       2=*,E13.5,/40X,* CLOSE =*,E13.5,/40X,* NWT    =*,I13,20X,*NESTA =*,I JTS 610
       313)                                                                JTS 620
        KCLOSE=0                                                           JTS 630
        IF(CLOSE.EQ.0.0) KCLOSE=1                                          JTS 640
        PRINT 80,TOL                                                       JTS 650
   80 FORMAT( 40X,* TOL     = *,E13.5)                                     JTS 660
        READ90,KCHECK,XMASS                                                JTS 670
   90 FORMAT(I5,E10.0)                                                     JTS 680
        IF(KCHECK.NE.2)GO TO 110                                           JTS 690
        PRINT 100,XMASS                                                    JTS 700
  100 FORMAT(//20X*MODES WILL NOT BE CHECKED*,//20X,*XMASS = *,E13.5)      JTS 710
        GO TO 130                                                          JTS 720
  110 PRINT 120,XMASS                                                      JTS 730
  120 FORMAT(//20X*MODES WILL BE CHECKED*,//20X,*XMASS = *,E13.5)          JTS 740
  130 IF(NWT.EQ.0)GO TO 145                                                JTS 750
        READ140,(PWMAT(I),I=1,NEXP)                                        JTS 760
  140 FORMAT (8E10.0)                                                      JTS 770
        READ140,(FWMAT(I),I=1,NEXP)                                        JTS 772
        GO TO 149                                                          JTS 773
  145 DO 146 I=1,NEXP                                                      JTS 775
  146 PWMAT(I)=FWMAT(I)=1.0                                                JTS 778
  149 PRINT 150                                                            JTS 780
  150 FORMAT(//10X,* RELATIVE MODE SHAPE WEIGHTING FACTORS * )             JTS 790
        PRINT 160,(PWMAT(I),I=1,NEXP)                                      JTS 800
  160 FORMAT(/ 1X,10E13.5)                                                 JTS 810
        PRINT 170                                                          JTS 830
  170 FORMAT(//10X,* RELATIVE MODE FREQUENCY WEIGHTING FACTORS * )         JTS 840
        PRINT 160,(FWMAT(I),I=1,NEXP)                                      JTS 850
  180 READ140,(EFREQ(I),I=1,NT)                                            JTS 860
        PRINT 190                                                          JTS 870
  190 FORMAT(//10X,* EXPERIMENTAL FREQUENCIES *)                           JTS 880
        PRINT 160,(EFREQ(I),I=1,NT)                                        JTS 890
        DO 200 I=1,NT                                                      JTS 900
  200 EOMEGS(I)=(6.283185*EFREQ(I))**2                                     JTS 910
        RNST=XMASS/(2.0*NESTA)                                             JTS 950
        WF=EOMEGS(NEXP)**2                                                 JTS 970
        DO 220 I=1,NEXP                                                    JTS 980
        PWMAT(I)=RNST*WF*PWMAT(I)                                          JTS1000
  220 FWMAT(I)=FWMAT(I)*WF/(EOMEGS(I)**2)                                  JTS1010
        PRINT 223                                                          JTS1020
```

Table A-8
(Cont'd.)

```
  223 FORMAT(//10X,* MODE SHAPE WEIGHTING FACTORS * )                      JTS1025
      PRINT 160,(PWMAT(I),I=1,NEXP)                                        JTS1030
      PRINT 226                                                            JTS1040
  226 FORMAT(//10X,* MODE FREQUENCY WEIGHTING FACTORS * )                  JTS1045
      PRINT 160,(FWMAT(I),I=1,NEXP)                                        JTS1050
  230 READ240,(KSTA(I),KVAR(I),SPRINGL(I),SPRINGU(I),KTYPE(I),I=1,NVSPR)  JTS1060
  240 FORMAT(2I4,2E8.0,I4)                                                 JTS1070
      PRINT 250                                                            JTS1080
  250 FORMAT(//22X,* K*,* KVAR(I)*,2X,* SPRINGL(I)*,2X,* SPRINGU(I)*,2X,  JTS1090
     1* KTYPE*)                                                            JTS1100
      PRINT 260,(KSTA(I),KVAR(I),SPRINGL(I),SPRINGU(I),KTYPE(I),I=1,NVSP  JTS1110
     1R)                                                                   JTS1120
  260 FORMAT(/ (20X,I4,I8,2E13.5,I6))                                      JTS1130
      DO 270 I=1,10                                                        JTS1140
      DO 270 J=1,NSTA                                                      JTS1150
      EPHI(J,I)=0.0                                                        JTS1160
  270 EPHIP(J,I)=0.0                                                       JTS1170
C                                                                          JTS1180
C     READING EXPERIMENTAL MODAL DATA                                      JTS1190
C                                                                          JTS1200
      IF(NESTA.EQ.NSTA)GO TO 290                                           JTS1210
      READ140,(XESTA(I),I=1, NESTA)                                        JTS1220
      PRINT 280                                                            JTS1230
  280 FORMAT(//30X,*MODE MEASUREMENT STATIONS, XESTA(I)*)                  JTS1240
      PRINT 160,(XESTA(I),I=1,NESTA)                                       JTS1250
  290 PRINT 300                                                            JTS1260
  300 FORMAT(1H1,20X,25H EXPERIMENTAL MODE SHAPES,//)                      JTS1270
      MSTA=NESTA                                                           JTS1280
      IF(NEXP.GT.5)MSTA=2*NESTA                                            JTS1290
      DO 320 IT=1,MSTA                                                     JTS1300
      READ330,J,K,(SHEL(L),L=1,5)                                          JTS1310
      PRINT 330,J,K,(SHEL(L),L=1,5)                                        JTS1320
      DO 310 L=1,5                                                         JTS1330
  310 EPHI(J,(K+L-1))=SHEL(L)                                              JTS1340
  320 CONTINUE                                                             JTS1350
  330 FORMAT(6X,2I3,5E12.5)                                                JTS1360
      PRINT 340                                                            JTS1370
  340 FORMAT(1H1,20X,25H EXPERIMENTAL MODE SLOPES,//)                      JTS1380
      DO 360 IT=1,MSTA                                                     JTS1390
      READ330,J,K,(SHEL(L),L=1,5)                                          JTS1400
      PRINT 330,J,K,(SHEL(L),L=1,5)                                        JTS1410
      DO 350 L=1,5                                                         JTS1420
  350 EPHIP(J,(K+L-1))=SHEL(L)                                             JTS1430
  360 CONTINUE                                                             JTS1440
C                                                                          JTS1450
C     READ BEAM DESCRIPTION                                                JTS1460
C                                                                          JTS1470
      NX=0                                                                 JTS1480
  370 NX=NX+1                                                              JTS1490
      READ380,(ITME(LL,NX),LL=1,5),(DAAT(KK,NX),KK=1,7)                    JTS1500
```

```
  380 FORMAT (2I4,3I2,2X,7E8.0)
      IF(ITME(1,NX).NE.0)GO TO 370
C
C     LAST DATA CARD HAS BEEN READ
C
      NCARD=NX
C
C     PRINT BEAM DESCRIPTION
C
      PRINT 390
  390 FORMAT(1H1,* BEAM DESCRIPTION READ BY PROGRAM JOINTS*///)
      DO 410 I=1,NCARD
      PRINT 400,(ITME(J,I),J=1,5),(DAAT(JJ,I),JJ=1,7)
  400 FORMAT ((5I4,4X,7E13.5))
  410 CONTINUE
C
C     SETTING STATIONS TO INTERNAL COUNTERS
C     DEFINE APPENDAGE NUMBERS = NA, TOTAL NUMBER = NAT, FIRST AND LAST
C     STATION NUMBERS = NAONE(NA) AND NAEND(NA),
C
      NAT=NA=NAONE(1)=1
      NN=1
      K=0
      DO 460 J=1,NSTA
      XSTA(J)=DAAT(3,NN)
      IF(K.NE.0)GO TO 420
      IF(ITME(4,NN).NE.0)GO TO 450
      IF(ITME(1,NN+1).EQ.0)GO TO 430
      IF(ITME(2,NN).NE.ITME(2,NN+1))GO TO 430
  420 NN=NN+1
      K=0
      GO TO 460
  430 NAEND(NA)=J+1
      IF(ITME(1,NN+1).EQ.0)GO TO 440
      NA=NA+1
      NAONE(NA)=J+2
      GO TO 450
  440 NAT=NA
  450 K=1
  460 CONTINUE
      PRINT 470,NAT
  470 FORMAT(/10X,*NAT = *,I3)
      PRINT 480
  480 FORMAT(/10X,*  J*,5X,*NAONE(J)*,5X,*NAEND(J)*)
      PRINT 490,(J,NAONE(J),NAEND(J),J=1,NAT)
  490 FORMAT(10X,I3,5X,I8,5X,I8)
C
C     COMPUTING GENERALIZED MASS FOR THE INPUT MODES
C
      DO 520 I=1,NEXP
```

Table A-8
(Cont'd.)

```
      NN=0
      JJ=0
      GM(I)=0.0
  500 NN=NN+1
      JJ=JJ+1
      IF(ITME(4,NN).NE.0)GO TO 510
      GM(I)=GM(I)+DAAT(2,NN)*EPHI(JJ,I)*EPHI(JJ,I)+DAAT(4,NN)*EPHIP(JJ,I
     1)*EPHIP(JJ,I)
      IF(ITME(2,NN).NE.ITME(2,NN+1)) JJ=JJ+1
      IF(JJ.LT.NSTA)GO TO 500
      GO TO 520
  510 JJ=JJ+1
      GO TO 500
  520 GM(I)=GM(I)/386.4
      PRINT 530
  530 FORMAT(/5X,* THE GENERALIZED MASS ASSOCIATED WITH THE INPUT MODES*
     1/)
      PRINT 540,(GM(I),I=1,NEXP)
  540 FORMAT(1X,5E20.8)
C     DEFINE STATION NUMBER OF LARGEST DISPLACEMENT FOR EACH
C     EXPERIMENTAL MODE NSMAXPH(I)
      DO 550 I=1,NEXP
      NSMAXPH(I)=1
      MAXSIGN(I)=1
      IF(EPHI(1,I).LT.0.0) MAXSIGN(I)=-1
      PHMAX=ABS(EPHI(1,I))
      NAE=NAEND(1)
      DO 550 J=2,NAE
      IF(ABS(EPHI(J,I)).LE.PHMAX)GO TO 550
      PHMAX=ABS(EPHI(J,I))
      MAXSIGN(I)=1
      IF(EPHI(J,I).LT.0.0) MAXSIGN(I)=-1
      NSMAXPH(I)=J
  550 CONTINUE
C
C     NORMALIZING THE INPUT MODES TO A GENERALIZED MASS OF 1.0
C
      DO 560 I=1,NEXP
      FACT=SQRT(1.0/GM(I))
      DO 560 J=1,NSTA
      EPHI(J,I)=FACT*EPHI(J,I)
  560 EPHIP(J,I)=FACT*EPHIP(J,I)
      KKKK=0
      DO 600 J=1,NVSPR
      NN=KSTA(J)
      IF(KTYPF(J).EQ.2)GO TO 570
      IF(DAAT(5,NN).EQ.0.)GO TO 580
      SPRING(J)=1.0/DAAT(5,NN)
      GO TO 600
  570 IF(DAAT(6,NN).EQ.0.)GO TO 580
```

```
      SPRING(J)=1.0/DAAT(6,NN)
      GO TO 600
  580 PRINT 590,J
  590 FORMAT(//6H  ****,18H COMPLIANCE NUMBER,I3,15H IS ZERO.  ****)
      ISTOP=1
  600 CONTINUE
      ITME(3,NCARD)=1
      IF(DAAT(4,NCARD).EQ.0.0) DAAT(4,NCARD)=250.
      IF(DAAT(3,NCARD).EQ.0.0) DAAT(3,NCARD)=1.10
      IF(DAAT(1,NCARD).EQ.0.0) DAAT(1,NCARD)=2.5
      SFREQ=DAAT(1,NCARD)
      STOPFR=DAAT(4,NCARD)
      DO 610 J=1,NVSPR
  610 SSPRING(J)=SPRING(J)
      JA=0
      JB=0
      JD=0
      MIKE=0
      DELF=DAAT(3,NCARD)
      DO 620 I=1,NT
  620 STFREQ(I)=EFREQ(I)
      IF(ISTOP.EQ.1)GO TO 10
      MWH=0
      IF(XMASS.GT.0.0) GO TO 630
      PRINT 625
  625 FORMAT(//10X,62H* MISSILE MASS HAS BEEN READ AS ZERO.  THIS CASE T
     1ERMINATED. *)
      GO TO 10
C
C     END OF INITIALIZATION PASS
C     GENERAL PASS
C
  630 CONTINUE
      DO 650 J=1,NVSPR
      NN=KSTA(J)
      IF(KTYPE(J).EQ.2)GO TO 640
      DAAT(5,NN)=1.0/SPRING(J)
      GO TO 650
  640 DAAT(6,NN)=1.0/SPRING(J)
  650 CONTINUE
      IF(ITER.EQ.1)GO TO 670
      DO 660 I=1,NT
  660 STFREQ(I)=TFREQ(I)
  670 CONTINUE
      NT=NCTM
      MTS=0
      DO 680 I=1,NT
      TFREQ(I)=0.0
      DO 680 K=1,NSTA
      TPHI(K,I)=0.0
```

```
  680 TPHIP(K,I)=0.0
      DAAT(1,NCARD)=SFREQ
C
C     SOLVE FOR NEW FREQUENCIES AND MODE SHAPES
C
      PRINT 690,ITER
  690 FORMAT(1H1,40X,21H INPUT FOR ITERATION ,I3/)
      LIME=0
      DO 830 I=1,NCTM
      DAAT(3,NCARD)=DELF
      DAAT(4,NCARD)=STOPER
      IF(MTS.EQ.1)GO TO 830
      IF(I.EQ.1)GO TO 760
      IF(KCLOSE.EQ.1)GO TO 730
      IF(STFREQ(I).NE.0.0)GO TO 710
      PRINT 700,I
  700 FORMAT(13H  *** STFREQ(,I2,35H) EQUALS 0.0, THIS CASE TERMINATED.)
      MIKE=1
      GO TO 810
  710 XFREQ=CLOSE* EFREQ(I)
      YFREQ=DELF*EFREQ(I-1)
      IF(XFREQ.GT.YFREQ)GO TO 720
      XFREQ= EFREQ(I-1)+( EFREQ(I)- EFREQ(I-1))/2.0
      DAAT(3,NCARD)=1.0+((EFREQ(I)-EFREQ(I-1))/(6.0*EFREQ(I)))
  720 DAAT(1,NCARD)=XFREQ
      GO TO 740
  730 DAAT(1,NCARD)=DAAT(3,NCARD)*TFREQ(I-1)
  740 IF(DAAT(1,NCARD).GT.DAAT(4,NCARD))GO TO 810
      PRINT 750,(ITME(J,NCARD),J=1,5),(DAAT(JJ,NCARD),JJ=1,7)
  750 FORMAT(/(5I4,4X,7E13.5))
  760 CALL MYKL(FREQ,GAM,LIME)
      LIME=1
      IF(FREQ.NE.0.)GO TO 780
      PRINT 770
  770 FORMAT(/* ERROR IN COMPUTED MODE FREQUENCIES.  FREQ=0.0, THIS CASE
     1 ABORTED *)
      MIKE=1
  780 CONTINUE
      IF(I.EQ.1)GO TO 790
      IF(FREQ.EQ.TFREQ(I-1))GO TO 820
  790 CONTINUE
      DO 800 K=1,NSTA
      TPHI(K,I)=VEC(4,K)
  800 TPHIP(K,I)=VEC(3,K)
      TFREQ(I)=FREQ
      GM(I)=GAM
      GO TO 830
  810 IF(MTS.EQ.1)GO TO 830
      NT=I
      MTS=1
```

```
      GO TO 830                                                         JTS3460
  820 NT=I-1                                                            JTS3470
      MTS=1                                                             JTS3480
  830 CONTINUE                                                          JTS3490
      IF(MIKE.EQ.1)GO TO 10                                             JTS3500
C                                                                       JTS3510
C     MATCHING CORRESPONDING MODES                                      JTS3520
C                                                                       JTS3530
C     FIND MISSING MODES                                                JTS3540
C                                                                       JTS3550
      NT=NCTM                                                           JTS3560
      DO 1070 I=1,NT                                                    JTS3570
      IF(KCHECK.EQ.2)GO TO 1040                                         JTS3580
      LBITE=0                                                           JTS3590
  840 NSGNCH=0                                                          JTS3600
      DO 860 NA=1,NAT                                                   JTS3610
      NSGN=1                                                            JTS3620
      IF(TPHIP(NAONE(NA),I).LT.0.0)NSGN=-1                              JTS3630
      N1=NAONE(NA)+1                                                    JTS3640
      N2=NAEND(NA)                                                      JTS3650
      DO 850 J=N1,N2                                                    JTS3660
      NSG=1                                                             JTS3670
      IF( TPHIP(J,I).LT.0.0)NSG=-1                                      JTS3680
      IF(NSG.EQ.NSGN)GO TO 850                                          JTS3690
      NSGN=NSG                                                          JTS3700
      NSGNCH=NSGNCH+1                                                   JTS3710
  850 CONTINUE                                                          JTS3720
  860 CONTINUE                                                          JTS3730
      IF(NSGNCH.EQ.I)GO TO 1040                                         JTS3740
      LBITE=LBITE+1                                                     JTS3750
      GO TO (940,960,870)LBITE                                          JTS3760
  870 PRINT 880                                                         JTS3770
  880 FORMAT(1H1,20X*MODES HAVE BEEN MISSED THREE TIMES.....CURRENT MODE JTS3780
     1S AND SLOPES*//)                                                  JTS3790
      NL=1                                                              JTS3800
  890 NN=NL+3                                                           JTS3810
      IF(NN.GT.NT)NN=NT                                                 JTS3820
      DO 900 KS=1,NSTA                                                  JTS3830
  900 PRINT 910,KS,(TPHI(KS,KM),TPHIP(KS,KM),KM=NL,NN)                  JTS3840
  910 FORMAT((2X,I4,4(3X,2E13.5)))                                      JTS3850
      NL=NL+4                                                           JTS3860
      IF(NL.LE.NT)GO TO 890                                             JTS3870
      PRINT 920                                                         JTS3880
  920 FORMAT(//20X*FREQUENCIES AND GENERALIZED MASSES* ,//)             JTS3890
      PRINT 930,(KM,TFREQ(KM),GM(KM),KM=1,NT)                           JTS3900
  930 FORMAT((10X,I5,2(10XE17.7)))                                      JTS3910
      GO TO 10                                                          JTS3920
  940 PRINT 950,I                                                       JTS3930
  950 FORMAT(//20X*MODE*,I5,3X*HAS BEEN MISSED ONCE*)                   JTS3940
      GO TO 980                                                         JTS3950
```

Table A-8
(Cont'd.)

```
  960 PRINT 970,I
  970 FORMAT(//20X*MODE*,I5,3X*HAS BEEN MISSED TWICE*)
  980 CONTINUE
      IF(NSGNCH.GT.NT)GO TO 1000
      MN=NSGNCH
      MM=MN+NT
      MI=I+NT
      DO 990 M=MN,NT
      TFREQ(-M+MM)=TFREQ(-M+MI)
      GM(-M+MM)=GM(-M+MI)
      DO 990 L=1,NSTA
      TPHI(L,-M+MM)=TPHI(L,-M+MI)
  990 TPHIP(L,-M+MM)=TPHIP(L,-M+MI)
      INF=MN-1
      DAAT(4,NCARD)=0.99*TFREQ(INF+1)
      GO TO 1010
 1000 INF=NT
      DAAT(4,NCARD)=0.99*TFREQ(NT)
 1010 DAAT(3,NCARD)=1.0+0.2*(DAAT(3,NCARD)-1.0)
      DO 1030 IN=I,INF
      DAAT(1,NCARD)=SFREQ*(0.9**LBITE)
      IF(IN.NE.1)DAAT(1,NCARD)=1.01*TFREQ(I-1)
      PRINT 750,(ITME(J,NCARD),J=1,5),(DAAT(JJ,NCARD),JJ=1,7)
      CALL MYKL(FREQ,GAM,LIME)
      DO 1020 K=1,NSTA
      TPHI(K ,IN)=VEC(4,K)
 1020 TPHIP(K,IN)=VEC(3,K)
      TFREQ(IN)=FREQ
 1030 GM(IN)=GAM
      GO TO 840
C     COMPARE POLARITY TO THAT OF EXPERIMENTAL MODE
C
 1040 CONTINUE
      IF(I.GT.NEXP)GO TO 1070
      NSIGN=1
      IF(TPHI(NSMAXPH(I),I).LT.0.0)NSIGN=-1
      IF(NSIGN.NE.MAXSIGN(I))GO TO 1050
      GO TO 1070
 1050 DO 1060 J=1,NSTA
      TPHI(J,I)=-TPHI(J,I)
 1060 TPHIP(J,I)=-TPHIP(J,I)
 1070 CONTINUE
      PRINT 1080
 1080 FORMAT(/*  COMPUTED GENERALIZED MASS FOR THE MYKL MODES ARE */)
      PRINT 1090,(GM(I),I=1,NT)
 1090 FORMAT(2X,10E13.5)
C
C     NORMALIZING MYKL MODES TO A GENERALIZED MASS OF 1.0
C
      DO 1100 I=1,NT
```

Table A-8
(Cont'd.)

```
      TOMEGS(I)=(6.283185*TFREQ(I))**2                                  JTS4460
      FACT=SQRT(1.0/GM(I))                                              JTS4470
      DO 1100 J=1,NSTA                                                  JTS4480
      TPHI(J,I)=FACT*TPHI(J,I)                                          JTS4490
 1100 TPHIP(J,I)=FACT*TPHIP(J,I)                                        JTS4500
      PRINT 1110                                                        JTS4510
 1110 FORMAT(/*  THE THEORETICAL MODES HAVE BEEN NORMALIZED *)           JTS4520
C                                                                       JTS4530
C     CHECK MODE SHAPE AND FREQUENCY                                    JTS4540
C     LOGIC FOR CONTROLING PROGRAM MYKL WILL BE LOCATED HERE            JTS4550
C                                                                       JTS4560
C     OBTAIN NEW ESTIMATES OF THE JOINT COMPLIANCES                     JTS4570
C                                                                       JTS4580
      CALL STEEP                                                        JTS4590
      IF(ITMAX.GT.1) GO TO 1115                                         JTS4593
      ITER=1                                                            JTS4594
      CALL RENORM                                                       JTS4595
      GO TO 10                                                          JTS4597
 1115 IF((MWH.LT.1).OR.(MWH.GT.2))GO TO 1120                            JTS4600
      CALL ALTER                                                        JTS4610
      GO TO 630                                                         JTS4620
 1120 IF(ISTOP.EQ.0)GO TO 1130                                          JTS4630
      CALL RENORM                                                       JTS4640
      GO TO 10                                                          JTS4650
 1130 IF(JA.EQ.2)GO TO 1140                                             JTS4660
      GO TO 630                                                         JTS4670
C                                                                       JTS4680
C     CONVERGENCE CHECK ON SOLUTION                                     JTS4690
C                                                                       JTS4700
 1140 KZERO=0                                                           JTS4710
      DO 1150 K=1,NVSPR                                                 JTS4720
      DELTAK=ASPRING(K)-SSPRING(K)                                      JTS4730
      IF(DELTAK.EQ.0.0) KZERO=1                                         JTS4740
      IF(KZERO.EQ.1)GO TO 1160                                          JTS4750
      DO 1150 J=1,NVSPR                                                 JTS4760
 1150 BB(K,J)=(AA(J,K)-SPFK(J))/DELTAK                                  JTS4770
 1160 CONTINUE                                                          JTS4780
      IF(KZERO.EQ.0)GO TO 1180                                          JTS4790
      PRINT 1170                                                        JTS4800
 1170 FORMAT(10X,37H DELTAK = 0.0, THIS CASF TERMINATED. )              JTS4810
      GO TO 10                                                          JTS4820
 1180 CONTINUE                                                          JTS4830
C                                                                       JTS4840
C     BB(J,K)=THE MATRIX OF SECOND ORDER DERIVATIVES                    JTS4850
C                                                                       JTS4860
      PRINT 1190                                                        JTS4870
 1190 FORMAT(//10X,* THE SECOND ORDER DERIVATIVES ARE */)               JTS4880
      DO 1200 J=1,NVSPR                                                 JTS4890
 1200 PRINT 1210,(BB(J,K),K=1,NVSPR)                                    JTS4900
 1210 FORMAT(1X,10E13.5)                                                JTS4910
```

Table A-8
(Cont'd.)

```
C
C     AVERAGING THE SECOND ORDER DERIVATIVES
C
      DO 1220 K=1,NVSPR
      DO 1220 J=1,NVSPR
 1220 AA(K,J)=(BB(K,J)+BB(J,K))/2.0
      DO 1230 J=1,NVSPR
      DO 1230 K=1,NVSPR
 1230 BB(J,K)=AA(J,K)
      PRINT 1240
 1240 FORMAT(//10X,* THE AVERAGED SECOND ORDER DERIVATIVES ARE */)
      DO 1250 J=1,NVSPR
 1250 PRINT 1210,(BB(J,K),K=1,NVSPR)
C
C     CALL INVERSION ROUTINE
C
      CALL MATNF 5 (BB,NVSPR,10,   1.0,DET,IERROR)
      PRINT 1260,DET
 1260 FORMAT(/* DET = *,E16.7)
      PRINT 1270
 1270 FORMAT(//10X,* THE INVERSE OF THE SECOND ORDER DERIVATIVES ARE */)
      DO 1280 J=1,NVSPR
 1280 PRINT 1210,(BB(J,K),K=1,NVSPR)
C
C     CHECKING THE INVERSE OF THE SECOND ORDER TERMS
C
      DO 1290 I=1,NVSPR
      DO 1290 J=1,NVSPR
      CC(I,J)=0.0
      DO 1290 K=1,NVSPR
 1290 CC(I,J)=CC(I,J)+AA(I,K)*BB(K,J)
      PRINT 1300
 1300 FORMAT(//*  THE INVERSE OF THE SECOND ORDER DERIVATIVES TIMES THE
     1SECOND ORDER DERIVATIVES EQUAL */)
      DO 1310 J=1,NVSPR
 1310 PRINT 1210,(CC(J,K),K=1,NVSPR)
C
C     COMPUTING NEW SPRINGS RATES UTILIZING SECOND ORDER TERMS
C
      DO 1340 J=1,NVSPR
      TEMP=0.0
      DO 1320 K=1,NVSPR
 1320 TEMP=TEMP+BB(J,K)*SPFK(K)
      SPRING(J)=SSPRING(J)-TEMP
      RATIO=ABS(SPRING(J)/SSPRING(J)-1.0)
      IF(RATIO.LT.0.025)GO TO 1330
      XNUM=ASPRING(J)-SSPRING(J)
      XDEN=SPRING(J)-SSPRING(J)
      IF(XDEN.EQ.0.0)GO TO 1330
      RATIO=XNUM/XDEN
```

Table A-8

(Cont'd.)

```
      IF(RATIO.LT.0.0) SPRING(J)=ASPRING(J)                            JTS5420
 1330 CONTINUE                                                         JTS5430
      IF(SPRING(J).LT.SPRINGL(J))SPRING(J)=SPRINGL(J)                  JTS5440
      IF(SPRING(J).GT.SPRINGU(J))SPRING(J)=SPRINGU(J)                  JTS5450
      COMP(J)=1.0/SPRING(J)                                            JTS5460
 1340 CONTINUE                                                         JTS5470
      PRINT 1350                                                       JTS5480
 1350 FORMAT(//20X,2H J,8X,5H K(J),9X,8H COMP(J),12X,8H SPFK(J),/)     JTS5490
      PRINT 1360,(J,SPRING(J),COMP(J),SPFK(J),J=1,NVSPR)               JTS5500
 1360 FORMAT(18X,I4,2E16.6,E20.6)                                      JTS5510
      IF(ITER.LT.ITMAX)GO TO 1380                                      JTS5520
      PRINT 1370                                                       JTS5530
 1370 FORMAT(//* THE MAXIMUM NUMBER OF ITERATIONS HAS BEEN EXCEEDED *) JTS5540
      ISTOP=1                                                          JTS5550
 1380 CONTINUE                                                         JTS5560
      MM=0                                                             JTS5570
      DO 1400 J=1,NVSPR                                                JTS5580
      RATIO=ABS(SPRING(J)/SSPRING(J)-1.0)                              JTS5590
      IF(RATIO-TOL)1390,1400,1400                                      JTS5600
 1390 MM=MM+1                                                          JTS5610
 1400 CONTINUE                                                         JTS5620
      IF(MM.LT.NVSPR)GO TO 1420                                        JTS5630
      PRINT 1410                                                       JTS5640
 1410 FORMAT(//*  THE MINIMUM COST FUNCTION HAS BEEN FOUND *)          JTS5650
      ISTOP=1                                                          JTS5660
 1420 CONTINUE                                                         JTS5670
      DO 1430 J=1,NVSPR                                                JTS5680
      OLDSPR(J)=SSPRING(J)                                             JTS5690
      SSPRING(J)=SPRING(J)                                             JTS5700
 1430 CONTINUE                                                         JTS5710
      IF(ISTOP.EQ.1)GO TO 630                                          JTS5720
      JD=0                                                             JTS5730
      JA=1                                                             JTS5740
      JB=0                                                             JTS5750
      MWM=0                                                            JTS5760
      GO TO 630                                                        JTS5770
      END                                                              JTS5780
```

Table A-9

FORTRAN Listing of Subroutine STEEP

```
      SUBROUTINE STEEP
C
C     ESTIMATE SPRING VALUES TO IMPROVE MATCH OF BEAM MODEL
C
      COMMON/1/ MWH, ISTOP,NSTA,NT,NEXP,STEP,ITMAX,TOL,ITER
      COMMON/2/     KKKK,ALPHA,F,PFK(20),INTEG(20)
      COMMON/3/PWMAT(10),FWMAT(10),EOMEGS(10),KVAR(20),SPRINGL(20),SPRIN
     1GU(20),EPHI(100,10),EPHIP(100,10),EFREQ(10),TFREQ(10)
      COMMON/4/TOMEGS(10),TPHI(100,10),TPHIP(100,10)
      COMMON/5/JA,JB,JC,FF,     SPFK(10),AA(10,10),ASPRING(20)
      COMMON/6/NVSPR,SPRING(10),SSPRING(10),KSTA(10),KTYPE(10),COMP(10)
      DIMENSION FACT(10),PXK(200),          FWI(10),FXI(10)
C
C     PRINTING OUT A COMPARISON OF EXPERIMENTAL AND THEORETICAL MODES
C
      PRINT 10, ITER
   10 FORMAT(1H1,* COMPARISON OF EXPERIMENTAL MODES TO THEORETICAL MODES
     1 FOR ITERATION NUMBER*,I3/)
      NL=1
   20 NN=NL+3
      IF(NN.GT.NT)    NN=NT
      DO 30 J=1,NSTA
   30 PRINT 40,  J,(EPHI(J,I),TPHI(J,I),I=NL,NN)
   40 FORMAT(2X,I4,  3X,2E13.5,3X,2E13.5,3X,2E13.5,3X,2E13.5)
      NL=NL+4
      IF(NL.LE.NT) GO TO 20
      PRINT 50
   50 FORMAT(1H1,* COMPARISON OF SLOPES -- EXPERIMENTAL TO THEORETICAL*/
     1)
      NL=1
   60 NN=NL+3
      IF(NN.GT.NT)    NN=NT
      DO 70 J=1,NSTA
   70 PRINT 40,  J,(EPHIP(J,I),TPHIP(J,I),I=NL,NN)
      NL=NL+4
      IF(NL.LE.NEXP) GO TO 60
      PRINT 80, ITER
   80 FORMAT(1H1,47X,* ITERATION*,I4//)
      PRINT 90
   90 FORMAT(10X,* MODE*,10X,* EXPERIMENTAL FREQ*,10X,* THEORETICAL FREQ
     1*/)
      PRINT 100,(I,EFREQ(I),TFREQ(I),I=1,NT)
  100 FORMAT(10X,I5,10X,E18.7,10X,E17.7)
C
C
C     COMPUTATION OF THE QUADRATIC COST FUNCTION
C
      FW=0.0
      FX=0.0
      NSP1=NSTA+1
```

```
      NSX2=NSTA*2
      DO 130 I=1,NEXP
      FWI(I)=0.5*FWMAT(I)*(EOMEGS(I)-TOMEGS(I))*(EOMEGS(I)-TOMEGS(I))
      FW=FW+FWI(I)
      FAC =0.0
      DO 110 J=1,NSTA
  110 FAC =FAC +(EPHI(J,I)-TPHI(J,I))*(EPHI(J,I)-TPHI(J,I))
      DO 120 J= NSP1,NSX2
      JJ=J-NSTA
  120 FAC =FAC +(EPHIP(JJ,I)-TPHIP(JJ,I))*(EPHIP(JJ,I)-TPHIP(JJ,I))
      FXI(I)=0.5*FAC*FWMAT(I)
  130 FX=FX+FXI(I)
      F=FW+FX
      PRINT 140,F,FW,FX
  140 FORMAT(//22H  THE COST FUNCTION = ,E13.5,10X,6H FW = ,E13.5,10X,6H
     1 FX = ,E13.5/)
      PRINT 150,(I,FWI(I),FXI(I),I=1,NEXP)
  150 FORMAT(38X,I3,10X,E13.5,16X,E13.5)
      IF(ITER.EQ.1) FF=F
      IF(JB.EQ.1) MWH=0
      IF(JB.NE.0)GO TO 160
      IF(ITER.EQ.1)GO TO 160
      IF(FF.GT.F) FF=F
      MWH=MWH+1
      IF(FF.GE.F) MWH=0
      IF((MWH.EQ.0).OR.(MWH.GT.2))GO TO 160
      GO TO 390
  160 IF(ISTOP.EQ.1) GO TO 390
C
C     COMPUTATION OF THE GRADIENTS FOR EACH UNKNOWN SPRING
C     POMEGK(PARTIAL DERIVATIVE OF OMEGA SQUARED WITH RESPECT TO SPRING
C    1RATES K)
C
      DO 280 J=1,NVSPR
      NN=KVAR(J)+1
      PFK(J)=0.0
      IF(JB.NE.0) AA(J,JB)=0.0
      DO 280 I=1,NEXP
      IF(KTYPE(J).EQ.1)GO TO 170
      POMEGK=(TPHIP(NN-1,I)-TPHIP(NN,I))**2
      GO TO 180
  170 POMEGK=(TPHI(NN-1,I)-TPHI(NN,I))**2
  180 CONTINUE
C
C     PXK(PARTIAL DERIVATIVE OF PHI WITH RESPECT TO SPRING RATES K)
C
      DO 190 NX=1,NSX2
  190 PXK(NX)=0.0
      DO 240 L=1,NT
      IF(L.EQ.I)GO TO 240
```

```
      IF(KTYPE(J).EQ.1)GO TO 200
      FACT(L)=(TPHIP(NN-1,L)*TPHIP(NN-1,I)-TPHIP(NN-1,L)*TPHIP(NN,I)-TPH
     1IP(NN,L)*TPHIP(NN-1,I)+TPHIP(NN,L)*TPHIP(NN,I))/(TOMEGS(I)-TOMEGS(
     2L))
      GO TO 210
  200 FACT(L)=(TPHI(NN-1,L)*TPHI(NN-1,I)-TPHI(NN-1,L)*TPHI(NN,I)-TPHI(NN
     1,L)*TPHI(NN-1,I)+TPHI(NN,L)*TPHI(NN,I))/(TOMEGS(I)-TOMEGS(L))
  210 CONTINUE
      DO 220 NX=1,NSTA
  220 PXK(NX)=PXK(NX)+FACT(L)*TPHI(NX,L)
      DO 230 NX=NSP1,NSX2
      NY=NX-NSTA
  230 PXK(NX)=PXK(NX)+FACT(L)*TPHIP(NY,L)
  240 CONTINUE
C
C     COMPUTATION OF PFK(J)--PARTIAL DERIVATIVE OF F WRT K
C
      PFKX=0.0
      PFKW=0.0
      DO 250 N=1,NSTA
  250 PFKX=PFKX+PWMAT(I)*(TPHI(N,I)-EPHI(N,I))*PXK(N)
      DO 260 N=NSP1,NSX2
      NY=N-NSTA
  260 PFKX=PFKX+PWMAT(I)*(TPHIP(NY,I) -EPHIP(NY,I))*PXK(N)
      PFKW=FWMAT(I)*(TOMEGS(I)-EOMEGS(I))*POMEGK
      PFK(J)=PFK(J)+PFKX+PFKW
      IF(JB.EQ.0)GO TO 270
      AA(J,JB)=AA(J,JB)+PFKX+PFKW
  270 CONTINUE
  280 CONTINUE
      IF(JB.EQ.NVSPR)GO TO 380
      IF(JD.EQ.1)GO TO 300
      JA=1
      JB=0
      JD=1
      DO 290 J=1,NVSPR
  290 SPFK(J)=PFK(J)
  300 CONTINUE
C
C     COMPUTING WHERE THE COST FUNCTION GOES TO ZERO
C
      JC=JB+1
      IF(SPFK(JC).GT.0.0)GO TO 310
      ALPHA=-STEP*SSPRING(JC)
      GO TO 320
  310 ALPHA=STEP*SSPRING(JC)
  320 CONTINUE
C
C     COMPUTING NEW GUESSES FOR THE VARIABLE SPRINGS
C
```

```
      IF(JB.EQ.0)GO TO 330
      SPRING(JB)=SSPRING(JB)
  330 CONTINUE
      JB=JB+1
      SPRING(JB)=SSPRING(JB)-ALPHA
      IF(SPRING(JB).LT.SPRINGL(JB))SPRING(JB)=SPRINGL(JB)
      IF(SPRING(JB).GT.SPRINGU(JB))SPRING(JB)=SPRINGU(JB)
      ASPRING(JB)=SPRING(JB)
      DO 340 J=1,NVSPR
  340 COMP(J)=1.0/SPRING(J)
      PRINT 350
  350 FORMAT(/20X,2H J,8X,5H K(J),          11X,7H PFK(J),12X,8H COMP
     1(J)/)
      PRINT 360,(J,SPRING(J),       PFK(J),COMP(J),J=1,NVSPR)
  360 FORMAT(18X,I4,E16.5,       2E18.5)
      PRINT 370,ALPHA
  370 FORMAT(/10X,*  ALPHA = *,E16.5)
      ITER=ITER+1
C
      GO TO 390
C
C
  380 JA=2
      ITER=ITER+1
C
C     RETURN TO PROGRAM JOINTS
C
  390 CONTINUE
      END
```

Table A-10
FORTRAN Listing of Subroutine ALTER

```
      SUBROUTINE ALTER
C
C     ESTIMATE NEW SPRING RATES WHEN THE COST FUNCTION HAS INCREASED
C
      COMMON/6/NVSPR,SPRING(10),SSPRING(10),KSTA(10),KTYPE(10),COMP(10)
      COMMON/7/XRATIO,OLDSPR(10)
      DIMENSION RATIO(10)
      DO 10 J=1,NVSPR
      RATIO(J)=0.0
      IF(OLDSPR(J).EQ.0.)GO TO 10
      RATIO(J)=SSPRING(J)/OLDSPR(J)
   10 CONTINUE
      IF(XRATIO.EQ.0.) XRATIO=0.5
      XRATIO=1.0+XRATIO
      YRATIO=1.0/XRATIO
      KOUNT=0
      DO 30 J=1,NVSPR
      IF(RATIO(J).LE.XRATIO)GO TO 20
      SSPRING(J)=XRATIO*OLDSPR(J)
      KOUNT=KOUNT+1
      GO TO 30
   20 IF(RATIO(J).GE.YRATIO)GO TO 30
      SSPRING(J)=YRATIO*OLDSPR(J)
      KOUNT=KOUNT+1
   30 CONTINUE
      IF(KOUNT.NE.0)GO TO 50
      DO 40 J=1,NVSPR
   40 SSPRING(J)=(SSPRING(J)-OLDSPR(J))/2.0+OLDSPR(J)
   50 DO 60 J=1,NVSPR
      SPRING(J)=SSPRING(J)
      COMP(J)=1.0/SSPRING(J)
   60 CONTINUE
      PRINT 70
   70 FORMAT(1H1,//20X,76H SINCE THE COST FUNCTION HAS INCREASED, NEW SP
     1RING RATES HAVE BEEN COMPUTED.//)
      PRINT 80
   80 FORMAT(/20X,2H J,8X,5H K(J),9X,8H COMP(J),/)
      PRINT 90,(J,SPRING(J),COMP(J),J=1,NVSPR)
   90 FORMAT(18X,I4,2E16.6)
      END
```

Table A-11

FORTRAN Listing of Subroutine RENORM

```
      SUBROUTINE RENORM
C
C     RENORMALIZATION OF THE EXPERIMENTAL AND THEORETICAL MODES
C
      COMMON/1/ MWH, ISTOP,NSTA,NT,NEXP,STEP,ITMAX,TOL,ITER
      COMMON/3/PWMAT(10),FWMAT(10),EOMEGS(10),KVAR(20),SPRINGL(20),SPRIN
     1GU(20),EPHI(100,10),EPHIP(100,10),EFREQ(10),TFREQ(10)
      COMMON/4/TOMEGS(10),TPHI(100,10),TPHIP(100,10)
      COMMON/8/KNORM,XSTA(100)
      DATA (MODE=10H MODE     ),(NAME1=10H EPHI     ),(NAME2=10H TPHI
     1 ),(NAME3=10H EPHIP    ),(NAME4=10H TPHIP    )
      DO 20 I=1,NEXP
      IF(EPHI(KNORM,I).EQ.0.)GO TO 20
      FACT=1.0/EPHI(KNORM,I)
      DO 10 J=1,NSTA
      EPHI(J,I)=FACT*EPHI(J,I)
      EPHIP(J,I)=FACT*EPHIP(J,I)
   10 CONTINUE
   20 CONTINUE
      DO 40 I=1,NT
      IF(TPHI(KNORM,I).EQ.0.)GO TO 40
      FACT=1.0/TPHI(KNORM,I)
      DO 30 J=1,NSTA
      TPHI(J,I)=FACT*TPHI(J,I)
      TPHIP(J,I)=FACT*TPHIP(J,I)
   30 CONTINUE
   40 CONTINUE
   50 PRINT 60, ITER
   60 FORMAT(1H1,* COMPARISON OF EXPERIMENTAL MODES TO THEORETICAL MODES
     1 FOR ITERATION NUMBER*,I3/)
      NL=1
      NN=NL+3
      IF(NN.GT.NEXP) NN=NEXP
      PRINT 70,(MODE,I,I=NL,NN)
   70 FORMAT(10X,4(18X,A6,I2))
      PRINT 80,(NAME1,NAME2,I=NL,NN)
   80 FORMAT(3X,2H K,6X,6H XSTA ,4(8X,A6,6X,A6))
      DO 90 J=1,NSTA
   90 PRINT 100,J,XSTA(J), (EPHI(J,I),TPHI(J,I),I=NL,NN)
  100 FORMAT(1X,I4,2X,E12.5,4(2X,2E12.5))
      NL=NL+4
      IF(NL.LE.NEXP) GO TO 50
  110 PRINT 120
  120 FORMAT(1H1,* COMPARISON OF SLOPES -- EXPERIMENTAL TO THEORETICAL*/
     1)
      NL=1
      NN=NL+3
      IF(NN.GT.NEXP) NN=NEXP
      PRINT 70,(MODE,I,I=NL,NN)
      PRINT 80,(NAME3,NAME4,I=NL,NN)
```

Table A-11
(Cont'd.)

```
      DO 130 J=1,NSTA
  130 PRINT 100,J,XSTA(J),(EPHIP(J,I),TPHIP(J,I),I=NL,NN)
      NL=NL+4
      IF(NL.LE.NEXP)GO TO 110
      END
```

Table A-12
FORTRAN Listing of Subroutine MYKL

```
      SUBROUTINE MYKL (FREQ,GAM,LIME)
C     MYKL MODIFIED TO LIMIT NUMBER OF INTERNAL STATIONS TO 100
      COMMON    FINK(300)
      COMMON    A(4,4,101),SAP(4,4),AP(4,4),VINV(4,4),ALV(4,4),T(4,4),AL
C     COMMON    A(4,4,300),SAP(4,4),AP(4,4),VINV(4,4),ALV(4,4),T(4,4),AL
     1VT(4,4),TAP(4,4,100),VEC(4,101),ITEM(6,101),DATA(8,101),I1(300),IR
C    1VT(4,4),TAP(4,4,100),VEC(4,300),ITEM(6,300),DATA(8,300),I1(300),IR
     2(300),OM(300),FUNC(300),R(3),KKK(100),MODE(100),JOINT(101),AL(4,4)
C    2(300),OM(300),FUNC(300),R(3),KKK(100),MODE(100),JOINT(300),AL(4,4)
     3,I6(101),PRNT(4),HOL(12)
C    3,I6(300),PRNT(4),HOL(12)
      COMMON    ICON(10),ICB(10),FPM(10,4,4),FQM(10,4,4),VSAVE(4),ARSTAR
     1(10,6,4),             ARPB(4,4),ARPA(4,4),APR(4,4),DANV(2,2),DENV(2,2
     2),THMAN(6,6),BMAN(6,6),BINV(6,6),RMUL(6,4)
      COMMON    I4(101)
C     COMMON    I4(300)
      COMMON    ITME(5,101),DAAT(7,101),IETM(5),DTAA(7)
C     COMMON    ITME(5,250),DAAT(7,250),IETM(5),DTAA(7)
   10 ITMIN=1
      ILAF=1
      N=0
      NX=0
   20 N=N+1
      NX=NX+1
      DO 30 I=1,5
   30 ITEM(I,N)=ITME(I,NX)
      DO 40 I=1,7
   40 DATA(I,N)=DAAT(I,NX)
      IF(LIME.EQ.1)GO TO 60
      WRITE(6,50) (ITEM(1,N),I=1,5),(DATA(J,N),J=1,7)
   50 FORMAT(5I4,4X,7(   E13.5))
   60 CONTINUE
      IF(ITEM(1,N))70,100,70
   70 ITEM(6,N)=ITEM(1,N)
      ITEM(1,N)=N
      IF(N.EQ.1)GO TO 20
      IF(ITEM(2,N).EQ.ITEM(2,N-1))GO TO 20
      DO 80 I=1,6
      ITEM(I,N+1)=ITEM(I,N)
   80 ITEM(I,N)=ITEM(I,N-1)
      ITEM(1,N)=N
      ITEM(1,N+1)=N+1
      ITEM(4,N)=0
      DO 90 J=1,7
      DATA(J,N+1)=DATA(J,N)
   90 DATA(J,N)=0.0
      DATA(3,N)=DATA(3,N-1)
      N=N+1
      GO TO 20
  100 DO 110 I=1,6
```

Table A-12
(Cont'd.)

```
      ITEM(I,N+1)=ITEM(I,N)
  110 ITEM(I,N)=ITEM(I,N-1)
      ITEM(1,N)=N
      ITEM(4,N)=0
      DO 120 J=1,7
      DATA(J,N+1)=DATA(J,N)
  120 DATA(J,N)=0.0
      DATA(3,N)=DATA(3,N-1)
      N=N+1
      NN=N-1
      M=N
      DO 150 I=2,NN
      N=I-1
      DATA(8,N)=DATA(3,I)-DATA(3,N)
      IF(ITEM(2,N)-ITEM(2,I))130,140,130
  130 DATA(8,N)=0.0
  140 DATA(8,I)=0.0
  150 CONTINUE
      DO 160 K=1,100
      DO 160 I=1,4
      DO 160 J=1,4
  160 A(I,J,K)=0.0
      KZ=0
      KOWT=1
      ITER=1
      W2=DATA(1,M)
      IF(W2)180,170,180
  170 W2=2.5
  180 W2=(W2*3.141593*2.0)**2
      EPS=DATA(2,M)
      IF(EPS)200,190,200
  190 EPS=.1E-4
  200 GAMA=DATA(3,M)
      IF(GAMA)220,210,220
  210 GAMA=1.10
  220 GUMMA=1.+(GAMA-1.)*.05
      UPBND=DATA(4,M)
      IF(UPBND)240,230,240
  230 UPBND=250.0
  240 UPBND=UPBND*6.283185
      K=1
      SAMA=GAMA
      DO 330 I=1,NN
      IF(ITEM(4,I)-1)250,280,300
  250 A(1,1,K)=1.0
      A(2,2,K)=1.0
      A(3,1,K)=-DATA(8,I)/DATA(1,I)
      IF(DATA(1,I).EQ.0.0)A(3,1,K)=0.0
      DATA(5,I)=DATA(5,I)/57.29578
      DATA(6,I)=DATA(6,I)/57.29578
```

```
      IF(ITEM(5,I))260,260,270                                          MYK1010
  260 A(1,2,K)=-DATA(8,I)                                               MYK1020
      A(3,2,K)=.5*DATA(8,I)**2/DATA(1,I)                                MYK1030
      IF(DATA(1,I).EQ.0.0)A(3,2,K)=0.0                                  MYK1040
      A(4,1,K)=-A(3,2,K)                                                MYK1050
      A(4,2,K)=DATA(8,I)**3/(6.0*DATA(1,I))                             MYK1060
      IF(DATA(1,I).EQ.0.0)A(4,2,K)=0.0                                  MYK1070
  270 K=K+1                                                             MYK1080
      GO TO 330                                                         MYK1090
  280 A(3,1,K)=-DATA(6,I)                                               MYK1100
      IF(ITEM(5,I))290,290,300                                          MYK1110
  290 A(4,2,K)=-DATA(5,I)                                               MYK1120
  300 KK=K+1                                                            MYK1130
      DATA(5,I)=DATA(5,I)/57.29578                                      MYK1140
      DATA(6,I)=DATA(6,I)/57.29578                                      MYK1150
      A(1,1,K)=1.0                                                      MYK1160
      A(1,1,KK)=1.0                                                     MYK1170
      A(2,2,K)=1.0                                                      MYK1180
      A(2,2,KK)=1.0                                                     MYK1190
      A(3,1,KK)=-DATA(8,I)/DATA(1,I)                                    MYK1200
      IF(DATA(1,I).EQ.0.0)A(3,1,KK)=0.0                                 MYK1210
      A(3,3,K)=1.0                                                      MYK1220
      A(3,3,KK)=1.0                                                     MYK1230
      A(4,4,K)=1.0                                                      MYK1240
      A(4,4,KK)=1.0                                                     MYK1250
      IF(ITEM(5,I))310,310,320                                          MYK1260
  310 A(1,2,KK)=-DATA(8,I)                                              MYK1270
      A(3,2,KK)=DATA(8,I)**2*.5/DATA(1,I)                               MYK1280
      IF(DATA(1,I).EQ.0.0)A(3,2,KK)=0.0                                 MYK1290
      A(4,1,KK)=-A(3,2,KK)                                              MYK1300
      A(4,2,KK)=DATA(8,I)**3/(6.0*DATA(1,I))                            MYK1310
      IF(DATA(1,I).EQ.0.0)A(4,2,KK)=0.0                                 MYK1320
      A(4,3,KK)=DATA(8,I)                                               MYK1330
  320 K=K+2                                                             MYK1340
  330 CONTINUE                                                          MYK1350
      NSTA=K-1                                                          MYK1360
      DO 340 I=1,NN                                                     MYK1370
      DATA(7,I)=DATA(7,I)/57.29578                                      MYK1380
      DATA(2,I)=DATA(2,I)/386.4                                         MYK1390
  340 DATA(4,I)=DATA(4,I)/386.4                                         MYK1400
      KORP=0                                                            MYK1410
      DO 360 I=1,NN                                                     MYK1420
      IF(ITEM(3,I)-KORP )360,360,350                                    MYK1430
  350 KORP =ITEM(3,I)                                                   MYK1440
  360 CONTINUE                                                          MYK1450
      K=1                                                               MYK1460
      DO 390 I=1,NN                                                     MYK1470
      IF(ITEM(4,I)-1)370,380,380                                        MYK1480
  370 I1(K)=ITEM(1,I)                                                   MYK1490
      I6(K)=ITEM(5,I)                                                   MYK1500
```

Table A-12
(Cont'd.)

```
      I4(K)=ITEM(4,I)
      IR(K)=KORP-ITEM(3,I)
      IF(ITEM(3,I).LT.0) IR(K)=-1
      K=K+1
      GO TO 390
  380 KK=K+1
      I1(K)=ITEM(1,I)
      I6(K)=ITEM(6,I)
      I1(KK)=I1(K)
      I6(KK)=I6(K)
      I4(K)=ITEM(4,I)
      I4(KK)=I4(K)
      IR(K)=KORP-ITEM(3,I)
      IF(ITEM(3,I).LT.0) IR(K)=-1
      IR(KK)=IR(K)
      K=K+2
  390 CONTINUE
      NSUP=NSTA
      DO 400 K=1,NSTA
      I=I1(K)
      IF(ITEM(3,I))410,400,400
  400 CONTINUE
      GO TO 420
  410 NSTA=K-1
  420 DIV=1.0
  430 DO 450 I=1,4
      DO 440 J=1,4
  440 SAP(I,J)=0.0
  450 SAP(I,I)=1.0
  460 JNT=1
      NOR=0
      KIAP=KORP
  470 K=1
  480 CONTINUE
      KS=K
      IF(IR(K).LT.0) GO TO 490
      IF(IR(K)+KIAP-KORP)1110,490,1110
  490 I=I1(K)
      MF=I
      J1=I+1
      IF(IR(K).GE.0) GO TO 510
      IF(J1-M)500,980,500
  500 IF(ITEM(2,I)-ITEM(2,J1))980,510,980
  510 IF(ITEM(4,I)-1)520,540,540
  520 A(1,3,K)=W2*DATA(4,I)
      A(1,4,K)=-W2*DATA(2,I)*DATA(8,I)
      A(2,4,K)=W2*DATA(2,I)
      A(3,3,K)=1.0+W2*DATA(4,I)*A(3,1,K)
      A(3,4,K)=W2*DATA(2,I)*A(3,2,K)
      A(4,3,K)=DATA(8,I)+W2*DATA(4,I)*A(4,1,K)
```

```
      A(4,4,K)=1.0+DATA(2,I)*H2*A(4,2,K)
      IF(ITEM(5,I))540,540,530
  530 A(4,3,K)=0.0
  540 IF(I4(K)-3)670,590,600
  550 NOR=NOR+1
      DO 560 J=1,4
      DO 560 L=1,4
  560 APR(     L,J)=AP(L,J)
      KQR=I6(K)
      ICB(NOR)=K
      DO 580 J=1,4
      DO 570 L=1,4
  570 SAP(L,J)=0.0
  580 SAP(J,J)=1.0
      GO TO 670
  590 IF(I4(K-1)-3)550,670,550
  600 IF(I4(K-1)-4)610,670,610
  610 KKEEP=K
      DO 620 J=1,4
      DO 620 L=1,4
  620 ARPB(L,J)=AP(L,J)
      KS1=NSTA+1
      DO 640 J=1,4
      DO 630 L=1,4
  630 SAP(L,J)=0.0
  640 SAP(J,J)=1.0
      DO 650 LX=KS1,NSUP
      IT=I1(LX)
      IF(ITEM(2,IT)-KQR)650,660,650
  650 CONTINUE
      WRITE(6,790)KQR
      GO TO 2190
  660 K=LX
      ICON(NOR)=K
      GO TO 480
  670 DO 690 L=1,4
      DO 690 J=1,4
      AP(L,J)=0.
      DO 690 IC=1,4
      AP(L,J)=AP(L,J)+A(L,IC,K)*SAP(IC,J)/DIV
      IF(AP(L,J)-1.0E+19)690,680,680
  680 DIV=DIV*1.0E+5
      GO TO 430
  690 CONTINUE
      DO 700 L=1,4
      DO 700 J=1,4
  700 SAP(L,J)=AP(L,J)
      IF(J1-M)710,720,710
  710 IF(ITEM(2,I)-ITEM(2,J1))720,1110,720
  720 AL(1,1)=SAP(1,3)
```

```
      AL(1,2)=SAP(1,4)                                                  MYK2510
      AL(2,1)=SAP(2,3)                                                  MYK2520
      AL(2,2)=SAP(2,4)                                                  MYK2530
      IF(KIAP)730,1130,730                                              MYK2540
  730 DETV=SAP(3,3)*SAP(4,4)-SAP(3,4)*SAP(4,3)                          MYK2550
      IF(DETV)740,2220,740                                              MYK2560
  740 VINV(1,1)=SAP(4,4)/DETV                                           MYK2570
      VINV(2,1)=SAP(4,3)/DETV*(-1.0)                                    MYK2580
      VINV(1,2)=SAP(3,4)/DETV*(-1.0)                                    MYK2590
      VINV(2,2)=SAP(3,3)/DETV                                           MYK2600
      ALV(1,1)=AL(1,1)*VINV(1,1)+AL(1,2)*VINV(2,1)                      MYK2610
      ALV(1,2)=AL(1,1)*VINV(1,2)+AL(1,2)*VINV(2,2)                      MYK2620
      ALV(2,1)=AL(2,1)*VINV(1,1)+AL(2,2)*VINV(2,1)                      MYK2630
      ALV(2,2)=AL(2,1)*VINV(1,2)+AL(2,2)*VINV(2,2)                      MYK2640
      DO 750 K2=2,NSUP                                                  MYK2650
      KQ=K2                                                             MYK2660
      IF(ITEM(2,I)-I6(K2))750,770,750                                   MYK2670
  750 CONTINUE                                                          MYK2680
      WRITE(6,760) I6(KQ)                                               MYK2690
  760 FORMAT(25H NO APPENDAGE STATION FORI3)                            MYK2700
      GO TO 2190                                                        MYK2710
  770 IQ=I1(KQ)                                                         MYK2720
      IF(ITEM(4,IQ)-2)780,800,780                                       MYK2730
  780 WRITE(6,790) I6(KQ)                                               MYK2740
  790 FORMAT(8H STATIONI3,28H IS NOT AN APPENDAGE STATION)              MYK2750
      GO TO 2190                                                        MYK2760
  800 IT=1+3*ITEM(5,IQ)+ITEM(5,I)                                       MYK2770
      T(1,1)=0.0                                                        MYK2780
      T(1,2)=0.0                                                        MYK2790
      T(2,1)=0.0                                                        MYK2800
      T(2,2)=0.0                                                        MYK2810
      RAD=SQRT((COS(DATA(7,IQ)))**2+(SIN(DATA(7,IQ))*COS(DATA(6,IQ)))**2 MYK2820
     1)                                                                 MYK2830
      IF(RAD)820,820,810                                                MYK2840
  810 CL=(COS(DATA(7,IQ))*COS(DATA(6,IQ)))/RAD                          MYK2850
      CU=SIN(DATA(7,IQ))*COS(DATA(6,IQ))/RAD                            MYK2860
      CV=COS(DATA(7,IQ))*SIN(DATA(6,IQ))/RAD                            MYK2870
      GO TO 830                                                         MYK2880
  820 CL=0.0                                                            MYK2890
      CU=SIN(DATA(5,IQ))                                                MYK2900
      CV=COS(DATA(5,IQ))                                                MYK2910
  830 GO TO (840,850,860,870,880,890,900,910,920),IT                    MYK2920
  840 T(1,1)=CL/SQRT(CL**2+CU**2)                                       MYK2930
      T(2,2)=CL/SQRT(CL**2+CV**2)                                       MYK2940
      T(2,2)=ABS(T(2,2))                                                MYK2950
      GO TO 930                                                         MYK2960
  850 T(1,1)=CU                                                         MYK2970
      GO TO 930                                                         MYK2980
  860 T(2,1)=-CV                                                        MYK2990
      GO TO 930                                                         MYK3000
```

```
 870 T(1,1)=-SQRT(1.0-CL**2)
     GO TO 930
 880 T(1,1)=CL
     GO TO 930
 890 GO TO 2200
 900 T(1,2)=SQRT(1.0-CL**2)
     GO TO 930
 910 GO TO 2200
 920 T(1,1)=CL
 930 ALVT(1,1)=ALV(1,1)*T(1,1)+ALV(1,2)*T(1,2)
     ALVT(1,2)=ALV(1,1)*T(2,1)+ALV(1,2)*T(2,2)
     ALVT(2,1)=ALV(2,1)*T(1,1)+ALV(2,2)*T(1,2)
     ALVT(2,2)=ALV(2,1)*T(2,1)+ALV(2,2)*T(2,2)
     A(1,3,KQ)=T(1,1)*ALVT(1,1)+T(1,2)*ALVT(2,1)
     A(1,4,KQ)=T(1,1)*ALVT(1,2)+T(1,2)*ALVT(2,2)
     A(2,3,KQ)=T(2,1)*ALVT(1,1)+T(2,2)*ALVT(2,1)
     A(2,4,KQ)=T(2,1)*ALVT(1,2)+T(2,2)*ALVT(2,2)
 940 TAP(1,1,JNT)=VINV(1,1)*T(1,1)+VINV(1,2)*T(1,2)
     TAP(1,2,JNT)=VINV(1,1)*T(2,1)+VINV(1,2)*T(2,2)
     TAP(2,1,JNT)=VINV(2,1)*T(1,1)+VINV(2,2)*T(1,2)
     TAP(2,2,JNT)=VINV(2,1)*T(2,1)+VINV(2,2)*T(2,2)
     JOINT(K)=JNT
     KKK(JNT)=KQ
     JNT=JNT+1
 950 DO 970 ISP=1,4
     DO 960 JSP=1,4
 960 SAP(ISP,JSP)=0.0
 970 SAP(ISP,ISP)=1.0
     GO TO 1110
 980 DO 990 J=1,4
     DO 990 L=1,4
 990 ARPA(L,J)=AP(L,J)
     DO 1000 I=1,2
     II=I+2
     DO 1000 J=1,2
1000 DANV(I,J)=ARPB(II,J)+ARPA(II,J)
     IF(ITEM(5,MF).NE.0) DANV(2,2)=1.0/DIV
     DEDET=1.0/(DANV(1,1)*DANV(2,2)-DANV(1,2)*DANV(2,1))
     DENV(1,1)=DANV(2,2)*DEDET
     DENV(2,2)=DANV(1,1)*DEDET
     DENV(1,2)=-DANV(1,2)*DEDET
     DENV(2,1)=-DANV(2,1)*DEDET
     DO 1010 J=1,6
     DO 1010 I=1,6
1010 THMAN(I,J)=0.0
     DO 1020 LL=1,5,2
     DO 1020 J=1,2
     JJ=J+LL-1
     DO 1020 I=1,2
     II=I+LL-1
```

Table A-12
(Cont'd.)

```
1020 THMAN(II,JJ)=DENV(I,J)
     BMAN(1,1)=-ARPA(3,1)-ARPB(3,1)
     BMAN(1,2)=-ARPA(3,2)-ARPB(3,2)
     BMAN(2,1)=-ARPA(4,1)-ARPB(4,1)
     BMAN(2,2)=-ARPA(4,2)-ARPB(4,2)
     BMAN(1,3)=ARPB(1,1)-ARPA(1,1)
     BMAN(1,4)=ARPB(1,2)-ARPA(1,2)
     BMAN(2,3)=ARPB(2,1)-ARPA(2,1)
     BMAN(2,4)=ARPB(2,2)-ARPA(2,2)
     BMAN(1,5)=-BMAN(1,3)
     BMAN(1,6)=-BMAN(1,4)
     BMAN(2,5)=-BMAN(2,3)
     BMAN(2,6)=-BMAN(2,4)
     BMAN(3,3)=-ARPA(3,1)
     BMAN(3,4)=-ARPA(3,2)
     BMAN(4,3)=-ARPA(4,1)
     BMAN(4,4)=-ARPA(4,2)
     BMAN(3,5)=-ARPB(3,1)
     BMAN(3,6)=-ARPB(3,2)
     BMAN(4,5)=-ARPB(4,1)
     BMAN(4,6)=-ARPB(4,2)
     BMAN(5,3)=-1.0
     BMAN(5,5)= 1.0
     BMAN(6,4)=-1.0
     BMAN(6,6)= 1.0
     DO 1030 I=1,6
     DO 1030 J=1,6
     BINV(I,J)=0.0
     DO 1030 MM=1,6
1030 BINV(I,J)=BINV(I,J)+BMAN(I,MM)*THMAN(MM,J)
     DO 1040 J=1,4
     DO 1040 I=1,6
1040 RMUL(I,J)=0.0
     DO 1050 J=1,2
     DO 1050 I=1,4
1050 RMUL(I,J)=-ARPB(I,J)
     DO 1060 J=3,4
     DO 1060 I=1,2
1060 RMUL(I,J)=-ARPB(I,J)-ARPA(I,J)
     DO 1070 J=3,4
     DO 1070 I=3,4
1070 RMUL(I,J)=-ARPB(I,J)
     DO 1080 I=3,4
     II=I+2
     DO 1080 J=3,4
1080 RMUL(II,J)=-ARPA(I,J)
     DO 1090 J=1,4
     DO 1090 I=1,6
     ARSTAR(NDR,I,J)=0.0
     DO 1090 MM=1,6
```

Table A-12
(Cont'd.)

```
1090 ARSTAR(NDR,I,J)=ARSTAR(NDR,I,J)+BINV(I,MM)*RMUL(MM,J)
     DO 1100 J=1,4
     DO 1100 I=1,4
     SAP(I,J)=0.0
     DO 1100 MM=1,4
1100 SAP(I,J)=SAP(I,J)+ARSTAR(NDR,I,MM)*APR(MM,J)
     K=KKEEP
     K=K+1
     GO TO 480
1110 K=K+1
     IF(K.LE.NSTA)GO TO 480
     IF(KIAP)480,480,1120
1120 KIAP=KIAP-1
     GO TO 470
1130 I2N=ITEM(2,M)
     KKK(JNT)=1
     JOINT(K)=JNT
     MODE(JNT)=ITEM(5,1)+1
     IF(I2N-7)1140,2240,2240
1140 IF(I2N)2190,2190,1150
1150 GO TO (1160,1190,1200,1230,1240,1250),I2N
1160 IF(ITEM(5,1))1180,1180,1170
1170 AP(2,4)=1.0/DIV
1180 FUNC(ITER)=AP(1,3)*AP(2,4)-AP(1,4)*AP(2,3)
     GO TO 1260
1190 FUNC(ITER)=AP(3,3)*AP(4,4)-AP(3,4)*AP(4,3)
     GO TO 1260
1200 IF(ITEM(5,1))1220,1220,1210
1210 AP(4,2)=1.0/DIV
1220 FUNC(ITER)=AP(3,1)*AP(4,2)-AP(3,2)*AP(4,1)
     GO TO 1260
1230 FUNC(ITER)=AP(1,3)*AP(4,4)-AP(1,4)*AP(4,3)
     GO TO 1260
1240 FUNC(ITER)=AP(3,2)*AP(4,3)-AP(4,2)*AP(3,3)
     GO TO 1260
1250 FUNC(ITER)=AP(1,2)*AP(4,3)-AP(1,3)*AP(4,2)
1260 OM(ITER)=SQRT(W2)
     PRNT(1)=ITER
     PRNT(2)=OM(ITER)/6.283185
     PRNT(3)=FUNC(ITER)
     GO TO (1270,1380),ILAF
1270 IF(KOWT.GT.1)GO TO 1330
1280 IF(ITHIN.LT.3) GO TO 1300
     OM(ITER+1)=OM(ITER)*GAMA
     IF(OM(ITER+1).GE.THIS)GO TO 1290
     GO TO 1310
1290 KOWT=1
     ITHIN=1
1300 OM(ITER+1)=OM(ITER)*GAMA
1310 ITER=ITER+1
```

```
      IF(ITER-298)1320,2190,2190                                        MYK4510
 1320 IF(OM(ITER).GT.UPBND)GO TO 2190                                   MYK4520
      KOWT=KOWT+1                                                       MYK4530
      W2=OM(ITER)**2                                                    MYK4540
      IF(W2.EQ.0.0)GO TO 2190                                           MYK4550
      GO TO 420                                                         MYK4560
 1330 IF((FUNC(ITER)/FUNC(ITER-1)).GT.0.0)GO TO 1350                    MYK4570
      ITHIN=1                                                           MYK4580
 1340 ILAF=2                                                            MYK4590
      SINLO=FUNC(ITER-1)                                                MYK4600
      SMX=ABS(SINLO)                                                    MYK4610
      SINHI=FUNC(ITER)                                                  MYK4620
      BIX=ABS(SINHI)                                                    MYK4630
      GOLO=OM(ITER-1)                                                   MYK4640
      GOHI=OM(ITER)                                                     MYK4650
      GO TO 1410                                                        MYK4660
 1350 IF(ITHIN.EQ.3)GO TO 1280                                          MYK4670
      FINK(ITER)=FUNC(ITER)-FUNC(ITER-1)                                MYK4680
      IF(KOWT.LT.3)GO TO 1280                                           MYK4690
      IF((FINK(ITER)/FINK(ITER-1)).LE.0.0)ITHIN=ITHIN+1                 MYK4700
      GO TO (1280,1360,1370),ITHIN                                      MYK4710
 1360 THAT=OM(ITER-1)                                                   MYK4720
      THEM=FUNC(ITER-1)                                                 MYK4730
      GO TO 1280                                                        MYK4740
 1370 THIS=OM(ITER)                                                     MYK4750
      OM(ITER)=THAT                                                     MYK4760
      FUNC(ITER)=THEM                                                   MYK4770
      GO TO 1280                                                        MYK4780
 1380 IF(FUNC(ITER)/SINLO)1390,1390,1400                                MYK4790
 1390 SINHI=FUNC(ITER)                                                  MYK4800
      GOHI=OM(ITER)                                                     MYK4810
      GO TO 1410                                                        MYK4820
 1400 SINLO=FUNC(ITER)                                                  MYK4830
      GOLO=OM(ITER)                                                     MYK4840
 1410 IF(KZ.LE.3)GO TO 1420                                             MYK4850
      OM(ITER+1)=(SINHI*GOLO-SINLO*GOHI)/(SINHI-SINLO)                  MYK4860
      OM(ITER+1)=ABS(OM(ITER+1))                                        MYK4870
      GO TO 1430                                                        MYK4880
 1420 OM(ITER+1)=(GOHI+GOLO)*.5                                         MYK4890
      IF(KZ.EQ.0)GO TO 1440                                             MYK4900
 1430 CONTINUE                                                          MYK4910
      IF(ABS(1.0-(OM(ITER+1)/OM(ITER))).LE.EPS)GO TO 1460               MYK4920
 1440 KZ=KZ+1                                                           MYK4930
      IF(KZ-16)1310,1310,1450                                           MYK4940
 1450 KOWT=1                                                            MYK4950
      KZ=0                                                              MYK4960
      ITHIN=1                                                           MYK4970
      ILAF=1                                                            MYK4980
      OM(ITER)=GOHI                                                     MYK4990
      FUNC(ITER)=SINHI                                                  MYK5000
```

```
      GO TO 1280
 1460 SAMBO=ABS(FUNC(ITER))
      IF(SAMBO-BIX)1470,1470,1450
 1470 IF(SAMBO-SMX)1480,1480,1450
 1480 OMEG=OM(ITER)
      IF(NOR.EQ.0)GO TO 1530
      DO 1520 LAP=1,NOR
      DO 1500 J=1,4
      DO 1490 I=1,4
      FPM(LAP,I,J)=0.0
 1490 FQM(LAP,I,J)=0.0
      FPM(LAP,J,J)=1.0
 1500 FQM(LAP,J,J)=1.0
      DO 1510 I=1,2
      II=I+4
      DO 1510 J=1,4
      FQM(LAP,I,J)=ARSTAR(LAP,II,J)
 1510 FPM(LAP,I,J)=FPM(LAP,I,J)-ARSTAR(LAP,II,J)
 1520 CONTINUE
 1530 CONTINUE
      KZ=0
      GO TO (1540,1580,1620,1660,1680,1700),I2N
 1540 IF(ITEM(5,1))1550,1550,1560
 1550 VEC(3,1)=-AP(1,4)/AP(1,3)
      VEC(4,1)=1.0
      GO TO 1570
 1560 VEC(3,1)=1.0
      VEC(4,1)=0.0
 1570 VEC(1,1)=0.0
      VEC(2,1)=0.0
      GO TO 1720
 1580 IF(ITEM(5,1))1590,1590,1600
 1590 VEC(3,1)=-AP(3,4)/AP(3,3)
      VEC(4,1)=1.0
      GO TO 1610
 1600 VEC(3,1)=1.0
      VEC(4,1)=0
 1610 VEC(1,1)=0
      VEC(2,1)=0.0
      GO TO 1720
 1620 IF(ITEM(5,1))1630,1630,1640
 1630 VEC(1,1)=-AP(3,2)/AP(3,1)
      VEC(2,1)=1.0
      GO TO 1650
 1640 VEC(1,1)=1.0
      VEC(2,1)=0.0
 1650 VEC(3,1)=0.0
      VEC(4,1)=0.0
      GO TO 1720
 1660 IF(ITEM(5,1))1670,1670,2240
```

Table A-12
(Cont'd.)

```
1670 VEC(1,1)=0.0
     VEC(2,1)=0.0
     VEC(3,1)=-AP(1,4)/AP(1,3)
     VEC(4,1)=1.0
     GO TO 1720
1680 IF(ITEM(5,1))1690,1690,2240
1690 VEC(1,1)=0.0
     VEC(2,1)=-AP(3,3)/AP(3,2)
     VEC(3,1)=1.0
     VEC(4,1)=0.0
     GO TO 1720
1700 IF(ITEM(5,1))1710,1710,2240
1710 VEC(1,1)=0.0
     VEC(2,1)=-AP(4,3)/AP(4,2)
     VEC(3,1)=1.0
     VEC(4,1)=0.0
1720 NSH=0
     DO 1870 K=2,KS
     I=I1(K)
     IF(I4(K)-3)1850,1730,1820
1730 IF(I4(K-1)-3)1850,1740,1850
1740 NSH=NSH+1
     DO 1750 J=1,4
1750 VSAVE(J)=VEC(J,K-1)
     DO 1760 J=1,4
     VEC(J,K)=0.0
     DO 1760 MM=1,4
1760 VEC(J,K)=VEC(J,K)+FPM(NSH,J,MM)*VSAVE(MM)
     KL=ICON(NSH)
     DO 1770 J=1,4
     VEC(J,KL)=0.0
     DO 1770 MM=1,4
1770 VEC(J,KL)=VEC(J,KL)+FQM(NSH,J,MM)*VSAVE(MM)
1780 KL=KL+1
     IF(KL.GT.NSJP)GO TO 1810
     I=I1(KL)
     IF(I.EQ.I1(KL-1))GO TO 1790
     IF(ITEM(2,I)-ITEM(2,I-1))1810,1790,1810
1790 DO 1800 J=1,4
     VEC(J,KL)=0.0
     DO 1800 MM=1,4
1800 VEC(J,KL)=VEC(J,KL)+A(J,MM,KL-1)*VEC(MM,KL-1)
     GO TO 1780
1810 CONTINUE
     GO TO 1870
1820 IF(I4(K-1)-4)1850,1830,1850
1830 DO 1840 J=1,4
     VEC(J,K)=0.0
     DO 1840 MM=1,4
1840 VEC(J,K)=VEC(J,K)+ARSTAR(NSH,J,MM)*VSAVE(MM)
```

Table A-12
(Cont'd.)

```
      GO TO 1870
 1850 DO 1860 J=1,4
      VEC(J,K)=0.0
      DO 1860 MM=1,4
 1860 VEC(J,K)=VEC(J,K)+A(J,MM,K-1)*VEC(MM,K-1)
 1870 CONTINUE
      IF(KORP)2010,2010,1880
 1880 KIAP=1
 1890 DO 1990 K=KS,NSTA
      I=I1(K)
      IF(ITEM(2,I)-ITEM(2,I-1))1910,1900,1910
 1900 IF(IR(K)+KIAP-KORP)1990,1970,1990
 1910 IF(IR(K)+KIAP-KORP)1990,1920,1990
 1920 DO 1930 K2=1,NSUP
      KQ=K2
      IF(ITEM(2,I)-I6(KQ))1930,1940,1930
 1930 CONTINUE
      GO TO 2190
 1940 VEC(1,K)=0.0
      VEC(2,K)=0.0
      DO 1950 J1=1,JNT
      J=J1
      IF(KKK(J1)-KQ)1950,1960,1950
 1950 CONTINUE
 1960 VEC(3,K)=TAP(1,1,J)*VEC(3,KQ)+TAP(1,2,J)*VEC(4,KQ)
      MODE(J)=ITEM(5,I)+1
      VEC(4,K)=TAP(2,1,J)*VEC(3,KQ)+TAP(2,2,J)*VEC(4,KQ)
      GO TO 1990
 1970 DO 1980 I=1,4
      VEC(I,K)=0.0
      DO 1980 J=1,4
 1980 VEC(I,K)=VEC(I,K)+A(I,J,K-1)*VEC(J,K-1)
 1990 CONTINUE
      IF(KIAP-KORP)2000,2010,2000
 2000 KIAP=KIAP+1
      GO TO 1890
 2010 GAM=0.0
      DO 2020 K=1,NSUP
      KN=K
      IF(ITEM(4,M)-I6(K))2020,2030,2020
 2020 CONTINUE
      GO TO 2080
 2030 IF(ITEM(5,KN)-1)2040,2050,2050
 2040 B=VEC(4,KN)
      GO TO 2060
 2050 B=VEC(3,KN)
 2060 DO 2070 K=1,NSUP
      DO 2070 J=1,4
 2070 VEC(J,K)=VEC(J,K)/B
 2080 DO 2090 K=1,NSUP
```

```
      I=I1(K)
 2030 GAM=GAM+DATA(4,I)*VEC(3,K)**2+DATA(2,I)*VEC(4,K)**2
      GK=GAM*OMEG**2
      IF(NOR)2100,2120,2100
 2100 JUG=JNT+NOR
      KKK(JUG)=KKK(JNT)
      MODE(JUG)=MODE(JNT)
      JU1=JUG-1
      J1=0
      DO 2110 J=JNT,JU1
      J1=J1+1
      KKK(J)=ICB(J1)
 2110 MODE(J)=MODE(JUG)
      JNT=JUG
 2120 CONTINUE
      DO 2170 JJ=1,JNT
      KQ=KKK(JJ)
      IQ=I6(KQ)
      II=MODE(JJ)
      IF(II)2190,2190,2130
 2130 GO TO (2140,2150,2160),II
 2140 GO TO 2170
 2150 GO TO 2170
 2160 GO TO 2170
 2170 CONTINUE
      FREQ=OMEG/6.283185
      FREP=OM(ITER+1)/6.283185
      ITEM(3,M)=ITEM(3,M)-1
      IF(ITEM(3,M))2190,2190,2180
 2180 KOHT=2
      OM(1)=GOHI
      FUNC(1)=SINHI
      IF(FUNC(1).EQ.0.0)FUNC(1)=-SINLO
      GAMA = SAMA
      ILAF=1
      OM(2)=GOHI*GAMA
      ITER=2
      MFAP=1
      W2=OM(2)**2
      ITHIN=1
      GO TO 420
 2190 RETURN
 2200 WRITE(6,2210)IT
 2210 FORMAT(29H NO T GIVEN FOR JOINT TYPE = I3)
      GO TO 2190
 2220 WRITE(6,2230)I6(KQ),KIAP
 2230 FORMAT(24H DETERMINANT V OF JOINT I3,17H APPENDAGE ORDER I3,5H = 0
     1.)
      GO TO 2190
 2240 WRITE(6,2250)I2N
```

Table A-12

(Cont'd.)

```
2250 FORMAT(25H BOUNDARY NOT IN TABLE = I3)                    MYK7010
     GO TO 2190                                                MYK7020
     END                                                       MYK7030
```

Table A-13
FORTRAN Listing of Subroutine MEMSET

```
      SUBROUTINE MEMSET (IA,IB)
      DIMENSION IA(1)
      K=IABS(LOCF(IB)-LOCF(IA))+1
      DO 10 J=1,K
   10 IA(J)=0
      END
```

Table A-14
FORTRAN Listing of Subroutine MATNF5

```
      SUBROUTINE MATNF5(A,N,NDIM,DETSCL,DET,IROAR)
      DIMENSION A(1)
      DIMENSION PIVOT(170),INDEX(170,2),IPIVOT(170)
   10 EQUIVALENCE(IROW,JROW),(ICOL,JCOL),(AMAX,T,SWAP)
C
C     BLOCK 100  INITIALIZE
C
   20 IROAR=0
      DET=DETSCL
   30 DO 40 J=1,N
   40 IPIVOT(J)=0
      DO 210 I=1,N
C
C     BLOCK 200  SEARCH FOR PIVOT ELEMENT
C
   50 AMAX=0.0
      DO 100 J=1,N
      IF(IPIVOT(J)-1)60,100,60
   60 DO 90 K=1,N
      IF(IPIVOT(K)-1)70,90,290
   70 JK=J+NDIM*(K-1)
      IF(ABS(AMAX)-ABS(A(JK)))80,90,90
   80 IROW=J
      ICOL=K
      AMAX=A(JK)
   90 CONTINUE
  100 CONTINUE
  110 IF(AMAX)120,300,120
C
C     BLOCK 300  INTERCHANGE ROWS TO PUT PIVOTAL ELEMENT ON DIAGONAL
C
  120 IPIVOT(ICOL)=IPIVOT(ICOL)+1
      IF(IROW-ICOL)130,150,130
  130 DET=-DET
      DO 140 L=1,N
      LD=NDIM*(L-1)
      IROL=IROW+LD
      ICLL=ICOL+LD
      SWAP=A(IROL)
      A(IROL)=A(ICLL)
  140 A(ICLL)=SWAP
  150 INDEX(I,1)=IROW
      INDEX(I,2)=ICOL
      ILOC=ICOL+NDIM*(ICOL-1)
      PIVOT(I)=A(ILOC)
      DET=DET*PIVOT(I)
C
C     BLOCK 400  DIVIDE PIVOT ROW BY PIVOT ELEMENT
C
  160 A(ILOC)=1.0
```

Table A-14
(Cont'd.)

```
      DO 170 L=1,N
      ICLL=ICOL+NDIM*(L-1)
      A(ICLL)=A(ICLL)/PIVOT(I)
  170 CONTINUE
C
C     BLOCK 500  REDUCE NON-PIVOT ROWS
C
  180 DO 210 L1=1,N
      IF(L1-ICOL)190,210,190
  190 ICOL=NDIM*(ICOL-1)
      L1C=L1+ICOL
      T=A(L1C)
      A(L1C)=0.0
      DO 200 L=1,N
      LD=NDIM*(L-1)
      L1D=L1+LD
      ICD=ICOL+LD
  200 A(L1D)=A(L1D)-A(ICD)*T
  210 CONTINUE
C
C     BLOCK 600  INTERCHANGE COLUMNS
C
  220 DO 250 I=1,N
      L=N+1-I
      IF(INDEX(L,1)-INDEX(L,2))230,250,230
  230 JROW=INDEX(L,1)
      JCOL=INDEX(L,2)
      JROW=NDIM*(JROW-1)
      JCCL=NDIM*(JCOL-1)
      DO 240 K=1,N
      KR=K+JROW
      KC=K+JCCL
      SWAP=A(KR)
      A(KR)=A(KC)
      A(KC)=SWAP
  240 CONTINUE
  250 CONTINUE
      RETURN
C
C     BLOCK 9000   ERROR INDICATIONS
C
  260 WRITE(6,270)IROAR
  270 FORMAT(31HO SUBROUTINE MATNF4 ERROR TYPE I5)
  280 CALL EXIT
  290 IROAR=1
      GO TO 260
  300 IROAR=-5
      RETURN
      END
```

TABLE A-15

SAMPLE DATA DECK LISTING FOR PROGRAM FILLIN

```
----------------------------     CARD COLUMNS     -----------------------------
00000000011111111112222222222333333333344444444445555555555666666666677777777778
12345678901234567890123456789012345678901234567890123456789012345678901234567890
--------------------------------------------------------------------------------

    FILLIN TEST CASE  TYPICAL MISSILE AIRFRAME
   1             0.16 +7    .040    7.8
  15             1.16 +8    .412   15.       2.447
  20             2.75 +8    .629   20.       7.002
  25             4.72 +8    .728   25.      11.50
  30             6.92 +8   1.003   30.15    20.13
  35             3.90 +8    .783   35.5     10.93
  37       2     3.83 +8           37.3
  39             2.51 +8   4.138   39.8     22.15
  45             3.59 +8   1.016   45.4     24.36
  46       1     5.81 +8           46.8                 .93 -7
  47             5.81 +8    .614   47.2     13.83
  48       3     1.57 +8           48.
  49             1.57 +8    .323   49.4      7.92
  55             1.57 +8    .560   55.      13.75
  60             1.57 +8   1.161   59.5     28.46
  61             4.53 +8           61.8
  62       1     4.53 +8           62.59                .62 -8
  63       4     3.23 +8           63.
  66             2.59 +8   3.106   66.      41.24
  67             3.56 +8    .809   67.97    11.32
  70       1     7.07 +8           70.                  .12 -6
  71             1.29 +8    .687   71.38    19.42
  76             4.88 +8    .925    7.4     26.13
  77       1     4.98 +8           77.6                 .62 -8
  78       2     4.54 +8           78.25
  79             4.54 +8    .846   79.      19.89
  80       1     8.02 +8           80.5                 .93 -7
  82             7.10 +8   7.075   82.      92.66
  90             5.26 +8   2.791   90.      81.50
 100             5.26 +8   3.000  100.      92.34
 110             5.26 +8   2.883  110.      88.78
 120             5.26 +8   2.883  120.      88.78
 130             5.26 +8   2.883  130.      88.78
 140             5.26 +8   2.883  140.      88.78
 150             5.26 +8   2.883  150.      88.78
 157             1.20 +9          157.5
 160             9.41 +8   4.468  160.     138.91
 168             1.23 +9   7.011  170.4     94.76
 170       1     2.47 +8          170.5                 .43 -7
 171             2.47 +8   1.387  171.7     26.71
 174             3.8A +8          174.
 178             5.98 +7   8.351  177.38 109.66
 182             5.98 +7   2.508  182.2     24.63
 191  37 1:      2.43 +5   1.132   30.3
 192  37 1: 1    2.43 +5           30.31        .19 -3
```

```
------------------------------  CARD COLUMNS  ------------------------------
00000000011111111112222222222333333333344444444445555555555666666666677777777778
12345678901234567890123456789012345678901234567890123456789012345678901234567890
--------------------------------------------------------------------------------

 193  37 1:       2.43 +5    .081    32.3
 194  37 1.       1.62 +6   2.251    35.3   18.60
 195  37 1: 1     8.09 +6            36.9                   .80 -5
 196  37 1.       8.09 +6    .453    37.02
 198  37 1:       8.09 +6            37.3
 315  78 1:       9.70 +7   5.049    72.9
 325  78 1.       1.21 +8   1.614    77.3
 326  78 1: 1     1.21 +8            78.           .26 -4   .32 -6
 330  78 1:       1.13 +7            78.25
 265  48-1: 1     5.66 +8            48.           .28 -4
 267  48-1:       5.66 +8   8.430    50.5    7.49
 268  48-1.       5.66 +8   4.431    55.     7.49
 269  48-1:       5.66 +8   9.717    59.5    8.20
 271  48-1. 1     5.66 +8            63.           .62 -4 1.
       1 3         40.               1.01   200.
   78   58   3
            7.5                 16.                 26.                 35.5
            40.5                45.                 48.5                52.
            57.                 62.                 66.                 69.5
            71.                 76.                 79.                 80.
            81.                 85.                 90.                 95.
            100.                105.                110.                115.
            120.                125.                130.                135.
            140.                145.                155.                160.
            165.                170.                171.                176.
            183.            37  30.             37  30.3            37  30.32
        37  32.             37  35.             37  36.89           37  37.
        37  37.3            78  70.5            78  75.             78   77.5
        78    78.01         78    78.25         48    45.           48   47.99
        48    49.5          48    55.           48    59.5          48    62.
        48    63.01         48    66.
        1  1   1.0          1.0         1.0
        2  1    .803         .905        .757
        3  1    .583         .813        .514
        4  1    .403         .706        .308
        5  1    .3           .655        .186
        6  1    .2           .639        .091
        7  1    .111         .579        .006
        8  1    .038         .521       -.043
        9  1   -.068         .353       -.103
       10  1   -.149         .212       -.131
       11  1   -.195         .094       -.117
       12  1   -.220        -.025       -.083
       13  1   -.234        -.081       -.048
       14  1   -.280        -.257        .015
       15  1   -.311        -.397        .049
```

Table A-15

(Cont'd.)

CARD COLUMNS

0000000001111111111222222222233333333334444444444555555555566666666667777777777(

123456'890123456789012345678901234567890123456789012345678901234567890123456789(

16	1	-.315	-.435	.069
17	1	-.311	-.436	.079
18	1	-.304	-.501	.126
19	1	-.306	-.616	.202
20	1	-.296	-.663	.250
21	1	-.280	-.701	.281
22	1	-.260	-.710	.308
23	1	-.242	-.709	.324
24	1	-.223	-.732	.342
25	1	-.198	-.755	.344
26	1	-.170	-.674	.336
27	1	-.143	-.641	.321
28	1	-.113	-.571	.298
29	1	-.079	-.504	.268
30	1	-.043	-.420	.229
31	1	.030	-.217	.141
32	1	.068	-.112	.09
33	1	.111	.072	.02
34	1	.148	.176	-.05
35	1	.161	.215	-.068
36	1	.237	.392	-.173
37	1	.268	.567	-.278
38	1	.797	-10.28	-.64
39	1	.78	-9.35	-.6
40	1	.65	-5.6	-.28
41	1	.53	-3.0	-.03
42	1	.42	-0.5	.17
43	1	.362	.691	.278
44	1	.36	.69	.275
45	1	.354	.687	.268
46	1	-.345	-.429	-.036
47	1	-.325	-.436	.013
48	1	-.321	-.439	.041
49	1	-.319	-.44	.046
50	1	-.311	-.441	.049
51	1	.2	.635	.09
52	1	.135	.59	.01
53	1	.103	.635	-.155
54	1	-.01	.68	-.265
55	1	-.10	.54	-.36
56	1	-.161	.487	-.422
57	1	-.15	.19	-.13
58	1	-.19	.1	-.115

TABLE A-16
SAMPLE DATA DECK LISTING FOR PROGRAM JOINTS

```
------------------------------    CARD COLUMNS    ------------------------------
00000000011111111112222222222333333333344444444445555555555666666666677777777778
12345678901234567890123456789012345678901234567890123456789012345678901234567890
--------------------------------------------------------------------------------

    PROGRAM JOINTS TEST CASE
    1    3    3    1   10    4   78   78  0.15      0.001          .9
    2   0.264
  1.0       1.0       1.0
  1.0       1.0       1.0
 59.3      116.      153.
  10   11   .1   +8   1.   +8    2
  21   26   .5   +7   5.   +7    2
  27   35   .1   +8   1.   +8    2
  48   58   .1   +6   1.   +6    2
         1  1  .99305E+00  .99665E+00  .99142E+00
         2  1  .82618E+00  .91618E+00  .78559E+00
         3  1  .77703E+00  .89471E+00  .73663E+00
         4  1  .66545E+00  .84066E+00  .60805E+00
         5  1  .53995E+00  .77872E+00  .46133E+00
         6  1  .41282E+00  .71442E+00  .31713E+00
         7  1  .37409E+00  .70447E+00  .27764E+00
         8  1  .37409E+00  .70447E+00  .27764E+00
         9  1  .31913E+00  .67842E+00  .21627E+00
        10  1  .19196E+00  .61390E+00  .86290E-01
        11  1  .15979E+00  .59723E+00  .57824E-01
        12  1  .15979E+00  .59723E+00  .57824E-01
        13  1  .15042E+00  .59237E+00  .49532E-01
        14  1  .13144E+00  .58253E+00  .32737E-01
        15  1  .13144E+00  .58253E+00  .32737E-01
        16  1  .10106E+00  .55586E+00  .96847E-02
        17  1 -.14839E-01  .41939E+00 -.66610E-01
        18  1 -.93783E-01  .29449E+00 -.98593E-01
        19  1 -.13327E+00  .22284E+00 -.11155E+00
        20  1 -.14322E+00  .19475E+00 -.11030E+00
        21  1 -.14322E+00  .19475E+00 -.11030E+00
        22  1 -.14822E+00  .18249E+00 -.10969E+00
        23  1 -.14822E+00  .18249E+00 -.10969E+00
        24  1 -.18578E+00  .90383E-01 -.10511E+00
        25  1 -.20661E+00  .25042E-01 -.88056E-01
        26  1 -.22617E+00 -.42329E-01 -.67804E-01
        27  1 -.22617E+00 -.42329E-01 -.67804E-01
        28  1 -.23708E+00 -.92267E-01 -.50985E-01
        29  1 -.29274E+00 -.32567E+00  .31853E-01
        30  1 -.29464E+00 -.33381E+00  .34456E-01
        31  1 -.29464E+00 -.33381E+00  .34456E-01
        32  1 -.30085E+00 -.36042E+00  .42963E-01
        33  1 -.30085E+00 -.36042E+00  .42963E-01
        34  1 -.30808E+00 -.39140E+00  .52867E-01
        35  1 -.31141E+00 -.42991E+00  .71247E-01
        36  1 -.31141E+00 -.42991E+00  .71247E-01
```

Table A-16
(Cont'd.)

```
-----------------------------  CARD COLUMNS  ------------------------------
00000000011111111112222222222333333333344444444445555555555666666666677777777778
12345678901234567890123456789012345678901234567890123456789012345678901234567890
--------------------------------------------------------------------------------

   37   1 -.31075E+00 -.45913E+00  .91805E-01
   38   1 -.30233E+00 -.58973E+00  .19073E+00
   39   1 -.27819E+00 -.68768E+00  .27681E+00
   40   1 -.24224E+00 -.71739E+00  .32324E+00
   41   1 -.19671E+00 -.71357E+00  .33832E+00
   42   1 -.14245E+00 -.63215E+00  .31740E+00
   43   1 -.78407E-01 -.49883E+00  .26426E+00
   44   1 -.75292E-02 -.31736E+00  .18385E+00
   45   1  .49843E-01 -.14328E+00  .10883E+00
   46   1  .69465E-01 -.82199E-01  .82546E-01
   47   1  .15548E+00  .20953E+00 -.65211E-01
   48   1  .15636E+00  .21245E+00 -.66965E-01
   49   1  .15636E+00  .21245E+00 -.66965E-01
   50   1  .16575E+00  .23778E+00 -.83601E-01
   51   1  .18630E+00  .30551E+00 -.12344E+00
   52   1  .21903E+00  .42658E+00 -.19370E+00
   53   1  .26103E+00  .54700E+00 -.26600E+00
   54   1  .26103E+00  .54700E+00 -.26600E+00
   55   1  .78000E+00 -.93500E+01 -.60000E+00
   56   1  .77943E+00 -.93198E+01 -.59867E+00
   57   1  .65071E+00 -.56155E+01 -.28149E+00
   58   1  .54672E+00 -.33377E+01 -.73377E-01
   59   1  .41079E+00 -.31895E+00  .18714E+00
   60   1  .36169E+00  .69730E+00  .27857E+00
   61   1  .36377E+00  .58673E+00  .26450E+00
   62   1  .35960E+00  .60980E+00  .27453E+00
   63   1  .35400E+00  .68700E+00  .26800E+00
   64   1  .35400E+00  .68700E+00  .26800E+00
   65   1 -.33433E+00 -.43273E+00 -.38667E-02
   66   1 -.32051E+00 -.43896E+00  .38411E-01
   67   1 -.32020E+00 -.43960E+00  .46600E-01
   68   1 -.31933E+00 -.43996E+00  .45875E-01
   69   1 -.31100E+00 -.44100E+00  .49000E-01
   70   1 -.31100E+00 -.44100E+00  .49000E-01
   71   1  .13478E+00  .58985E+00  .97324E-02
   72   1  .13382E+00  .87727E+00 -.12500E+00
   73   1  .82455E-01  .80682E+00 -.17500E+00
   74   1 -.10000E-01  .68000E+00 -.26500E+00
   75   1 -.10000E+00  .54000E+00 -.36000E+00
   76   1 -.18540E+00  .46580E+00 -.44680E+00
   77   1 -.14987E+00  .19030E+00 -.13005E+00
   78   1 -.14987E+00  .19030E+00 -.13005E+00
    1   1 -.23176E-01 -.11176E-01 -.28588E-01
    2   1 -.23176E-01 -.11176E-01 -.28588E-01
    3   1 -.19867E-01 -.96208E-02 -.22893E-01
    4   1 -.24768E-01 -.12001E-01 -.28537E-01
```

able A-16
(Cont'd.)

```
----------------------------- CARD COLUMNS -----------------------------
00000000011111111112222222222333333333344444444445555555555666666666677777777778
12345678901234567890123456789012345678901234567890123456789012345678901234567890
--------------------------------------------------------------------------------
```

5	1	-.21830E-01	-.11039E-01	-.24761E-01
6	1	-.25699E-01	-.12996E-01	-.29145E-01
7	1	-.21270E-01	-.10082E-01	-.23752E-01
8	1	-.21270E-01	-.10082E-01	-.23752E-01
9	1	-.22695E-01	-.10757E-01	-.25343E-01
10	1	-.22627E-01	-.11727E-01	-.20024E-01
11	1	-.22222E-01	-.35556E-02	-.21111E-01
12	1	-.20857E-01	-.16571E-01	-.14000E-01
13	1	-.23524E-01	-.12192E-01	-.20818E-01
14	1	-.23923E-01	-.12399E-01	-.21171E-01
15	1	-.23923E-01	-.12399E-01	-.21171E-01
16	1	-.21405E-01	-.22829E-01	-.15240E-01
17	1	-.19312E-01	-.27955E-01	-.10185E-01
18	1	-.16843E-01	-.30562E-01	-.55264E-02
19	1	-.17494E-01	- 31743E-01	-.57399E-02
20	1	-.16200E-01	-.28200E-01	-.56000E-02
21	1	-.71429E-02	-.34000E-01	.97143E-02
22	1	-.12229E-01	-.29990E-01	.14927E-02
23	1	-.12229E-01	-.29990E-01	.14927E-02
24	1	-.12812E-01	-.31418E-01	.15639E-02
25	1	-.94716E-02	-.33228E-01	.89118E-02
26	1	-.71429E-02	-.34000E-01	.97143E-02
27	1	-.92000E-02	-.35200E-01	.12600E-01
28	1	-.91541E-02	-.37813E-01	.12965E-01
29	1	-.94904E-02	-.40664E-01	.13000E-01
30	1	-.92000E-02	-.35200E-01	.12600E-01
31	1	-.40000E-02	-.38000E-01	.20000E-01
32	1	-.95946E-02	-.41111E-01	.13142E-01
33	1	-.95946E-02	-.41111E-01	.13142E-01
34	1	-.96866E-02	-.41505E-01	.13268E-01
35	1	-.40000E-02	-.38000E-01	.20000E-01
36	1	.17500E-02	-.16250E-01	.11750E-01
37	1	.82451E-03	-.17875E-01	.12834E-01
38	1	.92996E-03	-.17279E-01	.12805E-01
39	1	.31500E-02	-.65641E-02	.71590E-02
40	1	.38679E-02	-.18828E-02	.40726E-02
41	1	.49226E-02	.16749E-02	.77617E-03
42	1	.57506E-02	.11929E-01	-.31200E-02
43	1	.68015E-02	.14865E-01	-.62313E-02
44	1	.73400E-02	.19740E-01	-.88000E-02
45	1	.77870E-02	.24240E-01	-.10429E-01
46	1	.79106E-02	.24624E-01	-.10595E-01
47	1	.87572E-02	.29155E-01	-.17539E-01
48	1	.74000E-02	.20800E-01	-.14000E-01
49	1	.92000E-02	.35400E-01	-.21000E-01
50	1	.88731E-02	.29253E-01	-.17205E-01

Table A-16
(Cont'd.)

```
-----------------------------     CARD COLUMNS     --------------------------------
00000000011111111112222222222333333333344444444445555555555666666666677777777778
12345678901234567890123456789012345678901234567890123456789012345678901234567890
--------------------------------------------------------------------------------

      51  1  .89920E-02  .29645E-01 -.17435E-01
      52  1  .87143E-02  .25000E-01 -.15000E-01
      53  1  .87143F-02  .25000E-01 -.15000E-01
      54  1  .87143E-02  .25000E-01 -.15000E-01
      55  1 -.56667E-01  .31000E+01  .13333E+00
      56  1 -.56667E-01  .31000E+01  .13333E+00
      57  1 -.56667E-01  .31000E+01  .13333E+00
      58  1 -.40809E-01  .89668E+00  .78299E-01
      59  1 -.30688E-01  .63016E+00  .57143E-01
      60  1 -.30688E-01  .63016E+00  .57143E-01
      61  1 -.20000E-01 -.10000E-01 -.23333E-01
      62  1 -.20000E-01 -.10000E-01 -.23333E-01
      63  1 -.20000E-01 -.10000E-01 -.23333E-01
      64  1 -.20000E-01 -.10000E-01 -.23333E-01
      65  1  .44444E-02 -.15556E-02  .10889E-01
      66  1  .35587E-02 -.15063E-02  .11415E-01
      67  1  .16080E-02 -.12800E-02  .11200E-01
      68  1  .33333E-01 -.41667E-02  .12500E-01
      69  1  .33333E-01 -.41667E-02  .12500E-01
      70  1  .33333E-01 -.41667E-02  .12500E-01
      71  1 -.0207      -.0283      -.0202
      72  1 -.0207      -.0283      -.0202
      73  1 -.20545E-01 -.28182E-01 -.20000E-01
      74  1 -.20545E-01 -.28182E-01 -.20000E-01
      75  1 -.24400E-01 -.21200E-01 -.24800E-01
      76  1 -.24400E-01 -.21200E-01 -.24800E-01
      77  1 -.13378E-01 -.30100E-01  .0015056
      78  1 -.13378E-01 -.30100E-01  .0015056
  1             0.16 +7    .040    7.8
 15             1.16 +8    .412   15.        2.447
 20             2.75 +8    .629   20.        7.082
 25             4.72 +8    .728   25.       11.50
 30             6.92 +8   1.003   30.15     20.13
 35             3.90 +8    .783   35.5      10.93
 37      2      3.83 +8           37.3
 39             2.51 +8   4.138   39.8      22.15
 45             3.59 +8   1.016   45.4      24.36
 46      1      5.81 +8           46.8                          .93 -7
 47             5.81 +8    .614   47.2      13.83
 48      3      1.57 +8           48.
 49             1.57 +8    .323   49.4       7.92
 55             1.57 +8    .560   55.       13.75
 60             1.57 +8   1.161   59.5      28.46
 61             4.53 +8           61.8
 62      1      4.53 +8           62.59                         .62 -8
 63      4      3.23 +8           63.
```

Table A-16
(Cont'd.)

---------------------- CARD COLUMNS ----------------------

000000000111111111122222222223333333333444444444455555555556666666
123456789012345678901234567890123456789012345678901234567890123456

66			2.59 +8	3.106	66.	41.24		
67			3.56 +8	.809	67.97	11.32		
70		1	7.07 +8		70.			.12 -6
71			1.29 +8	.687	71.38	19.42		
76			4.89 +8	.925	77.4	26.13		
77		1	4.88 +8		77.6			.62 -8
78		2	4.54 +8		78.25			
79			4.54 +8	.846	79.	19.89		
80		1	8.02 +8		80.5			.93 -7
82			7.10 +8	7.075	82.	92.66		
90			5.26 +8	2.791	90.	81.50		
100			5.26 +8	3.000	100.	92.34		
110			5.26 +8	2.883	110.	88.78		
120			5.26 +8	2.883	120.	88.78		
130			5.26 +8	2.883	130.	88.78		
140			5.26 +8	2.883	140.	88.78		
150			5.26 +8	2.883	150.	88.78		
157			1.20 +9		157.5			
160			9.41 +8	4.468	160.	138.91		
168			1.23 +9	7.011	170.4	94.76		
170		1	2.47 +8		170.5			.43 -7
171			2.47 +8	1.387	171.7	26.71		
174			3.88 +8		174.			
178			5.98 +7	8.351	177.38	109.66		
182			5.98 +7	2.508	182.2	24.63		
191	37 1		2.43 +5	1.132	30.3			
192	37 1	1	2.43 +5		30.31		.19 -3	
193	37 1		2.43 +5	.081	32.3			
194	37 1		1.62 +6	2.251	35.3	18.60		
195	37 1	1	8.09 +6		36.9			.80 -5
196	37 1		8.09 +6	.453	37.02			
198	37 1		8.09 +6		37.3			
315	78 1		9.70 +7	5.049	72.9			
325	78 1		1.21 +8	1.614	77.3			
328	78 1	1	1.21 +8		78.		.26 -4	.32 -6
330	78 1		1.13 +7		78.25			
265	48-1	1	5.66 +8		48.		.28 -4	
267	48-1		5.66 +8	8.430	50.5	7.49		
268	48-1		5.66 +8	4.431	55.	7.49		
269	48-1		5.66 +8	9.717	59.5	8.20		
271	48-1	1	5.66 +8		63.		.62 -4 1.	
	1 3		40.		1.02	200.		

Table A-17

Key Output Data from Sample Data Deck

Parameter	Iteration		
	0	1	2
Cost Functions			
Overall	.68164 E + 12	.65905 E + 11	.36836 E + 11
Frequency	.17047 E + 12	.39695 E + 11	.96240 E + 10
Mode Shape	.51117 E + 12	.26210 E + 11	.27212 E + 11
Compliances			
C_1	.93000 E - 7	.83152 E - 7	.53820 E - 7
C_2	.12000 E - 6	.12038 E - 6	.80930 E - 7
C_3	.93000 E - 7	.60380 E - 7	.40304 E - 7
C_4	.30000 E - 5	.69565 E - 5	.59244 E - 5
Frequencies			
f_1	.4888485 E + 2	.4894103 E + 2	.5546776 E + 2
f_2	.1435402 E + 3	.1078903 E + 3	.1124721 E + 3
f_3	.1435414 E + 3	.1441162 E + 3	.1485364 E + 3

FIGURE A-1
SAMPLE APPLICATION
VALUES OF UNKNOWN JOINT
COMPLIANCES AND COST FUNCTION
VERSUS CYCLE NUMBER